COMPUTATIONAL EXPLORATION OF HYPERCOORDINATE ATOMS IN MOLECULES

by

KEIGO ITO

(Under the Direction of Paul von Ragué Schleyer)

ABSTRACT

This dissertation presents a computational exploration of unconventional molecules containing hypercoordinate atoms (i.e., those having a higher number of nearest neighboring atoms than expected by Lewis-based predictions). The four chapters in this dissertation discuss two different structural types: (a) those containing three-dimensional hypercoordinate environment (Chapters 2 and 3) and, (b) those having atoms exhibiting planar hypercoordination (Chapters 4 and 5). While di-coordinate bridging hydrogens are well known, higher hydrogen coordinations are rare. Chapter 2, entitled "Hypercoordinate Hydrogen in Scandium Hydride Clusters" demonstrates unusually high hydrogen coordinations (up to eight) in scandium hydride clusters. In contrast to known molecules containing hexacoordinate carbons, which have asymmetric environments, Chapter 3 (Synergistic Bonding in Three Dimensional Hypercoordinate Carbon) presents molecules with symmetrical three-dimensional hexacoordinate carbons (surrounded by six equivalent carbons). Achieving hypercoordination in planar geometries is especially challenging due to the reduction of out-of-plane bonding opportunities and increased steric repulsion between the ligands. Chapter 4, entitled "Myriad Planar Hexacoordinate Carbon Molecules Inviting Synthesis", focuses on the elaboration of planar hexacoordinate carbon cluster (CB_6^{2-}) based on a hydrocarbon grafting strategy. Chapter

5 (Cyclic Boron Clusters Enclosing Planar Hypercoordinate Cobalt, Iron and Nickel) illustrates cyclic boron clusters containing *octa*- or *nona*- planar hypercoordinate iron, cobalt, and nickel atoms. Although transition metals often have high coordination numbers (above six) in three-dimensional environments, such coordination numbers are unusual and difficult to achieve in planar geometries. The computational findings presented in this work contribute to the development of structural chemistry by proposing unconventional bonding environments.

INDEX WORDS: Hypercoordinate hydrogen, Scandium hydride cluster, Planar hypercoordinate carbon, CB_6^{2-} derivatives, Three-dimensional hypercoordinate carbon, Planar hypercoordinate transition metal, Double aromaticity

COMPUTATIONAL EXPLORATION OF HYPERCOORDINATE ATOMS IN MOLECULES

by

KEIGO ITO

B.S., California State University, Hayward, 2003

A Dissertation Submitted to the Graduate Faculty of The University of Georgia in Partial Fulfillment of the Requirements for the Degree

DOCTOR OF PHILOSOPHY

ATHENS, GEORGIA

2011

COMPUTATIONAL EXPLORATION OF HYPERCOORDINATE ATOMS IN MOLECULES

by

KEIGO ITO

Major Professor:	Paul von Ragué Schleyer
Committee:	Henry Fritz Schaefer III Nigel Graham Adams

Electronic Version Approved:

Maureen Grasso
Dean of the Graduate School
The University of Georgia
August 2011

DEDICATION

To Judy

ACKNOWLEDGEMENTS

I would like to express my sincere gratitude to those whom made my graduate school endeavor successful. First and foremost, I thank my advisor, Professor Paul Schleyer, for his guidance and patience. He game me the freedom to explore my own research projects and enabled me to become independent. His uncompromised expectation for a high research standard constantly challenged me to grow. I thank my mentors, Dr. Zhongfang Chen, Dr. Clémence Corminboeuf, and Dr. Chaitanya Wannere, who taught me the fundamentals in the chemical research. Additionally, I am thankful for my former and current co-workers in the Schleyer group, Matt, Debjani, and Chad for their help in research and friendship. I thank my American parents, Steve and Edith for their support. Their wicked jokes made me laugh and lightened up my mood. I also thank my birth parents. A large portion of my science-oriented mind originated from the way they raised me. Without their guidance, I would not have succeeded this far. A special and personal gratitude goes to my fiancé, Judy, for her continuous support and care. Her enthusiasm encouraged me to try out my ideas, and taught me not to fear the failure. Her emotional support gave me strength to "try again" when my spirit was crushed. For those and many other reasons, I am deeply indebted.

TABLE OF CONTENTS

Page

LIST OF TABLES

Page

LIST OF FIGURES

Page

CHAPTER 1

INTRODUCTION AND LITERATURE REVIEW

Hypercoordinate bonding[1] in molecules lead to fascinating structures that go beyond conventional expectations based on classical bonding rules.[2] Classical bonds involve two electrons between two atomic centers (2c-2e bonds), and the coordination number for each atom equals its expected valency. But non-classical bonds deviate from such anticipation. It is important to make a distinction between coordination (i.e. number of neighboring atom within a sum of their van der Waal's radii; a geometric criteria) and valency (i.e. the number of valence electron pairs involved in bonding; an electronic criteria).[3] Hence, elements displaying *hypercoordinate* bonding have higher numbers of neighboring atoms than expected by their classical valency. For example, boron clusters, due to their electron deficient nature, have the natural inclination to form networks of delocalized three-center-two-electron (3c-2e) bonds.[4] Hypercoordinate bonding can happen easily for electron deficient elements (e.g. B and Li), but are more difficult to achieve for other elements e.g. H, C, transition metals (as discussed here), which naturally favor classical bonding. The justification of hypercoordination, e.g. for carbons, also depends on the type (e.g. sp^2 or sp^3) of carbon considered. For example, four coordinations for an *sp2* carbon can be regarded as hypercoordination.

The focus of this dissertation is two-folds: (1) To propose widely applicable strategies for designing unconventional molecules containing hypercoordinate elements and (2) to suggest effective ways of increasing the experimental feasibility of synthesizing such species. Computational chemistry is a powerful tool for such purposes, as it offers a cheap and efficient alternative (compared to experiment) for exploring and predicting molecules

with hypercoordination bonding. The ability to simulate imaginative molecules also is one of the greatest strengths of such theoretical approach. The various chapters selected as a part of this dissertation demonstrate successful computational examples of inorganic and organic clusters with hypercoordinate hydrogen (chapter 2), carbon (chapters 3 and 4), and transition metals (chapter 5).

Although different elements require different bonding environments to achieve hypercoordinate bonding (i.e. based on various electron counting rules), the structural factors involved, i.e. competing electronic stabilization and steric repulsion, are quite similar. By definition, hypercoordination requires more than usual numbers of atoms or ligands to bind to one atom, either through favorable electrostatic interactions (as discussed in chapter 2 for various Sc-H clusters) or non-classical delocalized bonding mechanisms (as discussed in chapters 3 to 5). However, strategies to enhance electronic stabilization (e.g. by using delocalized bonding) are often offset by counteracting steric repulsion among surrounding ligands (chapters 2 and 4) or between the hypercoordinate element and encasing ring moiety (chapters 3 and 5).

Interestingly, the earliest example of molecules with non-classical bonding features precedes the conceptualization of classical bonding rules. Thomson discovered H_3^+, formed by three bridging hydrogens, in 1911.[5] Diborane, which contains two bridging hydrogen atoms, also was prepared as early as the late 19th century, although an ethane-like geometry was first assumed.[6] Apparent disagreements for the structure of diborane, between an ethane-like structure and a non-classical bridging structure (supported by the computed vibrational force constants and the experimental IR spectrum), resulted in a decade-long controversy.[7] Detailed investigations by Longuet-Higgins,[8] Pitzer,[9] and Lipscomb[4,10] led to

the conceptualization of (3c-2e) bonding, which added a new dimension to structural chemistry. However, hydrogen hypercoordination is not limited to 3c-2e bridging, but higher coordination can be achieved. Recent gas phase experiments observed tetracoordinate hydrogen containing hydrocarbon cation clusters in an ion beam in extremely cold environment.[11] When polar bonds are involved (e.g. between H's and more electropositive metallic elements), high-order hydrogen hypercoordination can be achieved. Wheatley and co-workers characterized organolithio clusters containing hydrogens with up to eight coordinations.[12] In chapter 2, we present hypercoordinate hydrogen in scandium hydride clusters, designed by combining 3c-2e bonds (delocalized bonding) and polar H-Sc bonds (electrostatic stabilization).

Violations of classical tetracoordination in carbons have received special attention. Hoffmann, Alder and Wilcox's (HAW) study of the interconversion of methane through the planar D_{4h} transition state marked a new chapter in hypercoordinate carbon chemistry.[13] Their conclusion, that planar hypercoordinate carbons can be stabilized by π-accepting/σ-donating ligands, encouraged the search for non-classical carbons, although they did not mention the possibility of competing steric factors. The first successful application of HAW's strategy was demonstrated in $C_3H_2Li_2$, by Jemmis and Schleyer,[14] in which lithium was utilized as a π-acceptor ligand. A more elegant example, D_{6h} CB_6^{2-}, was proposed by Exner and Schleyer in 2000; the electron deficient nature of boron encouraged deltahedral bonds, while the 6π electron aromaticity provided additional stability to retain the central planar hexacoordinate carbon.[15] Since the B_6 ligand is a ring, there is no steric repulsion between ligands. Although the –2 molecular charge makes CB_6^{2-} an unrealistic candidate for

experimental preparation in gas phase, this can be circumvent by a grafting strategy (see below), and is discussed in chapter 3.

Three dimensional hypercoordinate carbons (3dhC's) also can be realized by using delocalized 3c-2e bonds. Protonated- and diprotonated methane (CH_5^+ and CH_6^{2+}, respectively) preferred to form a mixture of classical 2c-2e and 3c-2e bonds (between the C and two H's), which result in asymmetric carbon centers. Unlike CH_6^{2+}, Minkin's $C_{13}H_8^{2+}$ hydrocarbon cluster with a three-dimensional hexacoordinate carbon formed three 3c-2e bonds (instead of a mixture of 3c-2e and 2c-2e bonds) symmetrically around the central carbon atom.[16] Minkin's example uses the hydrocarbon cage as a σ-donor/π-acceptor ligand, and thus can be considered as a three-dimensional extension of the HAW strategy. Chapter 4 utilizes a similar approach to design 3dhC's in hydrocarbon and carborane clusters.

Transition metal hypercoordinate bonding benefit additionally from the presence of d-orbitals. One of the most well-known example of hypercoordination in transition metal elements, the decacoordinate iron(II) in ferrocene, was achieved by Pauson and Kealy in 1951.[17] The initial (yet incorrect) structure based on classical 2c-2e bonds with a low symmetry failed to explain its IR spectrum, which suggested that ferrocene had a high symmetry. Woodward's proposal[18] of a sandwiched ferrocene structure inspired Dunitz to conceive a new type of bonding mechanism for organometallic molecules,[19] which utilized delocalized bonds between the iron d-orbitals and the cyclopentadiene π orbital (and thus, a high iron coordination number, consistent with the high symmetry of ferrocene). Hypercoordinate metal d-orbital to ring interactions are even stronger when the metals are encompassed by rings of appropriate size; such clusters benefit from both σ and π

delocalized bonding. Chapter 5 presents examples of double aromatic (π and radial σ aromaticity) boron rings containing hypercoordinate first row d-block elements.

While the numerous examples of molecules containing hypercoordinate elements force us to reconsider our views of such species as "rare exceptions," practical synthetic candidates must satisfy both theoretical and experimental requirements.[20] Hence, exotic molecules that are identified as "*thermochemically stable*," (e.g. based on computational explorations), may not necessarily be "*kinetically persistent*," and for the latter reason may have only fleeting existence in reality. Chapters 3 and 4 discuss specific charge compensation methods (i.e. by replacing charged elements or moieties with isoelectronic groups to obtain neutral species) and grafting strategies (i.e. by incorporating appropriate alkyl groups to the hypercoordinate moieties) that increase the kinetic persistence (structural rigidity), and thus experimental feasibility, of planar and three dimensional hypercoordinate carbons. Understanding hypercoordinate bonding and devising effective strategies to design molecules with unconventional structures open exciting synthetic opportunities for fundamental and applied fields of chemistry.

1.2 References

(1) Olah, G. A.; Prakash, G. K. S. *Chem. in Britain* **1983**, *19*, 916.

(2) Lewis, G. N. *J. Am. Chem. Soc.* **1916**, *38*, 762.

(3) Schleyer, P. v. R. *Chem. Eng. News* **1984**, 4.

(4) Lipscomb, W. N. *Acc. Chem. Res.* **1973**, *6*, 257.

(5) Thomson, J. J. *Phil. Mag.* **1911**, *21*, 225.

(6) Stock, A. *Hydrides of Boron and Silicon*; Cornell University Press: Ithaca, NY., 1933.

(7) Laszlo, P. *Angew. Chem. Int. Ed* **2000**, *39*, 2071.

(8) Longuet-Higgins, H. C.; Bell, R. P. *J. Chem. Soc.* **1943**, 250.

(9) Pitzer, K. S. *J. Am. Chem. Soc.* **1945**, *67*, 1126.

(10) Lipscomb, W. N. *J. Chem. Phys.* **1954**, *22*, 985.

(11) Douberly, G. E.; Ricks, A. M.; Ticknor, B. W.; McKee, W. C.; Schleyer, P. v. R.; Duncan, M. A. *J. Phys. Chem. A* **2008**, *112*, 1897.

(12) Haywood, J.; Wheatley, A. E. H. *Dalton Trans.* **2008**, 3378.

(13) Hoffmann, R.; Alder, R. W.; F., W. C. *J. Am. Chem. Soc.* **1970**, *92*, 4992.

(14) Collins, J. B.; Dill, J. D.; Jemmis, E. D.; Apeloig, Y.; Schleyer, P. v. R.; Seeger, R.; Pople, J. A. *J. Am. Chem. Soc.* **1976**, *98*, 5419.

(15) Exner, K.; Schleyer, P. v. R. *Science* **2000**, *290*, 1937.

(16) Minyaev, R. M.; Minkin, V. I.; Gribanova, T. N.; Starikov, A. G. *Mendeleev Commun.* **2004**, *14*, 47.

(17) Kealy; Pauson *Nature* **1951**, *168*, 1039.

(18) Wilkinson, G.; Rosenblum, M.; Whiting, M. C.; Woodward, R. B. *J. Am. Chem. Soc.* **1952**, *74*, 2125.

(19) Orgel, L. E.; Dunitz, J. D. *Nature* **1953**, *171*, 121.

(20) Hoffmann, R.; Schleyer, P. v. R.; Schaefer, H. F., III *Angew. Chem. Int. Ed.* **2008**, *47*, 7164.

CHAPTER 2

HYPERCOORDINATE HYDROGEN IN SCANDIUM HYDRIDE CLUSTERS[†]

[†] Keigo Ito and Paul von Ragué Schleyer
To be submitted to Theoretical Chemistry Accounts.

2.1 Abstract

Small to medium size scandium hydride cluster minima ($Sc_nH_m^x$: n=2–6, m=5–15, x=[+]-[–]), identified at the M06-2X/def2-TZVPP DFT level, are remarkably effective hosts for non-classical hypercoordinate hydrogens (up to eight coordination). Stochastic searches reveal D_{3h} $Sc_2H_5^+$, D_{4h} Sc_2H_6, D_{3h} $Sc_3H_8^+$, and D_{4h} $Sc_4H_{13}^-$ to be global minima. Hypercoordinate hydrogens maximize the thermochemical stability of $Sc_nH_m^x$ clusters, as they offer greater $H^{\delta-}$-$Sc^{\delta+}$ electrostatic attraction compared to the classical two-center-two-electron (terminal) H-Sc bonds. Following a simple electron counting guideline, fragments from small and medium-size clusters can be used as building blocks to design larger clusters (D_{3h} $Sc_5H_{16}^-$, D_{4h} $Sc_8H_{21}^{3+}$, and O_h $Sc_8H_{26}^{2-}$). Substitution of terminal hydrogens by methyl groups offer further prospects for bulk phase experimental realization of organoscandium hydride clusters having hypercoordinate hydrogens.

2.2 Introduction

Hydrogen hypercoordination in "electron deficient" molecules no longer are uncommon occurrences in main group and transition metal chemistry.[1-6] The bonding of such hydrogens differ from those in classical two-center, two-electron (2c-2e) arrangements or those involved in hydrogen bonds between donor atoms. Except for borane clusters, theoretical studies of such unusual bonding have largely been limited to individual cases. Dilthey's 1921 speculative depiction of bridging hydrogens in diborane[7,8] was ignored for two decades and was not established until Longuet-Higgins'[9] and Pitzer's[10] conceptualization of "three-center two-electron (3c-2e) bonds", widely generalized by Lipscomb.[11-13] H-bridged $C_2H_3^+$ and $C_2H_5^+$ are simple carbon-based examples where non-classical isomers with bridging hypercoordinate H's and more highly delocalized bonding

are preferred.[14] Alternative structures with classical 2c-2e bonds are possible, but all atoms in these isomers do not fulfill the octet rule. Hence, such "electron deficient" species are prone to exhibit hydrogen hypercoordination. Like boron, scandium also is an electron deficient element (both only have three valence electrons) and its derivatives may be good prospects for forming hypercoordinate hydrogens. Piers et al's recent synthesis of organoscandium hydride molecules containing a tetracoordinate hydrogen center ([ClScNDipp(THF)]$_3$[LiH(THF)] (Dipp = 2,6-^{i}Pr$_2$C$_6$H$_3$) (**a**), and DippNC(^{t}Bu)CHCH(^{t}Bu) (**b**) in Figure 2-1)[15] demonstrates the feasibility of scandium hydride clusters as hosts for hypercoordinate hydrogens. But what is the underlying reason for hydrogen hypercoordination in scandium hydride clusters?

As scandium is much more electropositive (1.20 in Allred-Rochow electronegativity scale)[16] than boron (2.01), a H-Sc bonds in scandium hydrides are expected to have higher polarity than a B-H bond in boranes. Transition metals have additional advantages promoting 3c-2e bonding and higher hydrogen hypercoordination due to their larger atomic radii and greater polarizability. The larger atomic radius of Sc, compared to B and Al, reduces steric repulsion but still offers significant orbital overlap to potential bridging (or higher coordination) hydrogens. Sc's greater polarizability also encourages delocalized bonding, ideal for hosting hypercoordinate hydrogens. While d-orbital[6,17-20] involvement is possible, the importance is marginal. This paper presents a series of scandium hydride clusters with hypercoordinate hydrogens and investigates the underlying reasons for the unusual bonding patterns.

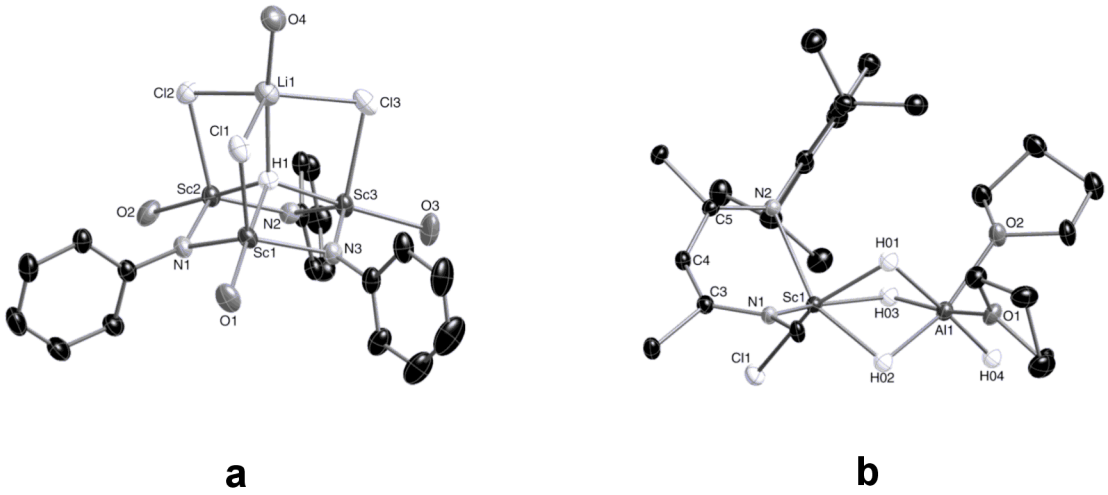

Figure 2-1. Structures of recently synthesized $[ClScNDipp(THF)]_3[LiH(THF)]$ (**a**) and DippNC(^{t}Bu)CHCH(^{t}Bu) (**b**). Reproduced with permission from ref. 15.

Since the conceptualization of 3c-2e bonds, many molecules with bridging hydrogens have been synthesized.[6,14,21-26] Like their boron counterparts, aluminum hydrides,[27-30] which have been produced in gas phase, were predicted to have bridging hydrogens (e.g. Figure 2-2, **c** and **d**).[29-32] Douberly et al.'s π-sandwiched proton between two acetylene moieties (Figure 2-2, **e**) demonstrates a remarkable viability of tetracoordinate hydrogen in gas phase despite its unfavorable thermochemical property; **e** was 74.7 kcal/mol above its global minimum isomer.[14] Strong hydrogen bond in HF_2^- can be considered as a hydrogen hypercoordination due to its unusually strong bond energy.[33-35] Hypercoordinate hydrogens in bulk phase (i.e. in solution or solid) were realized[6,17-20,36-43] in organometallic compounds (for example, $Ga_6H_6(CMe_3)_8$ (**f**),[44] $[Y(C_5Me_5)(OAr)(\mu\text{–}H)]_2$ (OAr = O-2,6-$C_6H_3{}^tBu_2$) (**g**),[45] $[(\eta_5\text{–}C_5Me_5)RuCl_2]_2$ (**h**),[46] $[Me_2Si(C_5Me_4)(\mu\text{-}PC_6H_{11})Y(\mu\text{-}H)]_4$ (**i**),[47] and $[Ag_4(\mu_4\text{-}H)(\mu_3\text{-}Ag)_4\{Se_2P(O\mathit{i}Pr)_2\}_6]^+$ (**j**),[48] and $[\{(Tp)LuH_2\}_6]$ (Tp = tris(pyrazolyl)hydroborate) (**k**)[49] in Figure 2-2). Higher hydrogen hypercoordination are

accessible by alternative strategies.[1,50] Wheatley et al. identified an octacoordinate hydrogen encapsulated by a cubic Li_8 core in $[(hpp)_6HLi_8]^+[ZnBu^t_3]^-$•0.5PhMe (hpp = 1,3,4,6,7,8-hexahydro-2H-pyrimido[1,2-*a*]pyrimidine) (Figure 2-2, **l**).[51]

Theoretical investigations of organic[52-55] and inorganic[56-58] clusters hosting hypercoordinate hydrogens are equally challenging and stimulate interesting hypercoordination strategies. Tantillo and Hoffmann's theoretical prediction of D_{3h} $C_{45}H_{23}^+$ (Figure 2-3, **m**) has two linearly-bridging hydrogens sandwiched between carbon atoms, but its two isomers with one and two classical C-H bonds were 20-30 kcal/mol lower in energy.[52] Tantillo's D_2 $C_8H_{13}^+$ example (Figure 2-3, **n**) contains a tetracoordinate hydrogen clamped between two C=C bonds, but is also much less stable than their classical counterparts.[54,55] Schleyer et al. explored the possibility of encapsulated endohedral hydrogen atom in dodecahedrane (Figure 2-3, **o**); this can be considered as hypercoordinate hydrogen with 20 coordinations![59,60] However, the exohedral C_s isomer (with a classical 2c-2e C-H bond counterpart) is more stable by 8 kcal/mol. Mebel et al's theoretical investigation of large borane clusters revealed a C_{3v} $B_{20}H_{21}^-$ global minimum containing a tricoordinate μ_3-H (Figure 2-3, **p**)[61] that is 6.6 kcal/mol more stable than the classical C_s isomer (with a vertex-bound μ_2-H). Similar face-capping μ_3-H's also have been demonstrated for alane clusters.[62,63] Hypercoordinate hydrogens in coinage metals[56,57] (e.g. Cu_3H_3 (**q**) in Figure 2-3) and titanium-doped nickel clusters,[58] ($TiNi_4H_2$ (**r**), Figure 2-3) have been demonstrated theoretically. Attempts to achieve bridging hydrogens through intramolecular hydrogen bonds also have been successful in rare occasions.[64,65]

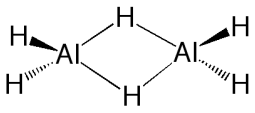

c (Al_2H_6)

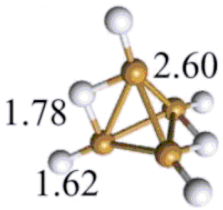

d (Al_4H_6)

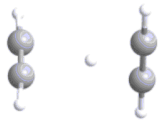

e ($C_4H_5^+$)

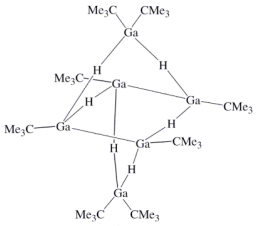

f ($Ga_6H_6(CMe_3)_8$)

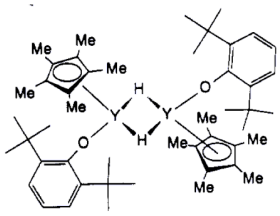

g ([Y(C_5Me_5)(OAr)(μ–H)]$_2$)

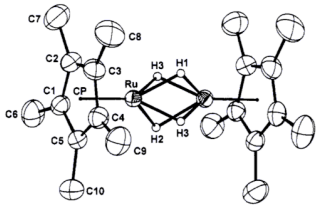

h ([(η_5–C_5Me_5)$RuCl_2$]$_2$)

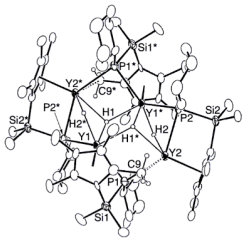

i ([$Me_2Si(C_5Me_4)(\mu$-PC_6H_{11})Y(μ-H)]$_4$)

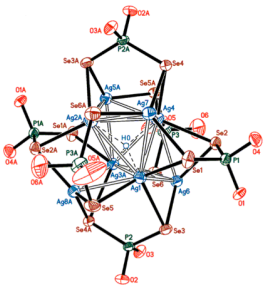

j ([$Ag_4(\mu_4$-H)(μ_3-Ag)$_4${$Se_2P(OiPr)_2$}$_6$]$^+$)

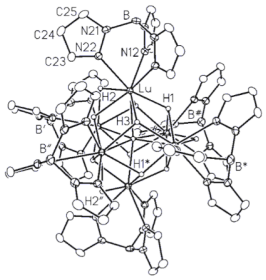

k ([{(Tp)LuH_2}$_6$])

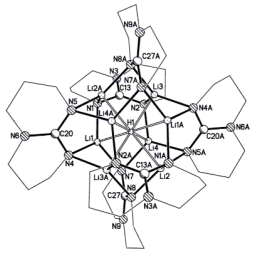

l ([(hpp)HLi]$^+$[$ZnBu^t$]$^-$ ·0.5PhMe)

Figure 2-2. Structures of experimentally realized clusters containing bridging hydrogens, Al_2H_6 (**c**), Al_4H_6 (**d**), $C_4H_5^+$ (**e**), $Ga_6H_6(CMe_3)_8$ (**f**), [Y(C_5Me_5)(OAr)(μ–H)]$_2$ (OAr = O-2,6-$C_6H_3{}^tBu_2$) (**g**), [(η_5–C_5Me_5)$RuCl_2$]$_2$ (**h**), [$Me_2Si(C_5Me_4)(\mu$-PC_6H_{11})Y(μ-H)]$_4$ (**i**), [$Ag_4(\mu_4$-H)(μ_3-Ag)$_4${$Se_2P(O^iPr)_2$}$_6$]$^+$ (**j**), [{(Tp)LuH_2}$_6$] (Tp = tris(pyrazolyl)hydroborate) (**k**), and [(hpp)$_6HLi_8$]$^+$[$ZnBut_3$]$^-$•0.5PhMe (hpp = 1,3,4,6,7,8-hexahydro-2H-pyrimido[1,2-a]pyrimidine) (**l**). Reproduced or adapted from refs. 31, 30, 14, 44, 45, 46, 47, 48, 49, and 51.

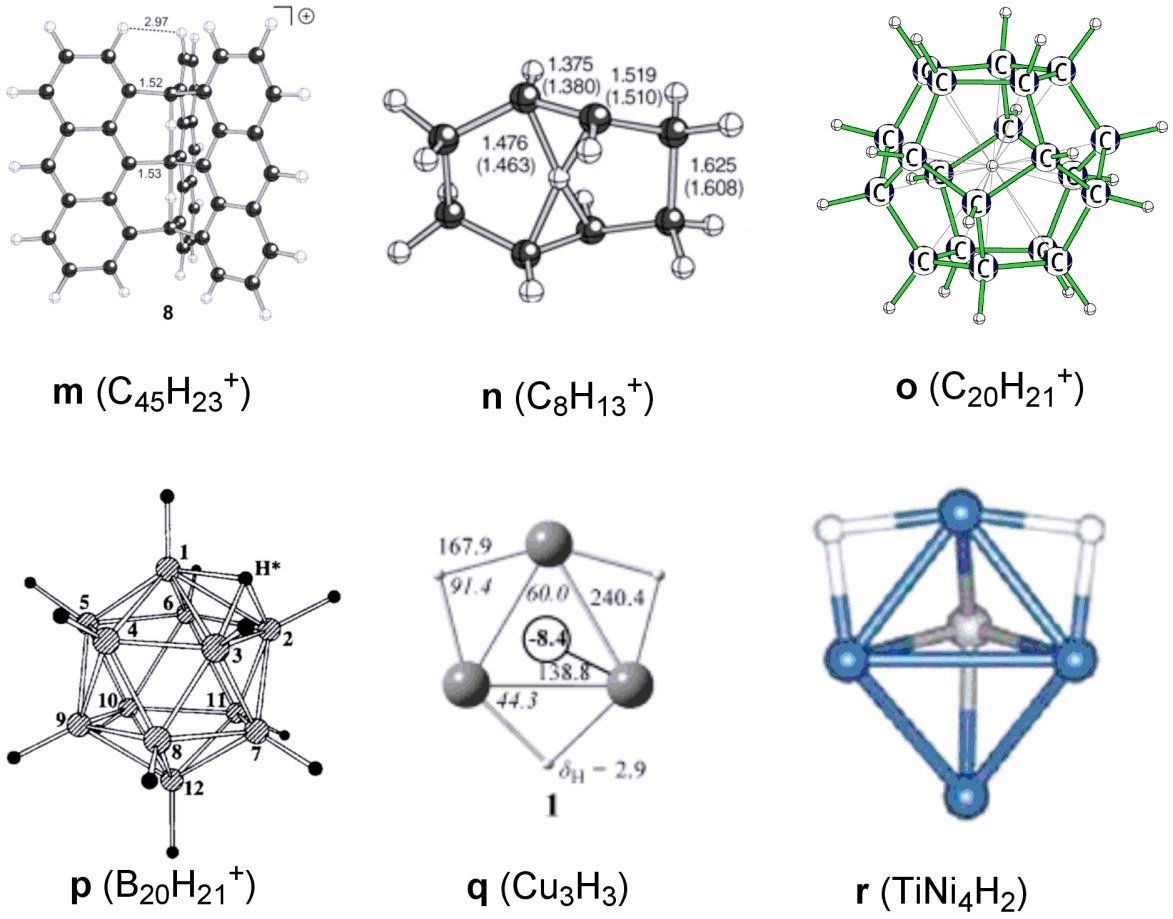

Figure 2-3. Structures of theoretically predicted clusters containing hypercoordinate hydrogens, $C_{45}H_{23}^+$ (**m**), $C_8H_{13}^+$ (**n**), $C_{20}H_{21}^+$ (**o**), $B_{20}H_{21}^-$ (**p**), Cu_3H_3 (**q**), and $TiNi_4H_2$ (**r**). Reproduced or adopted from refs. 52, 54, 60, 61, 56, and 58.

Despite prevalent experimental and theoretical examples of organic and inorganic clusters containing hydrogen hypercoordination, few provide solid rationales for their unusual bonding patterns. Gaining fundamental understanding of unusual bonding mechanisms, e.g. hydrogen hypercoordination, are important as they hold the key to opening new fields of chemistry.[66-68] The simplicity of scandium (first transition metal with only

three valence electrons) and its propensity to host hypercoordinate hydrogens makes it an attractive candidate for theoretical investigation. In this work, we propose a series of scandium hydride cluster minima containing hypercoordinate hydrogens and detailed examination of their unusual bonding.

2.3 Methods

Geometry optimizations and harmonic vibrational frequencies were computed at the M06-2X[69] DFT as implemented in NWChem[70] with the def2-TZVPP or def2-TZVP basis sets[71] obtained from the EMSL Basis set Exchange website.[72,73] The M06-2X bond distances and harmonic vibrational frequencies of ScH ($C_{\infty v}$)[74-78] and ScH_3 (D_{3h})[78,79] were more accurate than those of other DFT methods.[80] For all computations, radial and angular integration grid points were set to 100 and 1202, respectively, for hydrogen, and 160 and 1454, respectively, for scandium. Natural bond orbital (NBO),[81] natural population analysis (NPA),[82] natural steric analysis (NAS),[83-85] Wiberg bond indices (WBI)[86] were computed with the NBO 5.G program.[87] Potential energy surface scans of **1**-**7** were performed with Kick,[88-90] a stochastic search program, interfaced with Gaussian03 program.[91] Initial geometries, generated by Kick in a cell size ranging from 3.0 to 5.0 $Å^3$, were optimized at HF/STO-3G level with the Gaussian 03 program. The resulting isomers were further refined at the M06-2X/def2-TZVP level with NWChem. The electron density topologies were visualized with the MacMolPlt program[92] from the results obtained with GAMESS[93] at the M06-2X/def2-TZVPP level.

2.4 Small $Sc_2H_m^q$ Clusters

The simplest $Sc_2H_m^q$ cluster minima, D_{2h} Sc_2H_6 (**1**, local), D_{3h} $Sc_2H_5^+$ (**2**, global), D_{4h} Sc_2H_6 (**3**, global), and D_{5h} $Sc_2H_7^-$ (**4**, local) are stabilized by significant electrostatic attraction between the electronegative H's (Allred-Rochow electronegativity: 2.20) and electropositive Sc's (1.36)[16] As apparent from the valence bonding MO's of **2** (MO's 19–23, Figure 2-5), the $H^{\delta-}$-$Sc^{\delta+}$ interactions are highly polar (the majority electron density shifts towards the H's)[94] but none of the MO's show significant Sc-Sc interactions (Figure 2-5)! This is very different from boranes since their 3c-2e bonds are covalent in nature despite their electron deficient character. NPA charges reveal that the $Sc_2H_m^q$ clusters have extremely positively charged Sc's (ranging from +0.89 to +1.78 in **1** through **4**), even more so than that of ScH (Sc charge: +0.52). The terminal (classical 2c-2e bonding) and bridged (μ_2-H, non-classical 3c-2e bonding) H's have negative charges (ranging from –0.33 to –0.61 in **1** through **4**), but have rather different bonding strengths due to their difference connectivity to the Sc's.

Bridging Sc-H-Sc interactions are key to stabilizing the $Sc_2H_x^q$ clusters. The non-classical 3c-2e bonding (Sc-(μ_2-H)-Sc) offer much greater electrostatic stabilization than the terminal H's, since they have two (instead of one) adjacent Sc's. As a result, the bridging H's of **1** to **4** have greater vertical bond dissociation energies (VBDE) (78 to 91 kcal/mol, see Table 2-2) compared to the terminal H's (54 to 79 kcal/mol). The VBDE of ScH (47.9 kcal/mol) is even lower. The preference for bridging Sc-H-Sc motifs also is apparent from the 7.2 kcal/mol lower energy of the quadruply bridged **3** compared to its doubly bridged isomer, **1** (see Kick search below, and Figure 2-8). Computed Wiberg bond indices (WBI's) demonstrate convincingly that the bridged H's are *hypercoordinate* in nature. The total

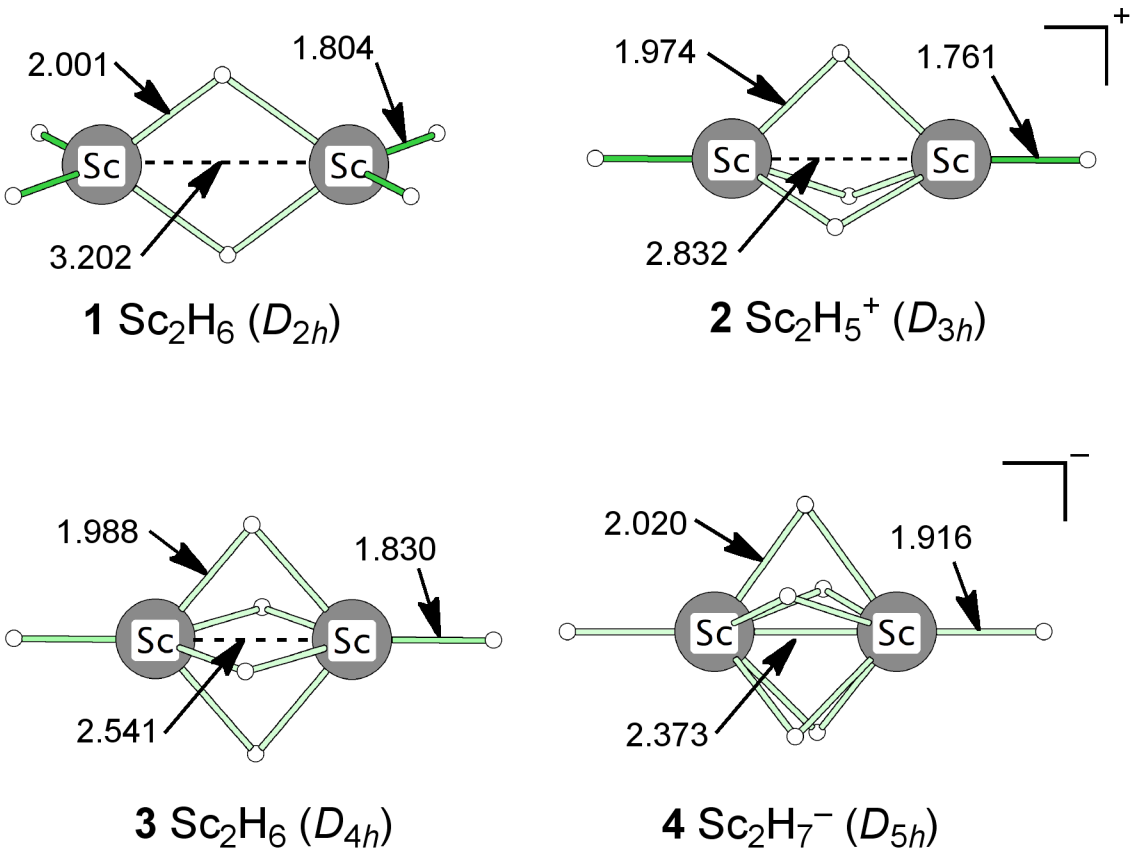

Figure 2-4. Structures and bond distances (in Å) of small scandium hydride cluster minima, **1** to **4**, computed at the M06-2X/def2-TZVPP level.

valences (the sum of all the WBI's) of the terminal (ranging from 0.71 to 0.81, Table 2) and bridged (0.63 to 0.89, Table 2-2) H's in **1** through **4** are close to the 0.76 of the H in ScH. Although the individual H-Sc WBI's of the bridging μ_2-H's (0.33 to 0.41, see Table 2-2) are rather small, the large numbers of interactions in **1** to **4** compensate for their weak interactions.

Increased numbers of bridging hydrogens in the $Sc_2H_x^q$ clusters lead to increased thermochemical stability (Figure 2-4), but such benefits are offset by increased steric repulsion ($NSA_{Tot.}$) (see Table 2-1). Shortening Sc-Sc bonds (from 3.20 Å in **1** [two μ_2-H's]

Table 2-1. Total energies ($E_{Tot.}$, in a.u.), zero point correction energies (ZPE, in kcal/mol), the lowest frequencies ($Freq_1$, in cm^{-1}), HOMO-LUMO gaps (Gap, in eV), total and individual natural steric analyses ($NSA_{Tot.}$ and $NSA_{Ind.}$, respectively, in kcal/mol)[§] and internuclear distances of adjacent bridging hydrogens (R_{H-H}, in Å) of cluster minima **1** thorough **4** and $C_{\infty v}$ ScH computed at the M06-2X/def2-TZVPP level.

	$E_{Tot.}$	ZPE	$Freq_1$	Gap	$NSA_{Tot.}$	$NSA_{Ind.}$	R_{H-H}
1	–1524.86297	22.1	241.7	6.9	17.8	7.9	2.400
2	–1524.04582	20.2	295.1	7.0	16.5	5.5	2.383
3	–1524.87561	24.0	337.6	6.8	32.8	8.2	2.163
4	–1525.47531	26.0	369.0	5.8	67.0	13.4	1.921
ScH	–761.17762	2.4	1689.5	4.5	-	-	-

§ $NSA_{Ind.}$ represents a natural steric exchange energy contribution from one Sc-(μ_2-H)-Sc bond, while $NSA_{Tot.}$ is a sum of $NSA_{Ind.}$ contributions from the Sc-(μ_2-H)-Sc bonds.

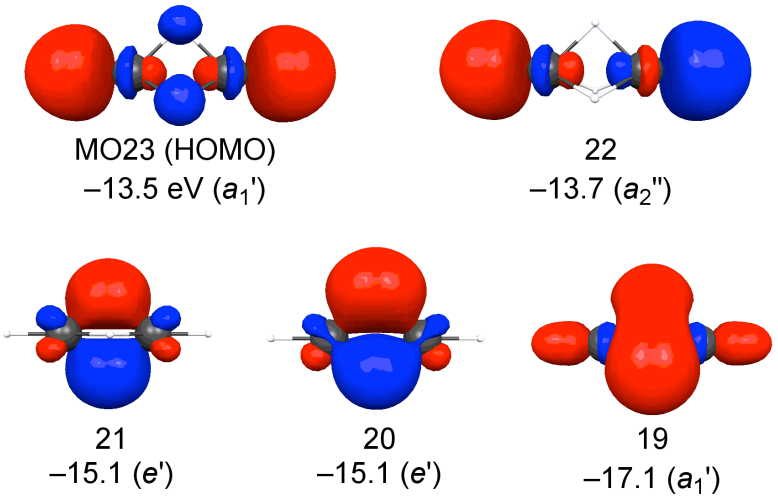

Figure 2-5. MO's of a representative cluster minimum, **2**, computed at the M06-2X/def2-TZVPP level. MO's 22 and 23 illustrate the terminal H-Sc bonds, and MO's 19-21 depict the bridging Sc-(μ_2-H)-Sc bonds.

Table 2-2. NPA charges (NPA), individual and total Wiberg Bond Indices ($WBI_{Ind.}$ and $WBI_{Tot.}$, respectively), and the vertical bond dissociation energies (VBDE, in kcal/mol) of cluster minima **1**-**4** and $C_{\infty v}$ Sc-H at the M06-2X/def2-TZVPP level.

		NPA	$WBI_{Ind.}$ (μ_n-H-Sc)	$WBI_{Tot.}$	VBDE
1	Sc	1.66	-	2.12	-
	μ_1-H	–0.53	0.59	0.72	69.8
	μ_2-H	–0.61	0.37	0.63	90.0
2	Sc	1.78	-	1.91	-
	μ_1-H	–0.45	0.73	0.81	54.1
	μ_2-H	–0.56	0.33	0.70	84.8
3	Sc	1.38	-	2.63	-
	μ_1-H	–0.49	0.69	0.76	73
	μ_2-H	–0.44	0.38	0.81	77.6
4	Sc	0.89	-	3.48	-
	μ_1-H	–0.54	0.63	0.71	78.8
	μ_2-H	–0.33	0.41	0.89	91.2
ScH	Sc	0.52	0.76	0.76	-
	μ_1-H	–0.52	0.76	0.76	47.9

to 2.37 Å in **4** [five μ_2-H's]), as well as increasing lowest vibrational frequencies (from 241.7 cm^{-1} in **1** to 369.0 cm^{-1} in **4**) documents the accumulating thermochemical stability due to the increasing number of bridging hydrogens. The increased steric repulsion, arises from greater numbers of adjacent bridging H's (one in **1** to five in **4**) and larger individual steric interactions ($NSA_{Ind.}$, Table 2-1), as a result of shorter internuclear distances ($R_{H\text{-}H}$, see Table 2-1). For this reason, the steric repulsion also increases as the number of bridging hydrogens increases; **4** displays significantly greater steric repulsion (**4**: 67 kcal/mol), when compared to **1** (17.8 kcal/mol). The Sc-(μ_2-H)$_3$-Sc moiety, e.g. in **2**, demonstrates an optimal balance for stabilizing Sc-H-Sc bonding interactions and destabilizing H···H steric repulsion. The Kick searches of **3** and **4** support the bridging hydrogen steric repulsion discussed in the NSA (see Structures section), and reveal that double (Sc-(μ_2-H)$_2$-Sc), triple (Sc-(μ_2-H)$_3$-Sc),

and quadruple bridge (Sc-(μ_2-H)$_4$-Sc) cluster cores are thermodynamically preferred over isomers with quintuple (Sc-(μ_2-H)$_5$-Sc) bridges. For example, Sc_2H_6 minima, **3**, **1**, and **3a**, are relatively close in energy to each other (see Figure 2-8). On the other hand, $Sc_2H_7^-$ minima (**4a**-**4c**), which contain the triple bridging motif, are more stable than **4** (with the quintuple bridge core) by as much as 39.3 kcal/mol! The above Kick search results demonstrate the basis for the successful use of double and triple bridge cluster core as building blocks.

2.5 Medium and Large Size Cluster Design Strategy

Medium (**5** to **8**) and large (**10** to **12**) size clusters can be designed based on a bottom-up building strategy (see below), involving favorable hypercoordinate hydrogen motifs, in combination with a simple electron counting guideline. The number of valence electrons involved in each of the Sc_nH_m clusters is key to maximizing their electrostatic attraction. This can be realized by considering formal negative charges for each of the H^-'s (two valence electrons) and positive charges for each of the Sc^{3+}'s (zero valence electrons), as expected by the ionic Lewis structures of the particular Sc_nH_m cluster (see, for example, **2** in Figure 2-6). On this basis, the optimal number of valence electrons for a given stoichiometry should equal twice the number of hydrogen atoms. For instance, the 11 valence electrons of neutral Sc_2H_5 are one too many. Instead, $Sc_2H_5^+$ (**2**, 2×5[H] = 10) is more favorable since it benefits from maximal electrostatic attraction between the H's and Sc's.

Successful applications of this cluster design strategy, by combinations of the Sc-(μ_2-H)$_2$-Sc and Sc-(μ_2-H)$_3$-Sc moieties of **1** and **2**, predicted various medium size cluster

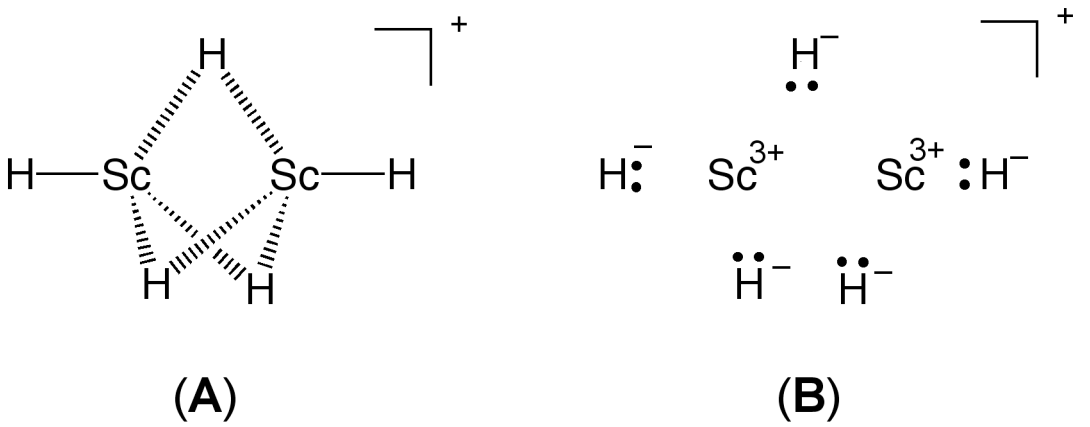

Figure 2-6. Covalent (**A**) and (**B**) ionic structure representations of the scandium hydride cluster cation, **2**. Dashed lines in (**A**) represent "partial" (i.e., "delocalized") bonds utilizing fewer than two bonding electrons.

minima (**5** to **8**) containing hydrogens with coordinations up to six (see Figure 2-7)! The three-membered ring $Sc_3H_8^+$ (**5**, D_{3h}) contains two face-capping hydrogens (μ_3-H's) above and below the Sc_3 framework. Both $Sc_4H_{11}^+$ (**6**, T_d) and $Sc_4H_{13}^-$ (**7**, D_{4h}) have encapsulated tetrahedral (μ_4-H_T) and square planar hydrogens (μ_4-H_{SP}), respectively. The central hydrogen of $Sc_6H_{15}^{3+}$ (**8**, O_h) reveals remarkable hexacoordination. Fragments of medium sized clusters (**5** to **8**) also can be used to design larger scandium hydride clusters (**10** to **12**). For example, D_{3h} $Sc_5H_{16}^-$ (**10**, see Figure 2-9**)** is conceived from the cluster **5** sandwiched between two fragments of **6**. D_{4h} $Sc_8H_{21}^{3+}$ (**11**, Figure 2-9**)** contains four units of **5** joined to the central square unit of **7**. O_h $Sc_8H_{26}^{2-}$ (**12**, Figure 2-9) is comprised of six clusters of **7** as faces of a cube. All of these species (**5** to **12**) are local minima, have appreciable lowest vibrational frequencies, as well as large HOMO-LUMO gaps, which suggest thermochemical stability (see Table 2-3 and Table 2-5). Like the smaller size clusters (**1** to **4**), **5** to **8** also display greater preference for hypercoordinate hydrogens, as documented

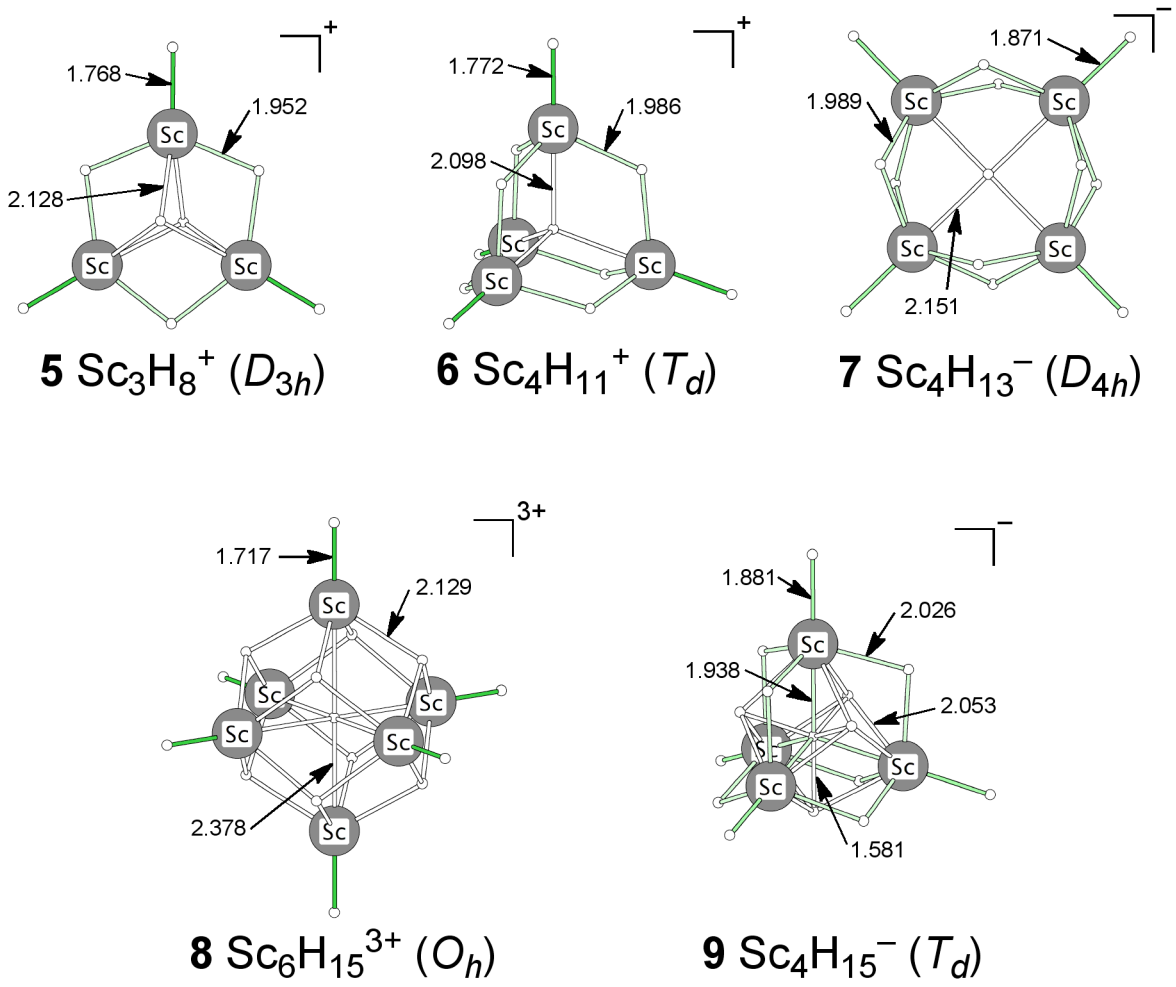

Figure 2-7. Structures and bond distances (in Å) of medium-sized scandium hydride cluster minima, **5** to **9**, computed at M06-2X/def2-TZVPP.

by their large VBDE's (ranging from 74.2 to 89.1 kcal/mol) compared to those of the terminal hydrogens (ranging from 33.4 to 87.7 kcal/mol). Although each of the individual hypercoordinate H-Sc interactions is weak, the collective $(\mu_n\text{-H})\text{-}(Sc)_n$ bonding is rather strong, due to large numbers of such interactions. Note that the $(\mu_n\text{-H})$-Sc distances in clusters **5** through **8** become longer as the hydrogen coordination increase from one to six (the corresponding individual WBI's decrease reciprocally), but the total valence of the

Table 2-3. Total energies ($E_{Tot.}$, in a.u.), zero point correction energies (ZPE, in kcal/mol), the lowest frequencies ($Freq_1$, in cm^{-1}), and HOMO-LUMO gaps (Gap, in eV) of cluster minima **5** thorough **9**, computed at the M06-2X/def2-TZVPP level.

	$E_{Tot.}$	ZPE	$Freq_1$	Gap
5	–2286.55889	33.1	240.9	6.5
6	–3049.04127	42.6	97.8	5.9
7	–3050.60913	54.1	76.2	6.9
8	–4571.97609	65.7	142.3	5.3
9	–3051.71485	62.7	143.3	7.0

Table 2-4. NPA charges (NPA), individual and total Wiberg Bond Indices ($WBI_{Ind.}$ and $WBI_{Tot.}$, respectively), and the vertical bond dissociation energies (VBDE, in kcal/mol) of cluster minima **5** through **9** at the M06-2X/def2-TZVPP level.

		NPA	$WBI_{Ind.}$ (μ_n-H-Sc)	$WBI_{Tot.}$	VBDE
5	Sc	1.65	-	2.12	-
	μ_1-H	–0.44	0.74	0.82	54.9
	μ_2-H	–0.52	0.36	0.74	85.3
	μ_3-H	–0.53	0.21	0.73	89.1
6	Sc	1.71	-	2.06	-
	μ_1-H	–0.46	0.73	0.8	67.2
	μ_2-H	–0.56	0.33	0.68	86.4
	μ_4-H	–0.61	0.13	0.73	81.4
7	Sc	1.39	-	2.59	-
	μ_1-H	–0.53	0.65	0.72	87.7
	μ_2-H	–0.49	0.36	0.76	86.6
	μ_4-H	–0.48	0.16	0.83	85.1
8	Sc	1.65	-	2.15	-
	μ_1-H	–0.35	0.82	0.89	33.4
	μ_3-H	–0.53	0.23	0.72	91.8
	μ_6-H	–0.51	0.10	0.76	74.2
9	Sc	0.90	-	3.33	-
	μ_1-H	–0.49	0.68	0.77	81.2
	μ_2-H	–0.35	0.38	0.88	77.1
	μ_4-H	–0.14	0.23	0.99	68.2
	μ_8-H	0.01	0.13	1.06	70.9
			(μ_4-H-μ_8-H) 0.13		

various hydrogens remains somewhat similar to that of ScH (0.76) regardless of their coordination numbers. The highly positive VBDE's of the tetra- and hexacoordinate hydrogens in **6** and **8** further rules out the possibility of the central hydrogens being a mere entrapment inside the cages (without any bonding interactions to the cages).

$Sc_4H_{15}^-$ (**9**, local T_d minima, see Figure 6) is an exception to the electron counting guideline, as the expected $Sc_4H_{15}^{3-}$ suffers from unfavorable electrostatic repulsion between the central hydrogen and four proximal face-capping hydrogens. $Sc_4H_{15}^{3-}$ has three degenerate imaginary frequencies due to a Jahn-Teller distortion (only one of the triply degenerate HOMO's is fully occupied). Removal of two electrons from the central hydrogen eliminates the undesirable electrostatic repulsion and facilitates covalent bonding between the octacoordinate central hydrogen (μ_8-H) and the surrounding four face-capping hydrogens (μ_4-H's). The covalent nature of the (μ_8-H)-(μ_4-H) bonds is confirmed by the hydrogen NPA charges: the negative partial charge of the μ_4-H's are greatly reduced (–0.14, see Table 2-4) compared to other face-capping hydrogens in **5** or **8** (both are –0.53) while the NPA partial charge on μ_8-H is essentially zero (0.01). The individual WBI's of (μ_8-H)-(μ_4-H) also are surprisingly large (0.13, see Table 2-4) despite the long 1.581 Å internuclear distance.

2.6 Chemical Viability and Generalization

Applications of "Kick," a stochastic search method, identified **2**, **3**, **4a**, **5**, **6a** and **7** as global minima (see Figure 2-8), and, hence, potential candidates for experimental realization in the gas phase (e.g. by a laser ablation). Notably, the only structural differences between the **2** (D_{3h}) and **5** (D_{3h}) global minima and their second lowest isomers **2a** (C_s) and **5a** (C_s),

respectively, are their terminal hydrogens positions; **2a** and **5a** have bent terminal H's (see Figure 2-8). Therefore, if $Sc_2H_5^+$ (**2** and **2a**) or $Sc_3H_8^+$ (**5** and **5a**) are experimentally produced and identified (e.g. via IR spectroscopy), these isomers might be vibrationally averaged. The energy of D_{4h} **7** also is close to its second lowest isomer, **7a** (C_{2v}), but the two structures are distinctly different. Despite their higher symmetry, **4** (D_{5h}) and **6** (T_d) are only local minima, 39.3 kcal/mol and 29.0 kcal/mol higher in energy than the global minima, **4a** (C_{2v}) and **6a** (C_s), respectively. Although its experimental realization of **6a**'s is not likely as a consequence, its quasi-tetrahedral tetracoordinate hydrogen atom at the center is intrigueing.[95]

Replacing the terminal hydrogens of selected scandium hydride clusters by suitable organic substituents offer further opportunities for bulk phase realization of organoscandium hydrides. For example, substituting the terminal hydrogens in 2 and 7 by methyl groups result in two D_{3h} minima (13a and 13b, see Figure 2-10) and C_4 $Sc_4H_9(CH_3)_4^-$ (14, see Figure 2-10), but does not disrupt the hydrogen hypercoordination. Although

Table 2-5. Total energies ($E_{Tot.}$, in a.u.), zero point correction energies (ZPE, in kcal/mol), the lowest frequencies ($Freq_1$, in cm^{-1}), and HOMO-LUMO gaps (Gap, in eV) of clusters **10** thorough **14**, computed at the M06-2X/TZVP level.

	$E_{Tot.}$	ZPE	$Freq_1$	Gap
10	–3813.09320	67.9	140.7	6.3
11	–6097.16270	95.2	49.6	6.3
12	–6101.24650	112.4	79.7	6.7
13a	–1602.70587	56.1	91.4	6.9
13b	–1602.70520	56.0	94.0	6.9
14	–3207.89232	125.8	25.6	6.7

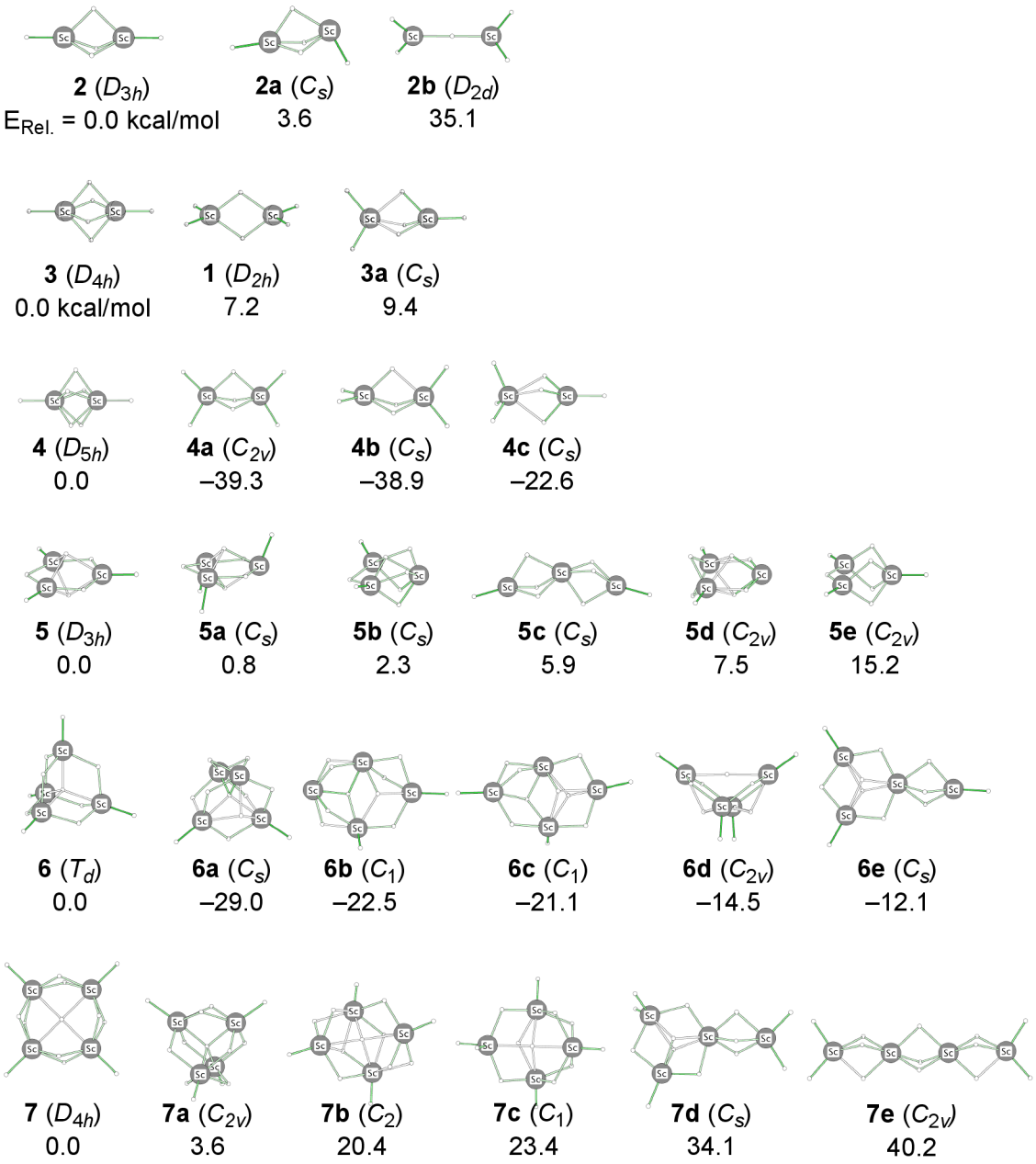

Figure 2-8. Isomers of **2**, **4**, **5**, **6**, and **7,** and their relative energies with respect to the proposed clusters, computed at M06-2X/def2-TZVP. All structures are minima, and relative energies include zero-point corrections.

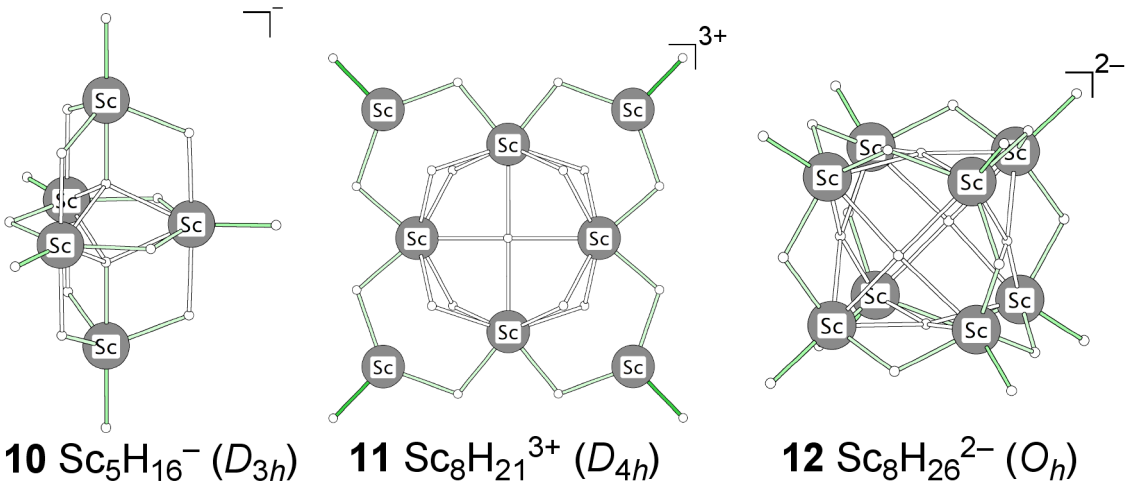

Figure 2-9. Structures of large scandium hydride cluster minima, **10** to **12**, computed at M06-2X/def2-TZVP.

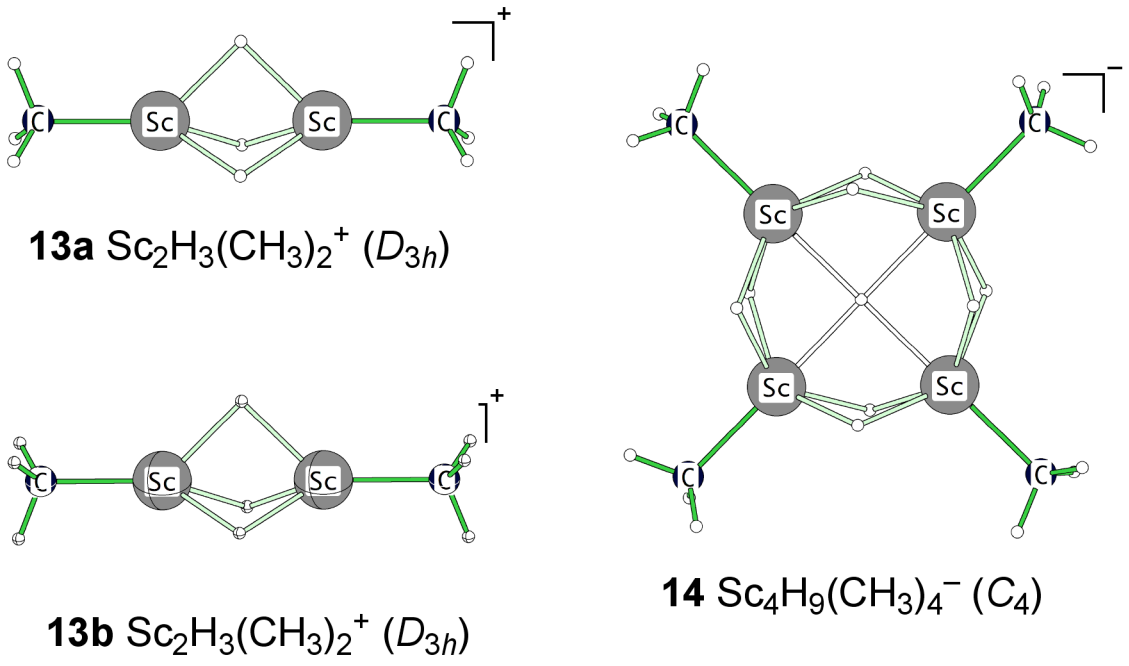

Figure 2-10. Structures of methyl-group grafted scandium hydride cluster minima, **13** to **15**, at M06-2X/def2-TZVP.

organoscandium molecules containing hypercoordinate hydrogens have been synthesized previously,[15] such examples are still rare. Our findings encourage synthetic attempts for "in solution" procedures.

2.7 Conclusions

Our theoretical investigation identified 14 scandium hydride cluster minima with unusual hypercoordinate hydrogen structural features. The proclivity of scandium hydride clusters to form hypercoordinate hydrogens originates from their tendency to maximize thermodynamic stability. Hypercoordinate Sc-(μ_n-H)-Sc bonds are significantly stronger than the terminal H-Sc interactions due to greater electrostatic attraction and large numbers of Sc-(μ_n-H)-Sc interactions. Our proposed design strategy can be employed to conceive larger scandium hydride clusters (by bottom-up building) and encourages attempts at bulk phase realization of organoscandium hydrides (via grafting strategies). Their high H/Sc ratios make the proposed clusters attractive candidates as hydrogen storage media. In view of the recent synthetic success of organoscandium clusters,[96-103] our theoretical prediction promotes experimental attempts to produce such unusual and beautiful molecules in gas and condensed phases. Scandium clusters containing other electronegative elements (e.g. halides) also offer exciting prospects for hypercoordinate chemistry.[3,39,104-106]

Acknowledgement

This work was supported by NSF Grant CHE-0716718.

2.8 References and Notes

(1) Haywood, J.; Wheatley, A. E. H. *Dalton Trans.* **2008**, 3378–3397.

(2) Hou, Z.; Nishiura, M.; Shima, T. *Eur. J. Inorg. Chem.* **2007**, 2535–2545.

(3) Arndt, S.; Okuda, J. *Chem. Rev.* **2002**, *102*, 1953–1976.

(4) Zeimentz, P. M.; Arndt, S.; Elvidge, B. R.; Okuda, J. *Chem. Rev.* **2006**, *106*, 2404–2433.

(5) Konkol, M.; Okuda, J. *Coord. Chem. Rev.* **2008**, *252*, 1577–1591.

(6) Marks, T. J.; Kolb, J. R. *Chem. Rev.* **1977**, *77*, 263–2293.

(7) Dilthey, W. *Z. Angew. Chem.* **1921**, *34*, 596.

(8) For a concise historical overview of diborane, see Laszlo, P (2000) Angew. Chem. Int. Ed. 39: 2071–2072.

(9) Longuet-Higgins, H. C. *J. Chim. Phys.* **1949**, *46*, 275.

(10) Pitzer, K. S. *J. Am. Chem. Soc.* **1945**, *67*, 1126–1132.

(11) Lipscomb, W. N. *J. Chem. Phys.* **1954**, *22*, 985–988.

(12) Lipscomb, W. N. *Acc. Chem. Res.* **1973**, *6*, 257–262.

(13) Lipscomb, W. N. *Science* **1977**, *196*, 1047–1055.

(14) Douberly, G. E.; Ricks, A. M.; Ticknor, B. W.; McKee, W. C.; Schleyer, P. v. R.; Duncan, M. A. *J. Phys. Chem. A* **2008**, *112*, 1897–1906.

(15) Conroy, K. D.; Piers, W. E.; Parvez, M. *Organometallics* **2009**, *28*, 6228–6233.

(16) Allred, A. L.; Rochow, E. G. *J. Inorg. Nucl. Chem.* **1958**, *5*, 264–268.

(17) Venanzi, L. M. *Coord. Chem. Rev.* **1982**, *43*, 251–274.

(18) Bau, R.; Drabnis, M. H. *Inorg. Chim. Acta* **1997**, *259*, 27–50.

(19) Ephritikhine, M. *Chem. Rev.* **1997**, *97*, 2193–2242.

(20) Suzuki, H. *Eur. J. Inorg. Chem.* **2002**, 1009–1023.

(21) Downs, A. J.; Goode, M. J.; Pulham, C. R. *J. Am. Chem. Soc.* **1989**, *111*, 1936–1937.

(22) Pulham, C. R.; Brian, P. T.; Downs, A. J.; Rankin, D. W. H.; Robertson, H. E. *J. Chem. Soc. Chem. Commun.* **1990**, 177–178.

(23) Kirchen, R. P.; Sorensen, T. S.; Wagstaff, K. *J. Am. Chem. Soc.* **1978**, *100*, 6761–6763.

(24) Kirchen, R. P.; Okazawa, N.; Ranganayakulu, K.; Rauk, A.; Sorensen, T. S. *J. Am. Chem. Soc.* **1981**, *103*, 597–604.

(25) Douberly, G. E.; Ricks, A. M.; Ticknor, B. W.; Schleyer, P. v. R.; Duncan, M. A. *J. Am. Chem. Soc.* **2007**, *129*, 13782–13783.

(26) Douberly, G. E.; Ricks, A. M.; Schleyer, P. v. R.; Duncan, M. A. *J. Chem. Phys.* **2008**, *128*, 021102-021101–021102-021104.

(27) Hara, M.; Domen, K.; Onishi, T.; Nozoye, H. *J. Phys. Chem.* **1991**, *95*, 6–7.

(28) Breisacher, P.; Siegel, B. *J. Am. Chem. Soc.* **1964**, *86*, 5053–5054.

(29) Li, X.; Grubisic, A.; Stokes, S. T.; Cordes, J.; Ganteför, G. F.; Bowen, K. H.; Kiran, B.; Willis, M.; Jena, P.; Burgert, R.; Schnöckel, H. *Science* **2007**, *315*, 356–358.

(30) Roach, P. J.; Reber, A. C.; Woodward, W. H.; Khanna, S. N.; Castleman, A. W., Jr. *Proc. Nat. Acad. Sci.* **2007**, *104*, 14565–14569.

(31) McKee, M. L. *J. Phys. Chem.* **1991**, *95*, 6519–6525.

(32) Rao, B. K.; Jena, P.; Burkart, S.; Ganteför, G.; Seifert, G. *Phys. Rev. Lett.* **2001**, *86*, 692–695.

(33) Emsley, J. *Chem. Soc. Rev.* **1980**, *9*, 91-124.

(34) Wenthold, P. G.; Squires, R. R. *J. Phys. Chem.* **1995**, *99*, 2002–2005.

(35) Davidson, E. R. *Int. J. Quant. Chem.* **2004**, *98*, 317–324.

(36) Evans, W. J.; Meadowns, J. H.; Wayda, A. L.; Hunter, W. E.; Atwood, J. L. *J. Am. Chem. Soc.* **1982**, *104*, 2008–2014.

(37) Kretschmer, W. P.; Troyanov, S. I.; Meetsma, A.; Hessen, B.; Teuben, J. H. *Organometallics* **1998**, *17*, 284–286.

(38) Tardif, O.; Nishiura, M.; Hou, Z. *Organometallics* **2003**, *22*, 1171–1173.

(39) Kirillov, E.; Lehmann, C. W.; Razavi, A.; Carpentier, J.-F. *Organometallics* **2004**, *23*, 2768–2777.

(40) Cui, D.; Tardif, O.; Hou, Z. *J. Am. Chem. Soc.* **2004**, *126*, 1312–1313.

(41) Li, X.; Baldamus, J.; Nishiura, M.; Tardif, O.; Hou, Z. *Angew. Chem. Int. Ed* **2006**, *45*, 8184–8188.

(42) Yousufuddin, M.; Gutmann, M. J.; Baldamus, J.; Tardif, O.; Hou, Z.; Mason, S. A.; McIntyre, G.; Bau, R. *J. Am. Chem. Soc.* **2008**, *130*, 3888–3891.

(43) Shima, T.; Hou, Z. *Organometallics* **2009**, *28*, 2244–2252.

(44) Uhl, W.; Cuypers, L.; Geiseler, G.; Harms, K.; Neumüller, B. *J. Chem. Soc., Dalton Trans.* **2001**, 2398–2400.

(45) Schaverien, C. J. *Organometallics* **1994**, *13*, 69–82.

(46) Suzuki, H.; Omori, H.; Lee, D. H.; Yoshida, Y.; Fukuishima, M.; Tanaka, M.; Moro-oka, Y. *Organometallics* **1994**, *13*, 1129–1146.

(47) Tardif, O.; Nishiura, M.; Hou, Z. *Tetrahedron* **2003**, *59*, 10525–10539.

(48) Liu, C. W.; Chang, H.-W.; Sarkar, B.; Saillard, J.-Y.; Kahlal, S.; Wu, Y.-Y. *Inorg. Chem.* **2010**, *49*, 468–475.

(49) Cheng, J.; Saliu, K.; Kiel, G. Y.; Ferguson, M. J.; McDonald, R.; Takats, J. *Angew. Chem. Int. Ed* **2008**, *47*, 4910–4913.

(50) Armstrong, D. R.; Clegg, W.; Davies, R. P.; Liddle, S. T.; Linton, D. J.; Raithby, P. R.; Snaith, R.; Wheatley, A. E. H. *Angew. Chem. Int. Ed* **1999**, *38*, 3367–3370.

(51) Boss, S. R.; Coles, M. P.; Eyre-Brook, V.; García, F.; Haigh, R.; Hitchcock, P. B.; McPartlin, M.; Morey, J. V.; Naka, H.; Raithby, P. R.; Sparkes, H.; Tate, C. W.; Wheatley, A. E. H. *Dalton Trans.* **2006**, 5574–5582.

(52) Tantillo, D. J.; Hoffmann, R. *J. Am. Chem. Soc.* **2003**, *125*, 4042–4043.

(53) Ponec, R.; Yuzhakov, G.; Tantillo, D. J. *J. Org. Chem.* **2004**, *69*, 2992–2996.

(54) Gutta, P.; Tantillo, D. J. *Angew. Chem.* **2005**, *117*, 2779–2783.

(55) Ponec, R.; Bultinck, P.; Gutta, P.; Tantillo, D. J. *J. Phys. Chem. A* **2006**, *110*, 3785–3789.

(56) Tsipis, A. C.; Tsipis, C. A. *J. Am. Chem. Soc.* **2003**, *125*, 1136–1137.

(57) Tsipis, A. C. *Organometallics* **2010**, *29*, 354–363.

(58) Venkataramanan, N. S.; Sahara, R.; Mizuseki, H.; Kawazoe, Y. *J. Phys. Chem. A* **2010**, *114*, 5049–5057.

(59) Moran, D.; Stahl, F.; Jemmis, E. D.; Schaefer, H. F., III; Schleyer, P. v. R. *J. Phys. Chem. A* **2002**, *106*, 5144–5154.

(60) Chen, Z.; Jiao, H.; Moran, D.; Hirsch, A.; Thiel, W.; Schleyer, P. v. R. *J. Phys. Chem. A* **2003**, *107*, 2075–2079.

(61) Mebel, A. M.; Najafian, K.; Charkin, O. P.; Schleyer, P. v. R. *J. Mol. Struct. THEOCHEM* **1999**, *461–462*, 187–202.

(62) Grubisic, A.; Li, X.; Stokes, S. T.; Cordes, J.; Ganteför, G. F.; Bowen, K. H.; Kiran, B.; Jena, P.; Burgert, R.; Schnöckel, H. *J. Am. Chem. Soc.* **2007**, *129*, 5969–5975.

(63) Fu, L.-J.; Jin, L.; Shao, C.-B.; Ding, Y.-H. *Inorg. Chem.* **2010**, *49*, 5276–5284.

(64) Reppé, A. K.; Bernstein, E. R. *J. Phys. Chem. A* **2000**, *104*, 6117–6128.

(65) Hargis, J. C.; Evangelista, F. A.; Ingels, J. B.; Schaefer, H. F., III *J. Am. Chem. Soc.* **2008**, *130*, 17471-17478.

(66) Williams, R. E. *Chem. Rev.* **1992**, *92*, 177–207.

(67) Fehlner, T. P. *Organometallics* **2000**, *19*, 2643–2651.

(68) Hosmane, N. S.; Maguire, J. A. *Eur. J. Inorg. Chem.* **2003**, 3989–3999.

(69) Zhao, Y.; Truhlar, D. G. *J. Chem. Phys.* **2006**, *125*, 194101.

(70) Bylaska, E. J.; de Jong, W. A.; Govind, N.; Kowalski, K.; Straatsma, T. P.; Valiev, M.; Wang, D.; Apra, E.; Windus, T. L.; Hammond, J.; Nichols, P.; Hirata, S.; Hackler, M. T.; Zhao, Y.; Fan, P.-D.; Harrison, R. J.; Dupuis, M.; Smith, D. M. A.; Nieplocha, J.; Tipparaju, V.; Krishnan, M.; Vazquez-Mayagoitia, A.; Wu, Q.; Van Voorhis, T.; Auer, A. A.; Nooijen, M.; Crosby, L. D.; Brown, E.; Cisneros, G.; Fann, G. I.; Fruchtl, H.; Garza, J.; Hirao, K.; Kendall, R.; Nichols, J. A.; Tsemekhman, K.; Wolinski, K.; Anchell, J.; Bernholdt, D.; Borowski, P.; Clark, T.; Clerc, D.; Dachsel, H.; Deegan, M.; Dyall, K.; Elwood, D.; Glendening, E.; Gutowski, M.; Hess, A.; Jaffe, J.; Johnson, B.; Ju, J.; Kobayashi, R.; Kutteh, R.; Lin, Z.; Littlefield, R.; Long, X.; Meng, B.; Nakajima, T.; Niu, S.; Pollack, L.; Rosing, M.; Sandrone, G.; Stave, M.; Taylor, H.; Thomas, G.; van Lenthe, J.; Wong, A.; Zhang, Z.; 5.1.1 ed.; Pacific Northwest National Laboratory, Richland, Washington 99352, USA: 2009.

(71) Weigend, F.; Ahlrichs, R. *Phys. Chem. Chem. Phys.* **2005**, *7*, 3297–3305.

(72) Feller, D. *J. Comput. Chem.* **1996**, *17*, 1571–1586.

(73) Schuchardt, K. L.; Didier, B. T.; Elsethagen, T.; Sun, L.; Gurumoorthi, V.; Chase, J.; Li, J.; Windus, T. L. *J. Chem. Inf. Model.* **2007**, *47*, 1045–1052.

(74) Ram, R. S.; Bernath, P. F. *J. Chem. Phys.* **1996**, *105*, 2668–2674.

(75) Ram, R. S.; Bernath, P. F. *J. Mol. Spectrosc.* **1997**, *183*, 263–272.

(76) Barone, V.; Adamo, C. *Int. J. Quant. Chem.* **1997**, *61*, 443–451.

(77) Wilson, D. J. D.; Marsden, C. J.; von Nagy-Felsobuki, E. I. *Phys. Chem. Chem. Phys.* **2003**, *5*, 252–258.

(78) Wang, X.; Chertihin, G.; Andrews, L. *J. Phys. Chem. A* **2002**, *106*, 9213–9225.

(79) Balabanov, N. B.; Boggs, J. E. *J. Phys. Chem. A* **2000**, *104*, 1597–1601.

(80) Other DFT methods include B3LYP, BP86., PBE, M05, M05-2X, M06, and B2PLYP.

(81) Foster, J. P.; Weinhold, F. *J. Am. Chem. Soc.* **1980**, *102*, 7211–7218.

(82) Reed, A. E.; Weinstock, R. B.; Weinhold, F. *J. Chem. Phys.* **1985**, *83*, 735–746.

(83) Badenhoop, J. K.; Wieinhold, F. *J. Chem. Phys.* **1997**, *107*, 5406–5421.

(84) Badenhoop, J. K.; Weinhold, F. *J. Chem. Phys.* **1997**, *107*, 5422–5432.

(85) Badenhoop, J. K.; Weinhold, F. *Int. J. Quantum Chem.* **1999**, *72*, 269–280.

(86) Wiberg, K. B. *Tetrahedron* **1968**, *24*, 1083–1096.

(87) Glendening, E. D.; Badenhoop, J. K.; Reed, A. E.; Carpenter, J. E.; Bohmann, J. A.; Morales, C. M.; Weinhold, F.; 5.G ed.; University of Wisconsin: Madison, WI, 2001.

(88) Saunders, M. *J. Am. Chem. Soc.* **1987**, *109*, 3150–3152.

(89) Bera, P. P.; Sattelmeyer, K. W.; Saunders, M.; Schaefer, H. F. I.; Schleyer, P. v. R. *J. Phys. Chem. A* **2006**, *110*, 4287–4290.

(90) Total number of Kick jobs were varied as follows: 3000 jobs for **2**, 3000 for **3**, 3500 for **4**, 4500 for **5**, 6500 for **6**, and 11500 for **7**. Kick search for **6** and **7** proved difficult due to their large molecule sizes. Because of the complexities, the proposed structures, T_d **6** and D_{4h} **7**, were not located by kick jobs. Furthermore, in many of initial kick results for **6** and **7**, a molecular hydrogen (H_2) separated away from the remainder of the clusters and formed $Sc_mH_{n-2}^X + H_2$ instead of $Sc_mH_n^X$. In such cases, the drifting hydrogen molecule was reattached to the cluster manually. Such a modification may result in the bias in stochastic method. Nevertheless, this biased kick search successfully located many isomers of **6** (**6a**-**6e**), all of which are much lower in energy compared to the proposed T_d structure. This demonstrates the efficacy of the biased method.

(91) Frisch, M. J.; Trucks, G. W.; Schlegel, H. B.; Scuseria, G. E.; Robb, M. A.; Cheeseman, J. R.; Montgomery, J., J. A.; Vreven, T.; Kudin, K. N.; Burant, J. C.; Millam, J. M.; Iyengar, S. S.; Tomasi, J.; Barone, V.; Mennucci, B.; Cossi, M.; Scalmani, G.; Rega, N.; Petersson, G. A.; Nakatsuji, H.; Hada, M.; Ehara, M.; Toyota, K.; Fukuda, R.; Hasegawa, J.; Ishida, M.; Nakajima, T.; Honda, Y.; Kitao, O.; Nakai, H.; Klene, M.; Li, X.; Knox, J. E.; Hratchian, H. P.; Cross, J. B.; Adamo, C.; Jaramillo, J.; Gomperts, R.; Stratmann, R. E.; Yazyev, O.; Austin, A. J.; Cammi, R.; Pomelli, C.; Ochterski, J. W.; Ayala, P. Y.; Morokuma, K.; Voth, G. A.; Salvador, P.; Dannenberg, J. J.; Zakrzewski, V. G.; Dapprich, S.; Daniels, A. D.; Strain, M. C.; Farkas, O.; Malick, D. K.; Rabuck, A. D.; Raghavachari, K.;

Foresman, J. B.; Ortiz, J. V.; Cui, Q.; Baboul, A. G.; Clifford, S.; Cioslowski, J.; Stefanov, B. B.; Liu, G.; Liashenko, A.; Piskorz, P.; Komaromi, I.; Martin, R. L.; Fox, D. J.; Keith, T.; Al-Laham, M. A.; Peng, C. Y.; Nanayakkara, A.; Challacombe, M.; Gill, P. M. W.; Johnson, B.; Chen, W.; Wong, M. W.; Gonzalez, C.; Pople, J. A.; Gaussian, Inc.: Wallingford, CT., 2004.

(92) Bode, B. M.; Gordon, M. S. *J. Mol. Graphics and Modeling* **1998**, *16*, 133–138.

(93) Schmidt, M. W.; Baldridge, K. K.; Boatz, J. A.; Elbert, S. T.; Gordon, M. S.; Jensen, J. J.; Koseki, S.; Matunaga, N.; Nguyen, K. A.; Su, S.; Windus, T. L.; Dupuis, M.; Montgomery, J. A. *J. Comput. Chem.* **1993**, *14*, 1347–1363.

(94) The H-Sc bonding are highly ionic; the H-Sc bond lengths of both the terminal (1.76 to 1.92 Å) and bridged (1.97 to 2.02 Å) H's are close to the sum of the effective Sc^{3+} (0.762 Å, see Stokłosa, A.; Laskowska, B. J. Chem. Crystallogr. 2008, 38, 913–925) and H^- (1.29 Å, see Libowitz, G. G.; Gibb, T. R. P., Jr. J. Phys. Chem. 1956, 510–511) ionic radii.

(95) We also characterized T_d $C_6H_{13}B_4^-$ with a tetracoordinate tetrahedral hydrogen as a local minima.

(96) Thompson, M. E.; Bercaw, J. E. *Pure Appl. Chem.* **1984**, *56*, 1–11.

(97) Sadow, A.; Tilley, T. D. *Angew. Chem. Int. Ed* **2003**, *42*, 803–805.

(98) Sadow, A.; Tilley, T. D. *J. Am. Chem. Soc.* **2003**, *125*, 7971–7977.

(99) Sadow, A. D.; Tilley, T. D. *J. Am. Chem. Soc.* **2005**, *127*, 643–656.

(100) Fontaine, F.-G.; Tilley, T. D. *Organometallics* **2005**, *24*, 4340–4342.

(101) Barros, N.; Eisenstein, O.; Maron, L.; Tilley, T. D. *Organometallics* **2006**, *25*, 5699–5708.

(102) Barros, N.; Eisenstein, O.; Maron, L.; Tilley, T. D. *Organometallics* **2008**, *27*, 2252–2257.

(103) Wadnerkar, N.; Kalamse, V.; Chaudhari, A. *J. Comput. Chem.* **2010**, *31*, 1656–1661.

(104) Arndt, S.; Voth, P.; Spaniol, T. P.; Okuda, J. *Organometallics* **2000**, *19*, 4690–4700.

(105) Piers, W. E.; Emslie, D. J. H. *Coord. Chem. Rev.* **2002**, *233–234*, 131–155.

(106) Wang, X.; Andrews, L. *J. Chem. Phys. A* **2010**, *114*, 2293–2299.

CHAPTER 3

SYNERGISTIC BONIDING IN THREE DIMENSIONAL HYPERCOORDINATE CARBON[†]

[†] Keigo Ito and Paul von Ragué Schleyer
To be submitted to Organic Letters

3.1 Abstract

Two three-dimensional hexacoordinate carbon (3dhC) clusters ($C_7H_6^{2+}$), based on three acetylene ligands (D_{3h}, local minimum) and a [6]trannulene ligand (D_{3d} , transition state), were designed employing the Dewar-Chatt-Duncanson bonding model. Both isomers benefit synergistically by three three-center-two-electron bonds and π-back bonding from the 3dhC lone pair (p_z) electrons to the ligands. Potentially viable analogs ($C_{15}H_{14}^{2+}$, and the isoelectronic $C_{13}H_{14}B_2$), i.e., by grafting C_4H_7 and C_3BH_7 groups to the two 3dhC prototypes, have much improved kinetic stabilities and offer synthetic prospect.

3.2 Introduction

Synergistic bonding effects, typically employed to describe the metal-carbon bonding interactions between a transition metal and ethylene, can play an important role in the designing of three-dimensional hypercoordinate hydrocarbons. As hydrocarbons usually display rather "regular" structural features, largely represented by the Lewis structure model and valence bond model, peculiar bonding patterns that deviate from such classical depictions, e.g. the bonding environment of planar hypercoordinate carbons (phC) and three-dimensional hexacoordinate (3dhC) carbons, attract great interest.[1-10] While detailed and systematic studies have been carried out for the phC's in the past four decades, the current understanding of the 3dhC's is much incomplete compared to the phC's. Nevertheless, the bonding mechanism of 3dhC's are, as we discover here, quite similar to that of phCs.

Monkhorst's 1968 theoretical study of the interconversion of a methane to its mirror replicate through a planar tetracoordinate transition state first triggered the idea of

hypercoordination in hydrocarbons.[11] But the square-planar transition state was deemed impossible to achieve due to the extremely large activation barrier (250 kcal/mol, later revised to 110 kcal/mol).[12,13] Following Monkhorst's work, Hoffmann, Alder, and Wilcox's (HAW) investigation of the molecular orbitals (MO's) interaction of D_{4h} methane concluded that a σ bond electron deficiency and a lack of π bonding (an unused p_z lone pair electrons) contributed to the high energy of planar tetracoordinate carbon.[14] To increase the thermochemical feasibility of achieving a planar tetracoordinate carbon, HAW suggested the use of π-acceptor ligands to strengthen the bonding interaction of the "unused" carbon p_z lone pair. When σ-donating but π-accepting ligands are involved, synergistic bonding between the central planar tetracoordinate carbon and surrounding ligands result in even stronger bonding interaction. For example, a phC in CB_6^{2-} benefits both from σ-bonding (σ electron donation from the B_6^{2-} ring to the central carbon) and π-back-bonding (π electron donation from the central carbon p_z lone pair to the peripheral B_6^{2-} ring).[15]

Although quite rare in classical organic chemistry, such synergistic bonding mechanisms are not unfamiliar in organometallic chemistry. A representative example is Zeise's salt,[16] $K[PtCl_3(C_2H_4)]\bullet H_2O$. In $K[PtCl_3(C_2H_4)]\bullet H_2O$, the ethylene ligands benefit *"synergistically"* from σ-type donation, from the filled ethylene π orbitals to the empty d orbital of the central Pt (dative bonding), as well as effective back-donation from the Pt lone pair electrons and ethylene π* orbital (π-back bonding). This explanation, first put forth by Dewar, Chatt, and Duncanson, i.e., Dewar-Chatt-Duncanson (DCD) model,[17,18] in the early 1950's illustrated the delocalized three-center-two-electron (3c-2e) metal-carbon bonding behavior of metal-alkene complexes generally. However, we emphasize here that the DCD

bonding model also can be employed to attain three dimensional hypercoordinate hydrocabon (3dhC) complexes.

Few theoretical explorations of ethylene-hypercoordinate carbon complexes have appeared in the literature. Minkin et al. proposed a D_{3h} $C_{13}H_{12}^{2+}$ cluster (**1,** see Figure 3-1) composed of two cyclohexane-like fragments joined by three C=C bonds encasing a 3dhC atom.[19] Their molecular orbital (MO) analysis reveals that the central carbon atom has significant interactions with the cage C=C π and π* orbital (the latter, as we find out, corresponds to π-back-donation). Inspired by Minkin's approach, Wang et al. used a similar strategy to design hexa- and octacoordinate carbon in the hydrocarbon cages.[20] Although not noted in their original papers these examples demonstrate the benefit of DCD-type synergistic bonding features in acheiving carbon hypercoordination and encourage further computational exploration.

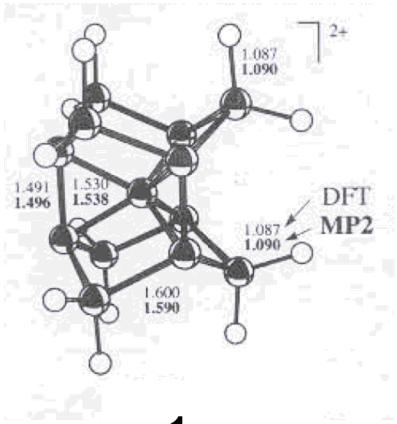

1

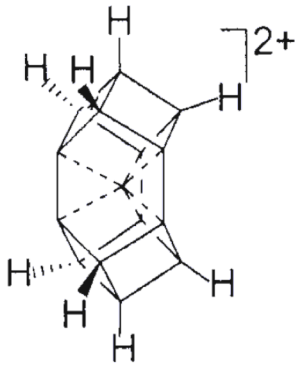

2

Figure 3-1. Geometries of $C_{13}H_{12}^{2+}$ (**1**) and $C_{15}H_8^{2+}$ (**2**)cluster.

3.3 Results and Discussion

Based on the DCD bonding model, we present two prototype 3dhC hydrocarbons: a tri-acetylene based cluster surrounding a 3dhC central carbon, D_{3h} $C_7H_6^{2+}$ (**3**), and a [6]trannulene-based[21] system encasing a 3dhC, D_{3d} $C_7H_6^{2+}$ (**4**) (see Figure 3-2) (both computed at the B3LYP/6-311+G** level,[22-26] as implemented in Gaussian 03).[27] Both clusters take advantage of synergistic bonding interactions between the central 3dhC and surrounding ligand, as illustrated by their molecular orbital (MO) analysis. In **3**, the three filled acetylene ligand π orbitals donate electrons to the in-plane σ* orbitals of the central 3dhC to form three 3c-2e dative bonds (see Figure 3, MO's 12, 18 and 19). This interaction is reinforced by π-back-donation bonding from the central 3dhC (p_z) lone pair to the empty antibonding (π*) orbitals of the ligands (see Figure 3-3, MO 20). The MO's of **4** display

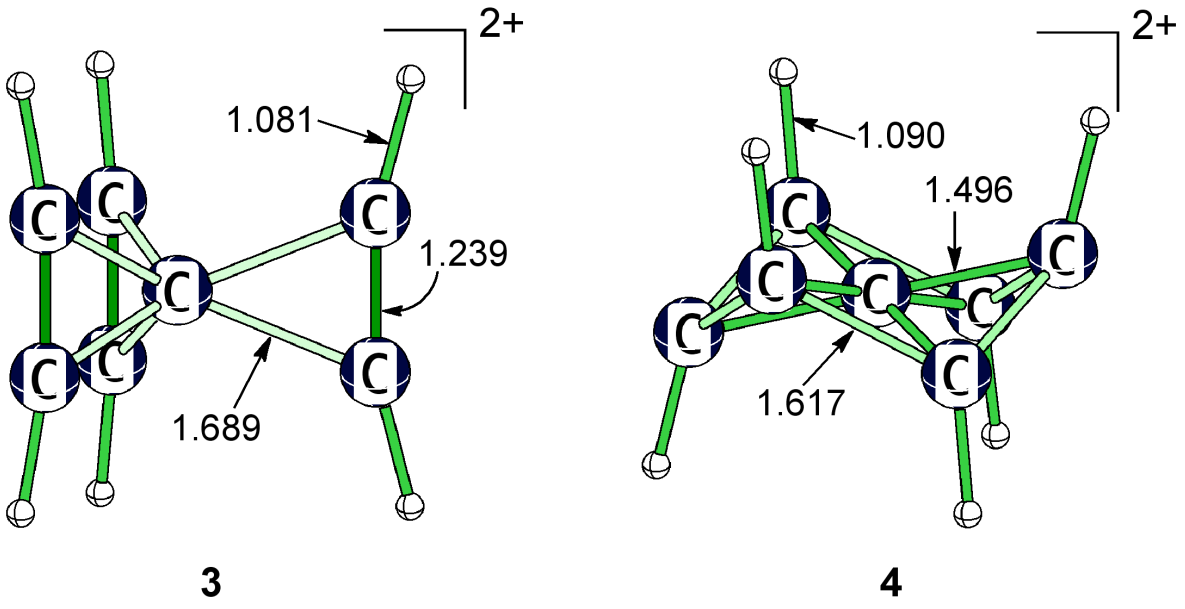

Figure 3-2. Geometries of **3** and **4** computed at B3LYP/6-311+G**. Bond distances are in Å.

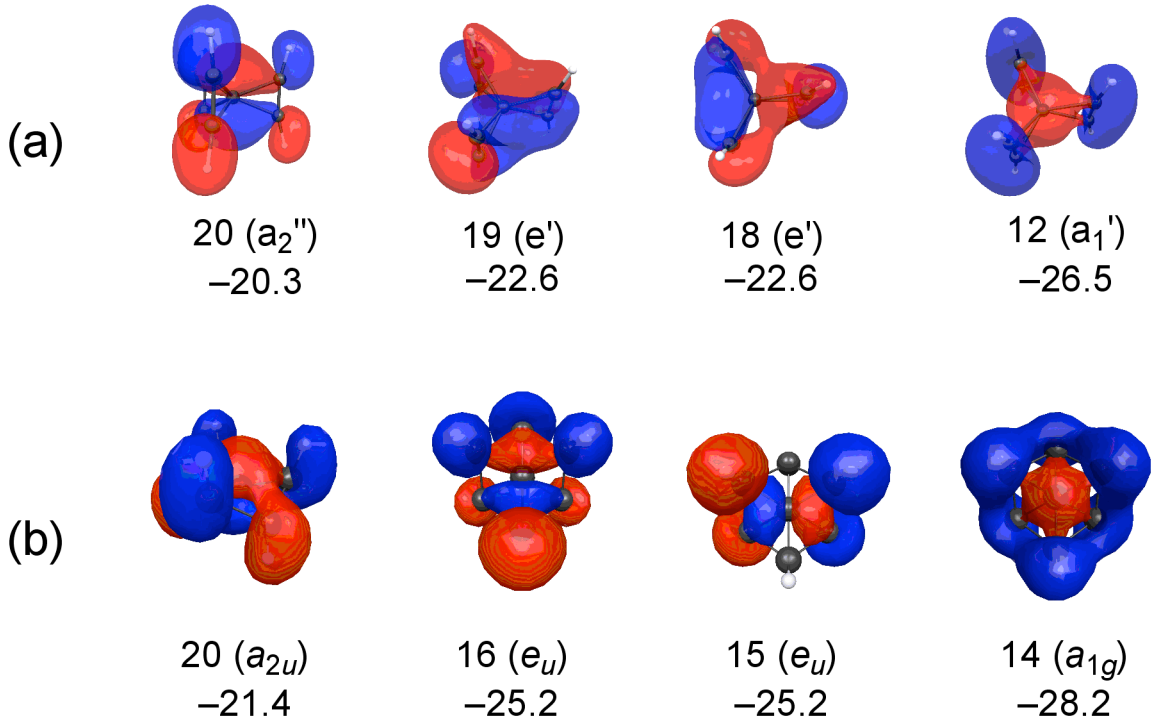

Figure 3-3. Synergistic bonding MO's of (a) **3** and (b) **4**, computed at the B3LYP/6-311+G** level using GAMESS[28].

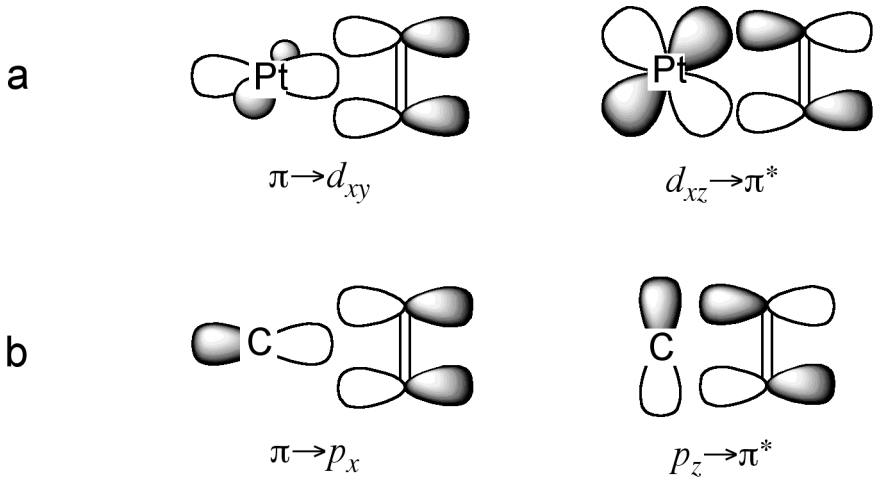

Figure 3-4. Illustrations of the synergistic bonding in (a) the DCD bond (e.g. Zeise's salt), and (b) the 3dhC (in **3**).

similar bonding characteristics. MO's 14, 15, and 16 correspond to the σ-type dative bonds (three 3c-2e bonds) between the ethylene moieties in [6]trannulene and the central 3dhC (see Figure 3). MO 20 corresponds to a π-back-donation from the 3dhC (p_z) lone pair to the [6]trannulene ring (see Figure 4-3). Schematic representations of the synergistic 3dhC-ligand interactions of **3** reveal apparent resemblance to the DCD-bonding model of metal-alkene complexes (Figure 3-4). But to what extent do the delocalized 3c-2e dative bonds and π-back-bonding of **3** and **4** compare, energetically, with classical covalent CC bonds (e.g. the C–C bond in ethane)?

The 3c-2e bond and π-back-bonding energies of **3** and **4** can be evaluated computationally by the block localized wavefunction (BLW) method.[29,30] The BLW method is designed specifically to evaluate electron delocalization energies, by comparing the energy of the molecule itself to the energy of a theoretical (localized) BLW reference. The wavefunction of the latter is computed by partitioning, i.e. "block-localizing," the molecule into various subspaces (each described by selected basis functions and numbers of electrons), in which the orbitals describing different subspaces are not allowed to interact. On this basis, the interaction of interest can selectively "turned off." For example, in **4**, the 3c-2e interaction energy between one of the ethylene moieties of the [6]trannulene ring and the central 3dhC is measured by "block-localizing" the interacting π orbital to the corresponding C=C moiety to disrupt the 3c-2e bonding, while the π-back-bonding is evaluated by "block-localizing" the p_z orbital of the 3dhC carbon to itself to disable π-back-bonding.

Table 3-1. The individual C_C-C_P Wiberg bond indices ($WBI_{Ind.}$), the central carbon total WBI ($WBI_{Tot.}$), and the BLW interaction energies (in kcal/mol) for the dative (BLW_D) and π-back-donation bonds (BLW_B). WBI's are computed by the NBO program at the B3LYP/6-311+G** level, and the BLW values are computed at the B3LYP/6-31G* level using GAMESS/BLW.

	$Freq_1$, cm^{-1}	$WBI_{Ind.}$	$WBI_{Tot.}$	BLW_D, kcal/mol	BLW_B, kcal/mol
3	139.2	0.64	3.89	300.6	98.4
4	*i*613.1	0.65	3.93	384.4	130.3
5	120.2	0.62	3.89	308.4	101.9
6	197.9	0.63	3.91	367.8	130.9
7	103.8	0.61	3.88	298.0	102.4
8	204.6	0.63	3.91	357.7	133.0

Based on this BLW procedure, both **3** and **4** reveal significant interaction energies between the central 3dhC and their surrounding ligands vertical BLW data computed at the B3LYP/6-31G* level using GAMESS).[28] In **3**, the three 3c-2e dative bonds contribute 300.6 kcal/mol (100.2 kcal/mol each), while the back-donation is worth 98.4 kcal/mol; both are energetically competitive when compared to ethane's C-C σ bond energy (86.6 kcal/mol). In **4**, the BLW estimated interaction energies for the three 3c-2e bonds (384.4 kcal/mol, 128.1 kcal/mol each) and the π back-donation bond (130.3 kcal/mol) are even greater. However, these stabilizing bonding interactions, are counterbalanced by coexisting steric factors (see viability section).

Although synergistic bonding is a key factor to the success of the DCD bonding model, steric repulsion between the individual ligands (e.g. between the three acetylene ligands in **3**) and between the central 3dhC and surrounding ligand (e.g., between the 3dhC and [6]trannulene ring in **4**) are involved simultaneously and contribute unfavorably to the formation of **3** and **4**. As a result, both **3** and **4** have rather low thermochemical and kinetic

stabilities. However, grafting and caging strategies, when applied to the prototypes **3** and **4**, offer effective remedy to such concerns as we discuss below.

While **3** is a local minimum (with an appreciable lowest vibrational frequency of 139.2 cm^{-1}), the activation barrier for isomerization to its isomer, **3a** (30.3 kcal/mol lower than **3**), is almost non-existent (0.07 kcal/mol). On this basis, **3** can almost be considered as a quasi-transition state. The isomer, **3a** (see Figure 3-5, displays only two delocalized 3c-2e bonds between the central carbon atom and two acetylene units, the third acetylene unit is isomerised to a vinyl moiety and connects to the central atom via a classical covalent C–C bond. To some extent, this rearrangement (in **3a**) relieves steric repulsion between the surrounding acetylene units in **3**. On the other hand, the **4** has one imaginary frequency (*i*613.1 cm^{-1}), which corresponds to the central carbonmoving up and down the [6]trannulene ring; an effort to reduce the steric repulsion between the 3dhC and trannulene ligand. Geometry optimization following the imaginary frequency leads to **4a** (local minimum, see Figure 3-5), which is 144.5 kcal/mol lower in energy!

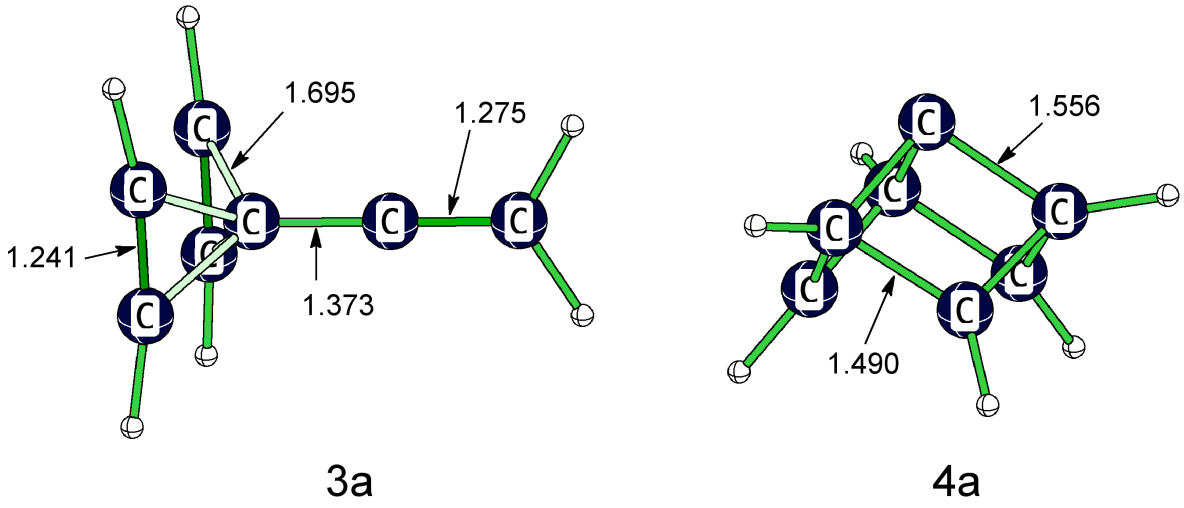

Figure 3-5. Geometries of **3a** and **4a**.

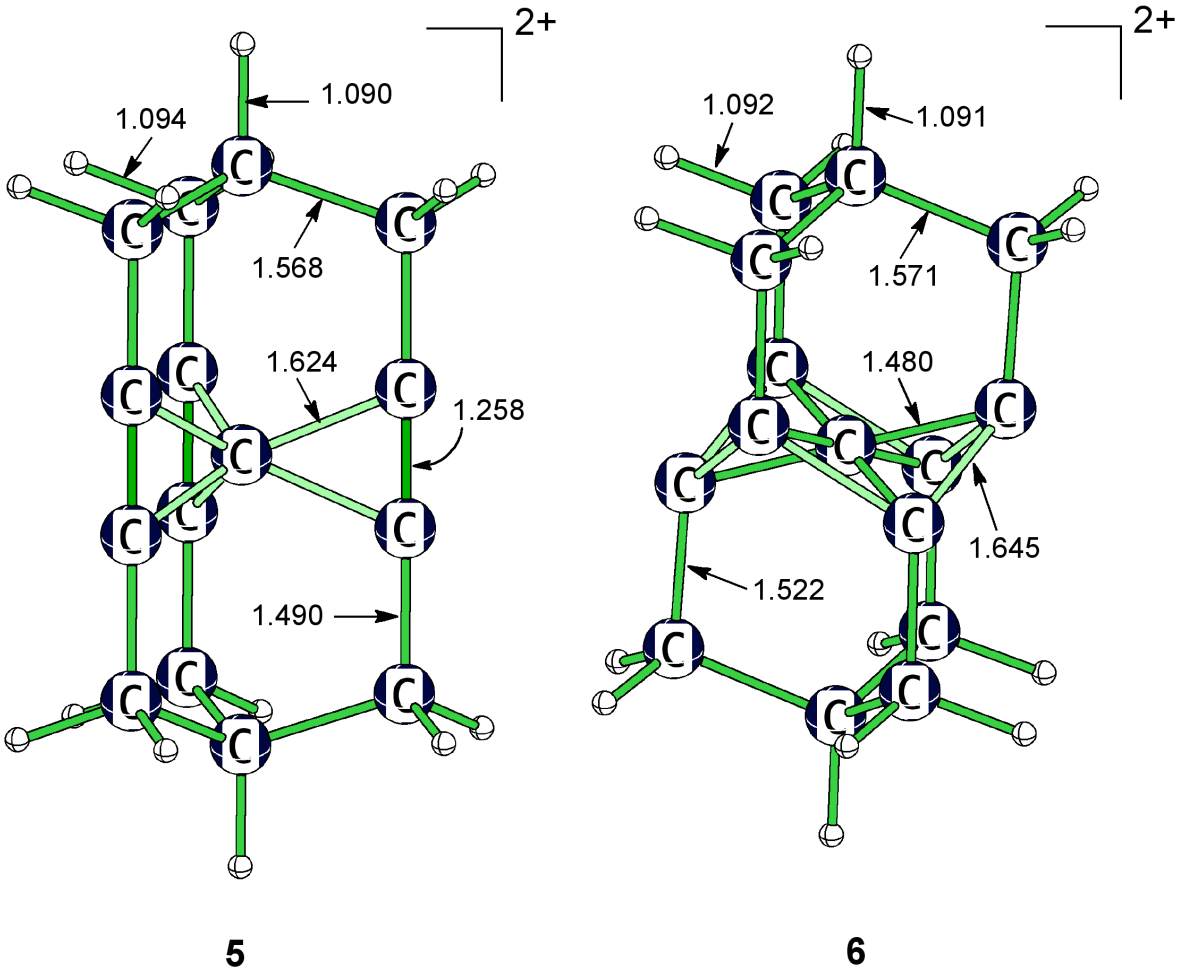

5 **6**

Figure 3-6. Geometries of **5** and **6**, computed at B3LYP/6-311+G**. Bond distances are in Å.

The kinetic stabilities of **3** and **4** can be improved dramatically by grafting suitable hydrocarbon moieties. Since **3** and **4** have a three-fold symmetry axis, C_{3v} C_4H_7 moietiescanbe grafted to the prototype clusters, to result in a D_{3h} and a D_{3d} $C_{15}H_{14}^{2+}$ minimum (see Figure 4-6, **5** and **6**). This substitution straps the floppy ligand carbons to two capping units, and makes the structure kinetically more stable towards isomerization. As a

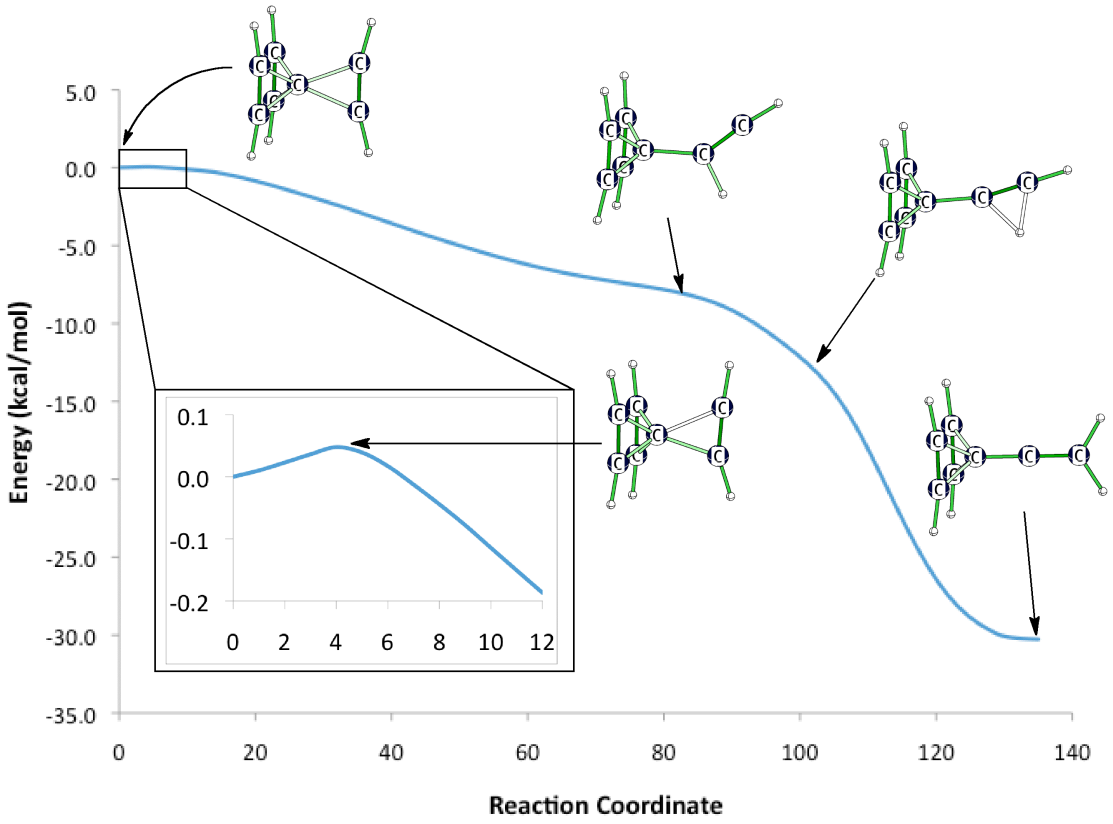

Figure 3-7. Reaction energy profile of isomerization from **3** to **3a**.

result, the activation energy of the bond dissociation between the central carbon (C_C) and a peripheral carbon (C_P) (10.4 kcal/mol) is significantly higher compared to the parent cluster **3** to **3a** (0.07 kcal/mol). Additionally, a dramatic blue-shift of the C_C-C_P stretching vibrational frequencies, from 306.2 and 423.5 cm^{-1} in **3** (see Table 3-1) to 459.4 and 559.7 cm^{-1} in **5** (Table 3-1), documents the increased structural rigidity of the 3dhC in **5**. The partially dissociated isomer, **5a** (see Figure 3-8), is only 2.4 kcal/mol lower in energy compared to **5**. Similarly, cluster **6** also displays increased structural rigidity. Although **4** has an imaginary frequency (*i*613.1 cm^{-1}) **6** is a local minimum with a lowest vibrational frequency of 196.1 cm^{-1}. In **6**, displacing the central carbon along the long axis of the cage is unfavorible energetically, and upon geometry optimization, the the central carbon returns

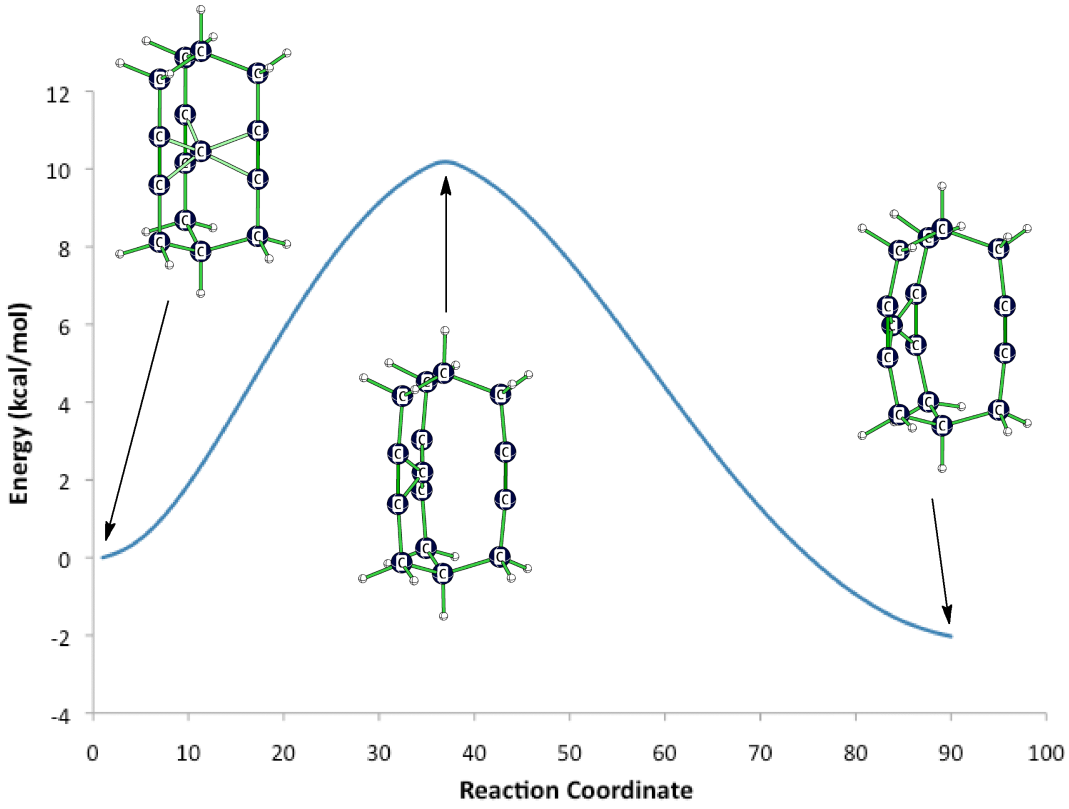

Figure 3-8. Reaction energy profile of isomerization from **5** to **5a**.

to the center of the cage. Although caging provides significant kinetic stabilization to the 3dhC prototypes proposed here, the bond C_C-C_P bond distance in **5** (1.624 Å) and **6** (1.480 Å) are not much different compared to those of **3** and **4**. Hence, caging does not perturb the local bonding environment around the hC's; the individual and total WBI's of **5** (0.62 and 3.89, respectively; see Table 3-1) and of **6** (0.63, and 3.91, respectively; Table 3-1), also are similar to those of **3** and **4**.

The apical carbon atoms of **5** and of **6** also can be substituted by boron atoms to obtain two isoelectronic neutral clusters. The resulting neutral clusters, D_{3h} and D_{3d}

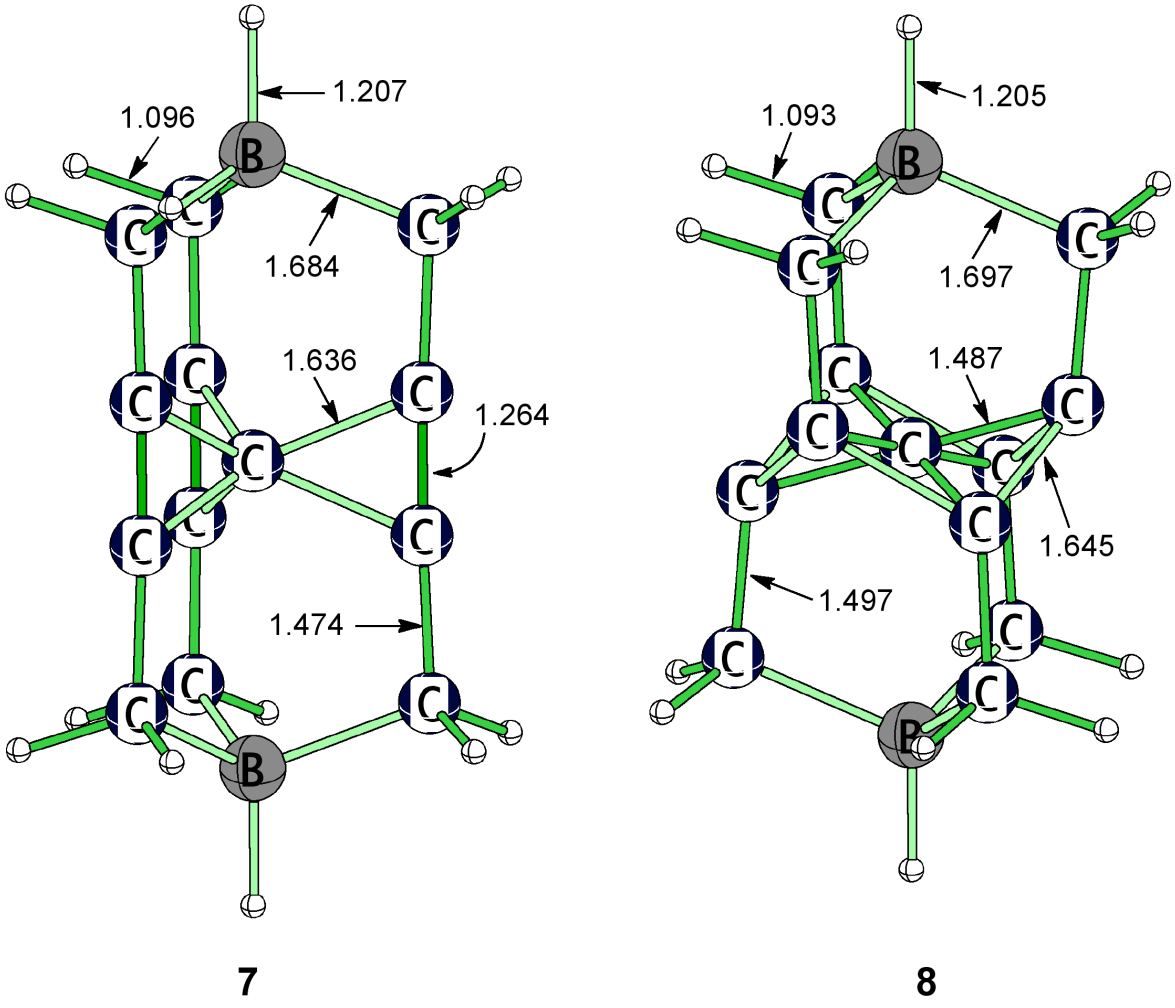

Figure 3-9. Geometries of caged carborane 3dhC clusters, **7** and **8**, computed at B3LYP/6-311+G**. Bond distances are in Å

$C_{13}H_{14}B_2$ (**7** and **8**, see Figure 3-9), are attractive targets for experimental liquid-phase synthesis. Similar to their hydrocarbon cage analogues, **5** and **6**, the C_3H_7B moieties of **7** and **8** provide increased kinetic stability to the 3dhC cores. In **7**, the C_C-C_P bond dissociation activation barrier is 8.6 kcal/mol, with appreciable corresponding vibrational frequencies (418.1 and 522.6 cm^{-1}). Like **6**, **8** is a minimum, and the vibrational frequency (418.1 and 522.6 cm^{-1}). Like **6**, **8** is a minimum, and the vibrational frequency corresponding to the

central carbon displacement along the axis of the cage is large (273.0 cm^{-1}). Since **7** and **8** are isoelectronic to **5** and **6**, while hC bonding mechanisms are not perturbed by the C/B substitution. The C_C-C_P bond distances in **7** (1.636 Å) and **8** (1.487 Å), are similar to those in **5** and **6**, and the WBI's show similar values ($WBI_{Ind.}$: 0.61 and 0.63, and $WBI_{Tot.}$: 3.88 and 3.91 for **7** and **8**, respectively; see Table 3-1).

3.4 Conclusions

We demonstrate that bonding mechanisms unfamiliar in organic chemistry, i.e. the DCD model, can be easily applied to offer unique bonding environments to achieve 3dhC. The synergistic bonding interactions of our proposed 3dhC clusters are energetically competitive to classical carbon- carbon covalent bonds. Although steric factors jeopardize the effectiveness of the DCD model, caging and grafting strategies circumvent such shortcomings and lead to increased thermochemical and kinetic stabilities. Applications of the DCD bonding model to hydrocarbon systems offer promising possibilities for hypercoordination chemistry.

Acknowledgment

This work was supported by NSF Grant CHE-0716718.

3.5 References

(1) Sorger, K.; Schleyer, P. v. R. *J. Mol. Struct. (THEOCHEM)* **1995**, *338*, 317–346.

(2) Röttger, D.; Erker, G. *Angew. Chem., Int. Ed. Engl.* **1997**, *36*, 812–827.

(3) Kuck, D. *Top. Curr. Chem.* **1998**, *196*, 168–220.

(4) Radom, L.; Rasmussen, D. R. *Pure Appl. Chem.* **1998**, *70*, 1977–1984.

(5) Rasul, G.; Prakash, G. K. S.; Olah, G. A. *Proc. Natl. Acad. Sci.* **1998**, *95*, 7257–7259.

(6) Erker, G. *Chem. Soc. Rev.* **1999**, *28*, 307–314.

(7) Siebert, W.; Gunale, A. *Chem. Soc. Rev.* **1999**, *28*, 367–371.

(8) Minkin, V. I.; Minyaev, R. M.; Hoffmann, R. *Russ. Cehm. Rev.* **2002**, *11*, 869–892.

(9) Keese, R. *Chem. Rev.* **2006**, *106*, 4787–4808.

(10) Merino, G.; Mendez-Rojas, M. A.; Vela, A.; Heine, T. *J. Comput. Chem.* **2007**, *28*, 362–372.

(11) Monkhorst, H. *Chem. Commun.* **1968**, *18*, 1111–1112.

(12) Pepper, M. J. M.; Shavitt, I.; Schleyer, P. v. R.; Glukhovtsev, M. N.; Janoschek, R.; Quack, M. *J. Comput. Chem.* **1995**, *16*, 2007.

(13) Minyaev, R. M.; Gribanova, T. N. *Izv. Acad. Nauk, Ser. Khim.* **2000**, 786.

(14) Hoffmann, R.; Alder, R. W.; F., W. C. *J. Am. Chem. Soc.* **1970**, *92*, 4992–4993.

(15) Exner, K.; Schleyer, P. v. R. *Science* **2000**, *290*, 1937–1940.

(16) Zeise, W. C. *Ann. Phys.* **1831**, *97*, 497–541.

(17) Dewar, M. J. S. *Bull. Soc. Chim. Fr.* **1951**, *18*, C. 71–C. 79.

(18) Chatt, J.; Duncanson, L. A. *J. Chem. Soc.* **1953**, 2939–2947.

(19) Minyaev, R. M.; Minkin, V. I.; Gribanova, T. N.; Starikov, A. G. *Mendeleev Commun.* **2004**, *14*, 47–48.

(20) Wang, Y.; Huang, Y.; Liu, R. *Chem. Eur. J.* **2006**, *12*, 3610-3616.

(21) Fokin, A. A.; Jiao, H.; Schleyer, P. v. R. *J. Am. Chem. Soc.* **1998**, *120*, 9364–9365.

(22) Becke, A. D. *Phys. Rev. A* **1988**, *38*, 3098–3100.

(23) Lee, C.; Yang, W.; Parr, R. G. *Phys. Rev. B* **1988**, *37*, 785–789.

(24) McLean, A. D.; Chandler, G. S. *J. Chem. Phys.* **1980**, *72*, 5639–5648.

(25) Raghavachari, K.; Binkley, J. S.; Seeger, R.; Pople, J. A. *J. Chem. Phys.* **1980**, *72*, 650–654.

(26) Raghavachari, K.; Trucks, G. W. *J. Chem. Phys.* **1989**, *91*, 1062–1065.

(27) Frisch, M. J.; Trucks, G. W.; Schlegel, H. B.; Scuseria, G. E.; Robb, M. A.; Cheeseman, J. R.; Montgomery, J., J. A.; Vreven, T.; Kudin, K. N.; Burant, J. C.; Millam, J. M.; Iyengar, S. S.; Tomasi, J.; Barone, V.; Mennucci, B.; Cossi, M.; Scalmani, G.; Rega, N.; Petersson, G. A.; Nakatsuji, H.; Hada, M.; Ehara, M.; Toyota, K.; Fukuda, R.; Hasegawa, J.; Ishida, M.; Nakajima, T.; Honda, Y.; Kitao, O.; Nakai, H.; Klene, M.; Li, X.; Knox, J. E.; Hratchian, H. P.; Cross, J. B.; Adamo, C.; Jaramillo, J.; Gomperts, R.; Stratmann, R. E.; Yazyev, O.; Austin, A. J.; Cammi, R.; Pomelli, C.; Ochterski, J. W.; Ayala, P. Y.; Morokuma, K.; Voth, G. A.; Salvador, P.; Dannenberg, J. J.; Zakrzewski, V. G.; Dapprich, S.; Daniels, A. D.; Strain, M. C.; Farkas, O.; Malick, D. K.; Rabuck, A. D.; Raghavachari, K.; Foresman, J. B.; Ortiz, J. V.; Cui, Q.; Baboul, A. G.; Clifford, S.; Cioslowski, J.; Stefanov, B. B.; Liu, G.; Liashenko, A.; Piskorz, P.; Komaromi, I.; Martin, R. L.; Fox, D. J.; Keith, T.; Al-Laham, M. A.; Peng, C. Y.; Nanayakkara, A.; Challacombe,

M.; Gill, P. M. W.; Johnson, B.; Chen, W.; Wong, M. W.; Gonzalez, C.; Pople, J. A.; Gaussian, Inc.: Wallingford, CT., 2004.

(28) Perdew, J. P.; Burke, K.; Wang, Y. *Phys. Rev. B* **1996**, *54*, 16533.

(29) Mo, Y.; Peyerimhoff, S. D. *J. Chem. Phys.* **1998**, *109*, 1687–1697.

(30) Mo, Y.; Song, L.; Lin, Y. *J. Phys. Chem. A* **2007**, *111*, 8291–8301.

CHAPTER 4

MYRIAD PLANAR HEXACOORDINATE CARBON MOLECULES INVITING SYNTHESIS[†]

[†] Keigo Ito, Zhongfang Chen, Clémence Corminboeuf, Chaitannya S. Wannere, Qian Shu Li, Xiu Hui Zhang, and Paul v. R. Schleyer *Journal of the American Chemical Society*, **2007**, *129*, 1510-1511. Reprinted here with permission of publisher.

4.1 Abstract

The prototypal hexacoordinate carbon (phC) molecule, CB_6^{2-} (D_{6h}), can be annulated by inserting arenes, olefins, or other one or two atom bridging groups into a perimeter B−B bond. Two single-atom units also can bridge opposite CB_6 edges. These strategies allow the design of limitless phC derivatives based on CB_6 as a building block unit. Illustrative examples, shown to be viable computationally, offer possibilities for experimental realization. These phC's involve multicenter deltahedral σ bonding, common for boron but unusual for carbon, in the ring planes, as well as π delocalization.

4.2 Introduction

Molecules with planar hexacoordinate carbons (phC) are exciting prospects. They violate both the usual maximum tetracoordination of carbon and its proclivity for three-dimensional bonding. Two independent research groups discovered phC examples computationally in 2000. Exner and Schleyer's CB_6^{2-} (Figure 4-1, **1**) and the isoelectronic C_3B_4 isomers (e.g., **2**) have six aromatic π electrons.[1] Minyaev and Gribanova proposed heteroatomic extensions of **1** with eight-membered ring perimeters (Figure 4-1, **3**, X = NH and O).[2] We confirm these to be minima, despite having eight, rather than six π electrons.

In contrast to this limited number of phC's, Wang and Schleyer predicted numerous molecules with planar pentacoordinate carbons (ppC) in 2001. They showed how ppC chemistry might offer unlimited possibilities for generalization and experimental realization.[3] Appropriate ppC structural units can be grafted onto virtually any arene or unsaturated ring having three adjacent CH groups. Likewise, generally applicable construction principles allow the incorporation of phC structural units, based on simple

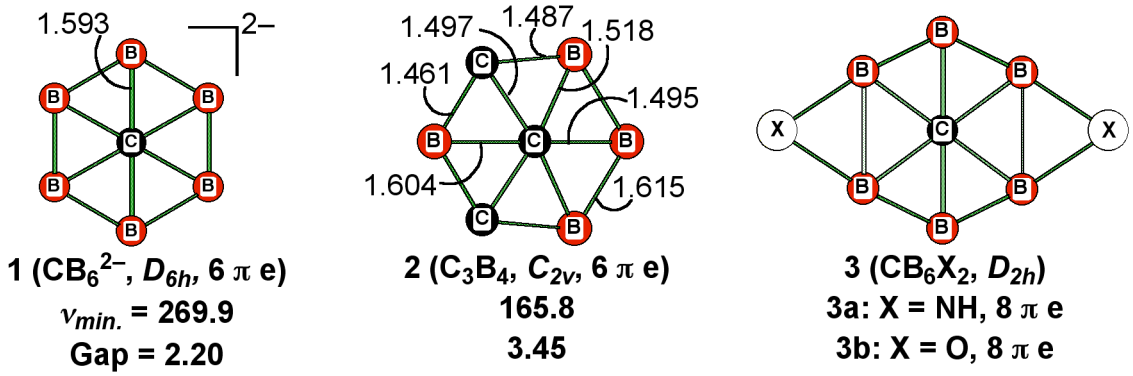

Figure 4-1. Previously reported phC minima.1 Bond lengths in Å, the lowest frequency (υ_{min}) in cm-1, HOMO-LUMO energy separation (Gap) in eV.

elaborations of **1** and **3**. The preparation of numerous planar tetracoordinate carbon compounds following theoretical predictions[4] offers hope for the realization of phC's.

Akin to principles devised for ppC's,[3] building block strategies facilitate the design of numerous molecules with phC's. The initial idea was based on the finding that C_{2v} $CH_2B_6^{2-}$ (**4**), the 1,2-dihydro derivative of **1**, retains the phC despite its ruptured BB ring bond[3] (albeit with somewhat elongated CB bond lengths). As in the design of ppC molecules,[3] the opened edge of **4** can be bridged and the ring closed by appropriate atoms and groups. The selection of phC examples in Figure 4-2 retains the planar hexacoordinate carbon CB_6 unit. Like **3**, more than one bridge is possible. Consequently, phC's can be grafted onto myriad systems.

The planar hypercoordinate bonding principles for phCs, like those for ppCs,[3] are general and are easily extended to other combinations of atoms, with elements other than carbon in the centers.[2] Thus, Minkin et al. computed examples of planar hexacoordinate boron species in 2001,[5] and the boron analogue of **4**, C_{2v} $H_2B_7^-$, was reported recently by Boldyrev and co-workers.[6] As in earlier studies of planar hypercoordination,[1,4] we focus

here on carbon as the central element since violations of the conventional tetrahedral tetracoordinate bonding of carbon seem more unusual. While all our new phC molecules are local minima,[7] their isomers (e.g., with boron in the center and carbon on the outside) can be lower in energy. However, such species are no less interesting inherently and illustrate the generality of the bonding principles.

4.3 Results and Discussion

The two hydrogens in **4** provide substitution sites. Ring closure, for example, by replacing both the H's, as well as the two negative charges, of **4** with a CH=CH bridge, results in the neutral six π electron $C_3H_2B_6$ (**5**). The appreciable vertical ionization potentials (VIP) of **5** and other neutral species imply stability (Table 3-1). The six Wiberg bond indices (WBI) to the central carbon in **5**, ranging from 0.46 to 0.80, document the hexacoordination to the B_6 ring. The total WBI (3.86) of the central carbon does not violate octet rule expectations. Exchanging the central carbon with the three unique borons resulted in isomers (with hexacoordinate borons in the center and carbons in the perimeter) ranging between 18.5 and 30.8 kcal/mol lower in energy. However, a Born-Oppenheimer molecular dynamics simulation[8] (BOMD, Figure 3-3 for the trajectory), using the deMon 2004 program,[9] demonstrates the viability of **5** as a local minimum and its resistance toward isomerization. Searches only located high-energy transition states for isomerization.

Benzannulation of **5** gives **6**, the 10 π electron analogue of naphthalene. Similarly, the replacement of vicinal hydrogens in benzene and essentially all arenes by a CB_6 group (i.e., **4** without its H's) can yield new phC candidates. The tropylium ion derivative,

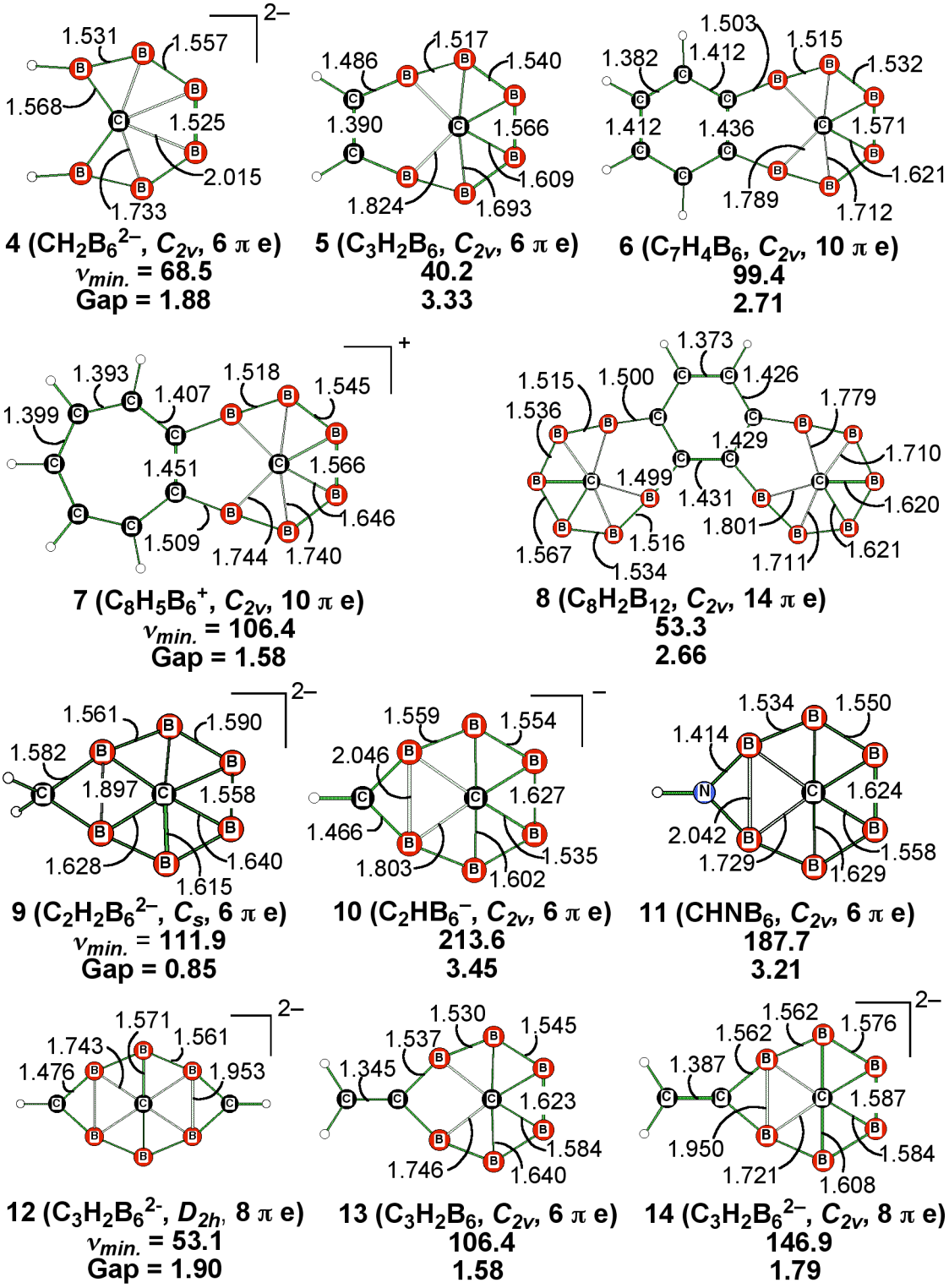

Figure 4-2. Examples of phC minima optimized at B3LYP/6-311+G**. Bond distances are in Å, the lowest frequency (vmin) in cm-1, HOMO-LUMO energy separation (Gap) in eV.

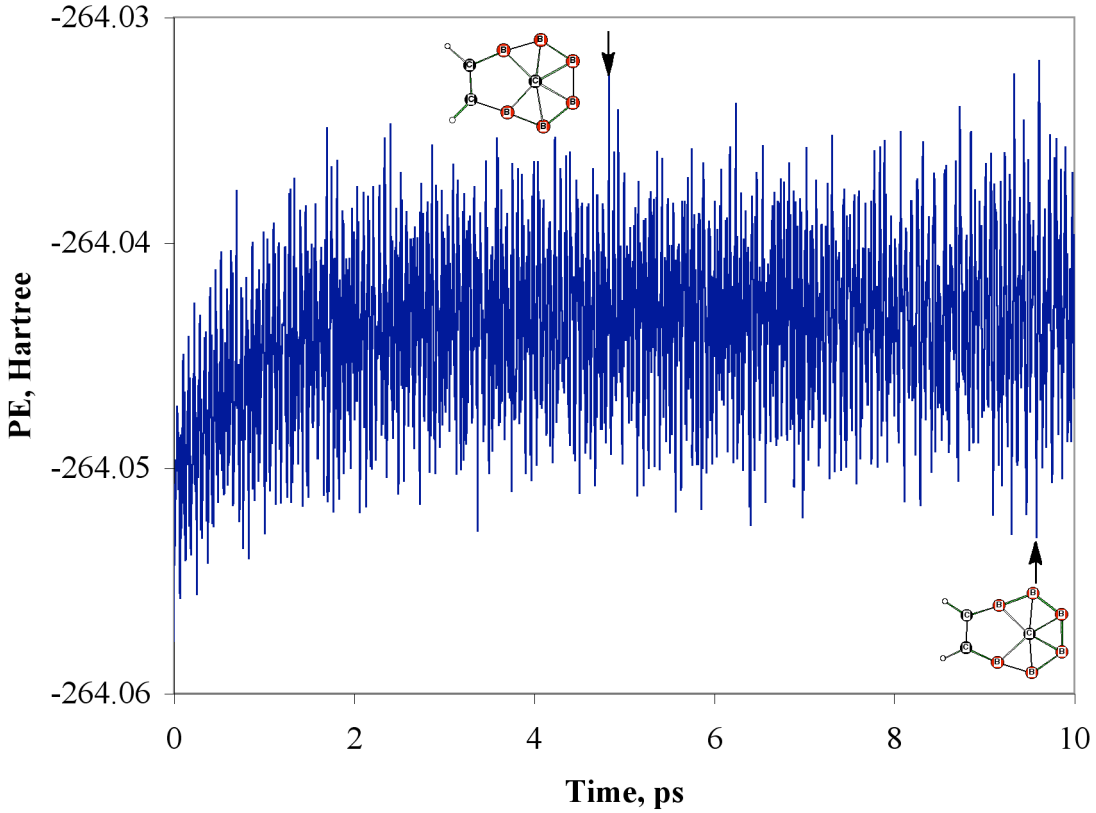

Figure 4-3. Potential energy of **5** along the MD trajectory at PBE/DZVP/Gen-A2* level. Born-Oppenheimer molecular dynamics simulation was performed for 10 ps after 2 ps of equilibration with the interval of 0.5 fs at 300 K using deMon 2004.

$C_8H_5B_6^+$ (**7**), exemplifies other bicyclic systems. The tricyclic minimum, C_{2v} $C_8H_2B_{12}$ (**8**), has two CB_6 units, each with a phC, grafted *meta* onto benzene.

Elaborations of **4** with single-atom bridges result in phC minima with seven-membered ring perimeters. For example, a methylene group can replace the two H's in **4** and bridge the CB_6^{2-} unit to give C_s $C_2H_2B_6^{2-}$ (**9**). While the methylene carbon in **9** deviates slightly from the CB_6 plane, the planarity of the CB_6 moiety is nearly exact. Replacing the

Table 4-1. Summary of properties of phC molecules. The total energies ($E_{Tot.}$) are in hartrees;, unscaled ZPE in kcal/mol, the out-of-plane component of the NICS tensor ($NICS(1)_{zz}$) and the dissection into the σ ($NICS(1)_{\sigma zz}$), radial MO's ($NICS(1)_{Radialzz}$), and π ($NICS(1)_{\pi zz}$) are in ppm. NICS(1) were computed at 1.0 Å above the phC perpendicular to the ring plane. Geometry optimization and NICS calculations were performed at the B3LYP/6-311+G** and PW91PW91/6-311G* levels, respectively.

Molecule	$E_{Tot.}$	ZPE	$NICS(1)_{zz}$	$NICS(1)\sigma_{zz}$	$NICS(1)_{Radialzz}$	$NICS(1)_{\pi zz}$
1	–186.91984	15.7	–50.8	4.0	–19.0	–30.2
2	–213.40785	18.0	–49.5	–5.6	–10.9	–27.3
4	–188.17008	25.3	–50.1	–15.7	–6.3†	–22.2
4b	–175.09552	26.8	-	-	-	-
5	–264.47528	36.9	–45.0	–3.9	–14.2	–18.5
5a	–264.51786	38.9	-	-	-	-
5b	–264.52730	38.7	-	-	-	-
5c	–264.50718	38.5	-	-	-	-
6	–418.15993	66.8	–38.8	–0.5	–16.3	–12.1
7	–456.58917	77.5	–51.0	1.0	–17.9	–24.1
8	–604.00925	70.5	–43.8	–1.7	–14.3	–16.4
9	–226.28524	31.4	–54.3	–17.2	–7.0†	–24.4*[1]
10	–225.82816	26.6	–45.9	–3.1	–19.6	–16.4
11	–242.44471	27.6	–35.5	–0.5	–21.6	–6.5
12	–264.49012	34.9	–46.8	–9.1	–17.6	–12.6
13	–264.42058	36.7	66.2	–0.7	–21.5	95.7
14	–264.41737	35.0	–53.4	–12.4	–11.0	–23.2
15	–341.89894	56.8	–0.4	–3.1	–21.5	32.7
16	–341.90133	54.4	–55.8	–7.5	–18.0	–22.1

*[1] HOMO, HOMO–1, HOMO–7 and HOMO–10 were grouped as π MO's. †Due to significant mixings of radial orbitals and σ orbitals, $NICS(1)_{Radialzz}$ may be inaccurate.

two H's in **4** with CH- results in C_{2v} $C_2HB_6^-$ (**10**); planarity is retained. Heteroatomic bridging groups such as NH can result in favorable neutral phC minima, such as $CHNB_6$ (**11**).

The phC units in **4-11** have $4n + 2$ π electrons. Their aromaticity is demonstrated by refined nucleus-independent chemical shift (NICS) indices, such as the perpendicular tensor components, 1 Å above the central carbons ($NICS(1)_{\pi zz}$).[13] The $NICS(1)_{zz}$ grid of **5** and the large negative value (–45.0) above the ring center indicate the presence of a strong induced diatropic ring current, with a shielding zone inside and a deshielding zone outside (see Figure 4-4). Dissection of $NICS(1)_{zz}$ shows that the shielding tensor contributions from the π MO and from the in-plane radial σ MO sets are both diatropic ($NICS(1)_{\pi zz}$) –18.5; $NICS(1)_{radialzz}$) –14.3. See Figure 4-5 and Table 4-1 for NICS(1) and dissected NICS(1) of **5**). Schleyer et al. coined the term "doubly aromatic"[10] for such situations. The $NICS(1)_{zz}$

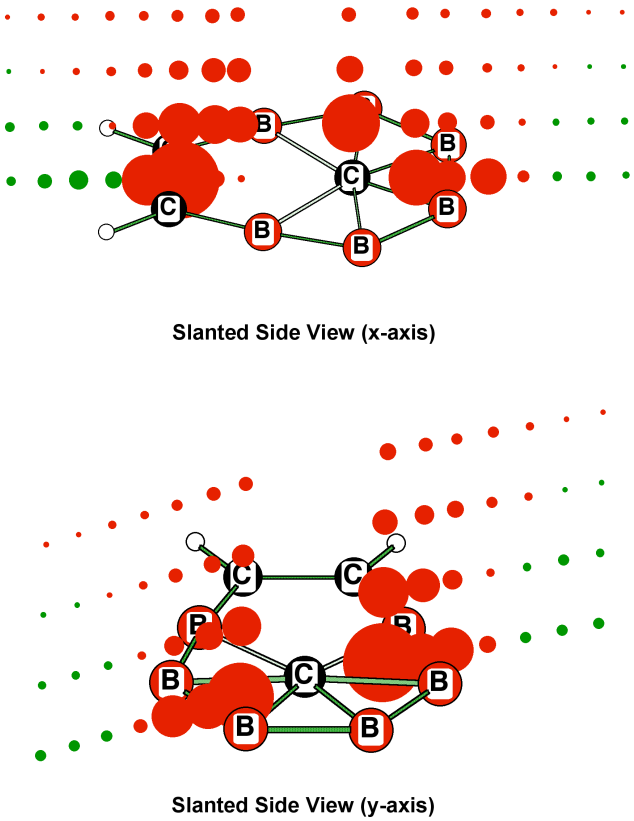

Figure 4-4. $NICS_{zz}$ grid of **5**, computed at PW91/6-311G* level. NICS probes are spaced at 1.0 Å apart.

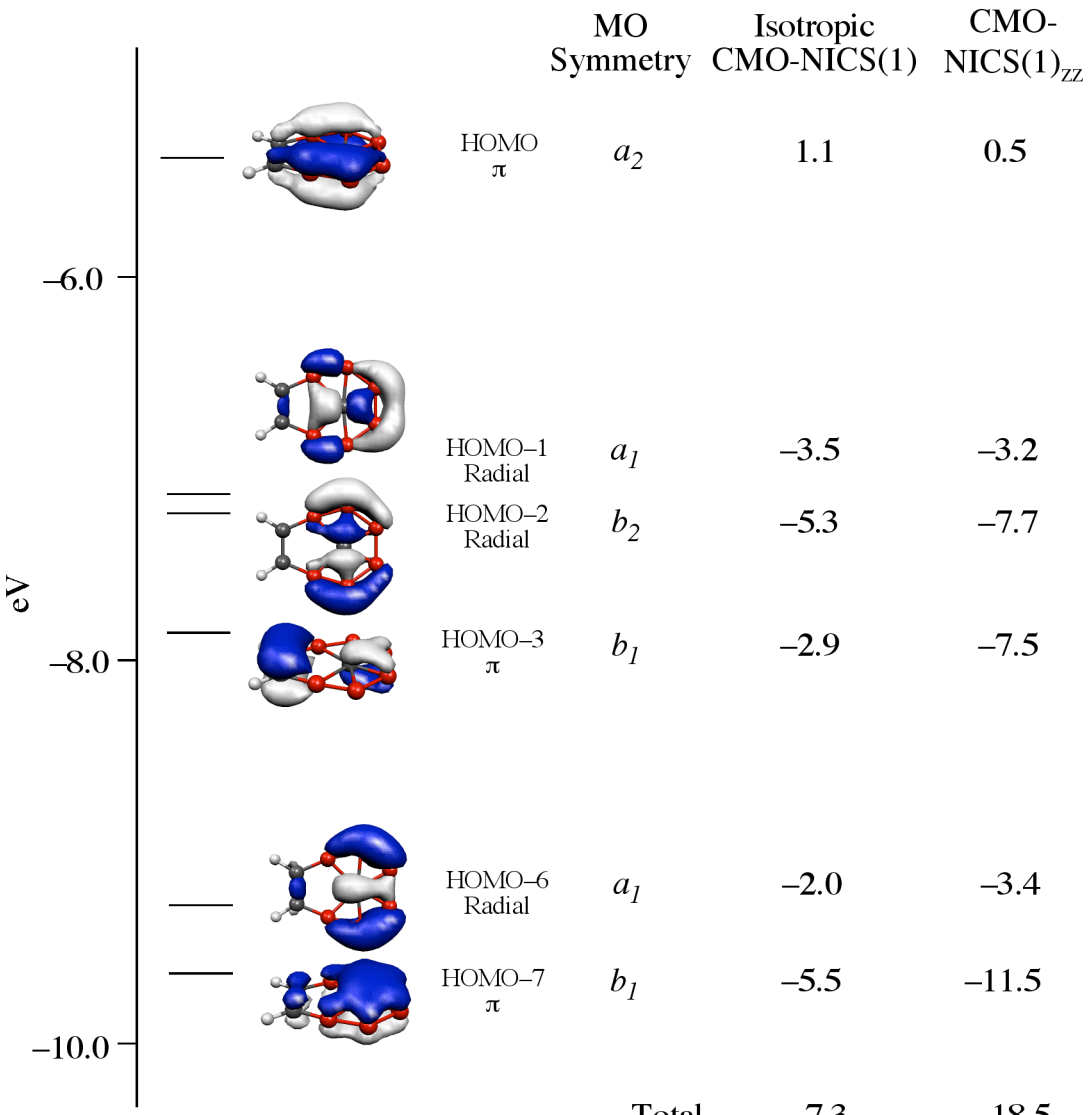

Figure 4-5. CMO dissection of isotropic NICS(1)$_{\pi}$ and NICS(1)$_{\pi zz}$ of the Hückel aromatic **5**, $C_3H_2B_6$ (C_{2v}) at PW91PW91/6-311G* are shown. Total$_{\pi}$ is a sum of contributions from all π MO's, and Total$_{Radial}$ is a sum of contributions from all radial MO's. Total value includes contributions from σ, radial, π and core electrons.

results for **5** indicate that both π and radial MO's help to achieve the planar geometry with a phC. Planar hypercoordination may benefit even more from σ MO stabilization than from the π MO system. **4a**,[6] with only four π electrons, also illustrates this point.

Two-fold bridging of **1** on opposite edges results in an eight-membered ring perimeter exemplified by Minyaev's phC molecules, **3** (X = NH and O), which have eight π

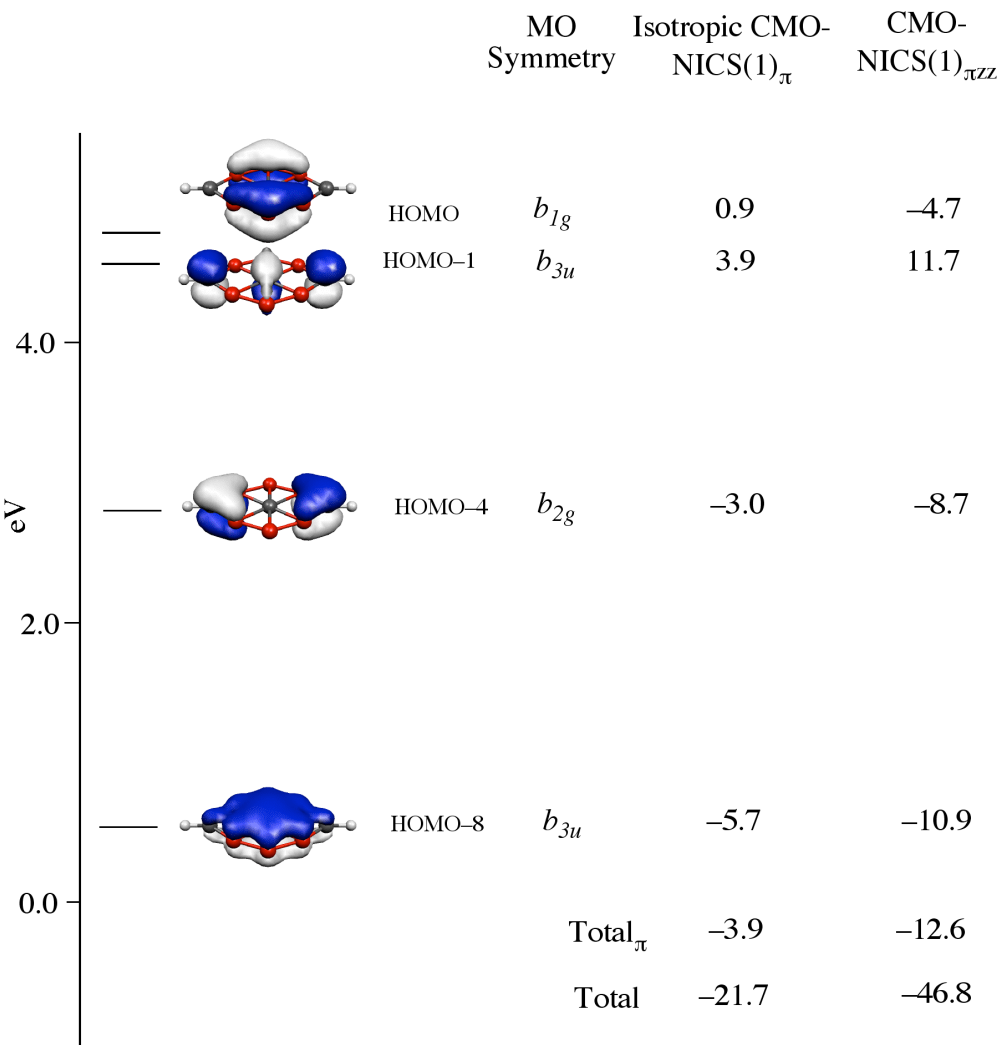

Figure 4-6. CMO dissection of isotropic NICS(1)$_{\pi}$ and NICS(1)$_{\pi zz}$ of **12**, $C_3H_2B_6^{2-}$ (D_{2h}) at PW91PW91/6-311G*. Total$_{\pi}$ is a sum of contributions from all π MO's. Total value includes contributions from σ, radial, π and core electrons.

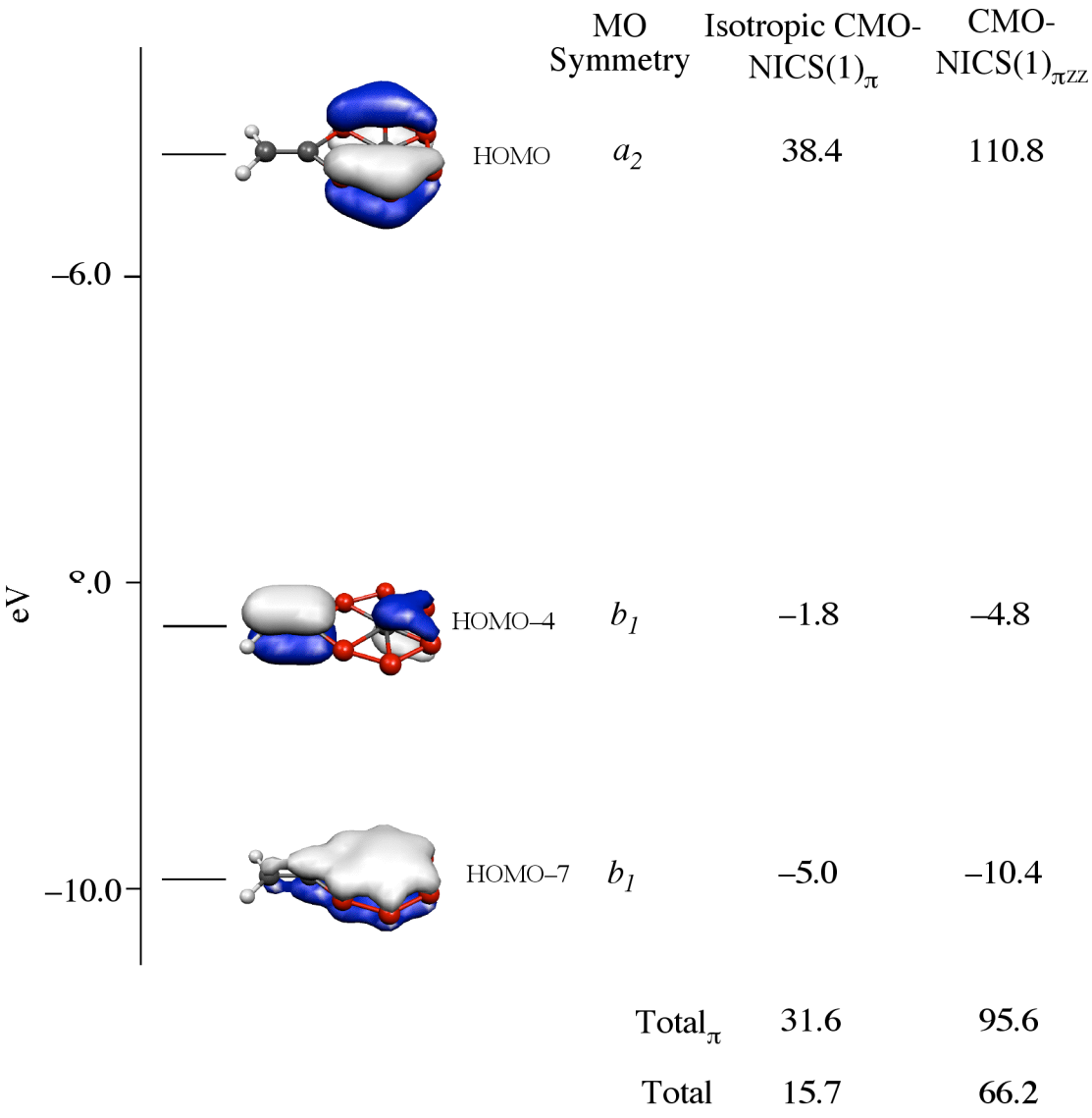

Figure 4-7. CMO dissection of isotropic NICS(1)$_\pi$ and NICS(1)$_{\pi zz}$ of the **13**, $C_3H_2B_6$ (C_{2v}) at PW91PW91/6-311G* level are shown. Total$_\pi$ is a sum of contributions from all π MO's. Total value includes contributions from σ, radial, π and core electrons.

electrons. The isoelectronic **12** (i.e., D_{2h} $C_3H_2B_6^{2-}$ where X = CH^- in **3**) also has eight π electrons, but two of these (in HOMO–1) are nonbonding due to remoteness of the CH units; the remaining six π electrons are delocalized in the central CB_6 moiety (see Figure 3-

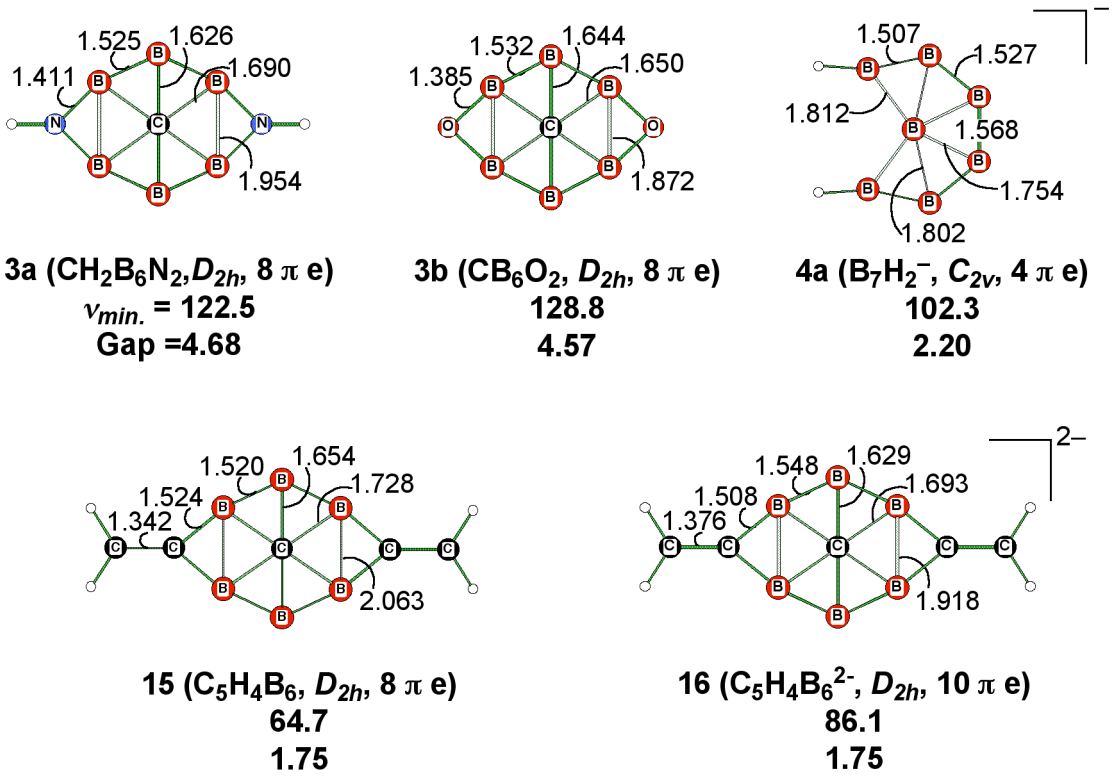

3a ($CH_2B_6N_2$,D_{2h}, 8 π e)
$\nu_{min.}$ = 122.5
Gap =4.68

3b (CB_6O_2, D_{2h}, 8 π e)
128.8
4.57

4a ($B_7H_2^-$, C_{2v}, 4 π e)
102.3
2.20

15 ($C_5H_4B_6$, D_{2h}, 8 π e)
64.7
1.75

16 ($C_5H_4B_6^{2-}$, D_{2h}, 10 π e)
86.1
1.75

Figure 4-8. Planar hypercoordinate boron and phC minima optimized at B3LYP/6-311+G**. Bond distances are shown in Å, the lowest frequency ($\upsilon_{min.}$) in cm^{-1}, HOMO-LUMO energy separation (Gap) in eV.

6; neutral D_{2h} $C_3H_2B_6$ is a triplet). Replacing two H's in **4** with an exocyclic C=CH_2 results in C_{2v} $C_3H_2B_6$ (**13**), a phC minimum. Although **13** has a total of six π electrons, two of these are localized as a C=C π bond (HOMO–4; see Figure 4-7). Four π electrons remain for the CB_6 moiety, and a +66.2 paratropic NICS(1)$_{zz}$ value for **13** results. The C_{2v} $C_3H_2B_6^{2-}$ dianion (**14**), with six of the eight π electrons on the CB_6 unit, results in a –53.4 diatropic NICS(1)$_{zz}$ value, thus **14** may be more viable than **13**. Double C=CH_2 bridging gives the eight π electron phC minimum, D_{2h} $C_5H_4B_6$ (**15**; see Figure 4-8 for details). However, akin to **13**, **15** has four π electrons localized on exocyclic C=C bonds; only four π electrons

remain on the CB unit. As expected, the 10 π electron dianion D_{2h} $C_5H_4B_6^{2-}$ (**16**; see Figure 4-8) has six π electrons on the CB_6 unit and a diatropic NICS(1)$_{zz}$ (–55.8). Molecules like **3** (X = NH and O), **12**, and **14** demonstrate that the total π electron count is less important than the number of π electrons associated with the phC moiety. Evidently, delocalized bonding of the σ system is needed to achieve planar hypercoordination.

4.4 Conclusions

CB_6 units with planar hexacoordinate carbons (or borons) can be grafted onto olefins, arenes, or saturated carbon systems. Most of these new phC candidates are doubly aromatic with delocalized σ as well as π systems, but a total of $4n$+2 π electrons is not required. All these phC derivatives provide additional examples of deltahedral bonding involving carbon and offer many opportunities for experimental realization.

Acknowledgment

This work was supported by the National Science Foundation Grant CHE-0209857 in Georgia, and by National Natural Science Foundation Grant 29873006 in China. We thank Abdolreza Sadjadi for helpful discussions. We thank Prof. Weinhold for making an earlier version of the NBO 5.0g program available to us.

4.5 References

(1) Exner, K.; Schleyer, P. v. R. *Science* **2000**, *290*, 1937-1940.

(2) Minyaev, R. M.; Gribanova, T. N. *Izv. Akad. Nauk. Ser. Khim.* **2000**, *5*,786-796; *Russ. Chem. Bull.* **2000**, *49*, 783-793.

(3) (a) Wang, Z.; Schleyer, P. v. R. *Science* **2001**, *292*, 2465-2469. (b) Li,S. D.; Miao, C. Q.; Guo, J. C.; Ren, G. M. *J. Am. Chem. Soc.* **2004**, *126*, 16227-16231.

(4) (a) Minkin, V. I.; Minyaev, R. M.; Hoffmann, R. *Russ. Chem. Re*V. **2002**, *71*, 869-892. (b) Sorger, K.; Schleyer, P. v. R. *THEOCHEM* **1995**, *338*, 317-346. (c) Ro ttger, D.; Erker, G. *Angew. Chem., Int. Ed. Engl.* **1997**, *36*, 812-827. (d) Radom, L.; Rasmussen, D. R. *Pure Appl. Chem.* **1998**, *70*, 1977-1984. (e) Siebert, W.; Gunale, A. *Chem. Soc. Re*V. **1999**, *28*, 367-371. (f) Choukroun, R.; Cassoux, P. *Acc. Chem. Res.* **1999**, *32*, 494-502.

(5) (a) Gribanova, T. N.; Minyaev, R. M.; Minkin, V. I. *Mendelee*V *Commun.* **2001**, 169-170. (b) Gribanova, T. N.; Minyaev, R. M.; Minkin, V. I. *Russ. J. Inorg. Chem.* **2001**, *46*, 1207-1210 (translated from *Zh. Neorg. Khim.* **2001**, *46*, 1340-1343).

(6) Alexandrova, A. N.; Koyle, E.; Boldyrev, A. I. *J. Mol. Model.* **2006**, *12*, 569-576.

(7) All the phC's, optimized with Gaussian 03 (see ref 11) at the B3LYP/ 6-311+G** DFT level, were minima, and their wavefunctions were stable. Magnetic shielding — a good measure of aromaticity or antiaromaticity — were evaluated by nucleus-independent chemical shift methods (NICS, see ref 12). In particular, out-of-plane (*zz*) tensor component contribution from individual canonical molecular orbitals to NICS (CMO-NICS; see ref 13) computed using the NBO 5.0g program (ref 14) at the GIAO/ PW91PW91/6-311G* level was used to analyze the behavior of the radial

and π MO's.

(8) BOMD was carried out on **5** for 10 ps after 2 ps of equilibration with the interval of 0.5 fs at 300 K at the PBE/DZVP/Gen-A2* level.

(9) Köster, A. M.; Lores, R.; Geudtner, G.; Goursot, A.;Heine, T.; Patchkovskii, S.; Reveles, J. U.; Vela, A.; Salahub, D. R. deMon; *NRC*: Ottawa, Canada, 2004.

(10) Chandrasekhar, J.; Jemmis, E. D.; Schleyer, P. v. R. *Tetrahedron Lett.* **1979**, *39*, 3707-3710.

(11) Frisch, M. J.; Trucks, G. W.; Schlegel, H. B.; Scuseria, G. E.; Robb, M. A.; Cheeseman, J. R.; Montgomery, J., J. A.; Vreven, T.; Kudin, K. N.; Burant, J. C.; Millam, J. M.; Iyengar, S. S.; Tomasi, J.; Barone, V.; Mennucci, B.; Cossi, M.; Scalmani, G.; Rega, N.; Petersson, G. A.; Nakatsuji, H.; Hada, M.; Ehara, M.; Toyota, K.; Fukuda, R.; Hasegawa, J.; Ishida, M.; Nakajima, T.; Honda, Y.; Kitao, O.; Nakai, H.; Klene, M.; Li, X.; Knox, J. E.; Hratchian, H. P.; Cross, J. B.; Adamo, C.; Jaramillo, J.; Gomperts, R.; Stratmann, R. E.; Yazyev, O.; Austin, A. J.; Cammi, R.; Pomelli, C.; Ochterski, J. W.; Ayala, P. Y.; Morokuma, K.; Voth, G. A.; Salvador, P.; Dannenberg, J. J.; Zakrzewski, V. G.; Dapprich, S.; Daniels, A. D.; Strain, M. C.; Farkas, O.; Malick, D. K.; Rabuck, A. D.; Raghavachari, K.; Foresman, J. B.; Ortiz, J. V.; Cui, Q.; Baboul, A. G.; Clifford, S.; Cioslowski, J.; Stefanov, B. B.; Liu, G.; Liashenko, A.; Piskorz, P.; Komaromi, I.; Martin, R. L.; Fox, D. J.; Keith, T.; Al-Laham, M. A.; Peng, C. Y.; Nanayakkara, A.; Challacombe, M.; Gill, P. M. W.; Johnson, B.; Chen, W.; Wong, M. W.; Gonzalez, C.; Pople, J. A.; Gaussian, Inc.: Wallingford, CT., 2004.

(12) Schleyer, P. v. R.; Maerker, C.; Dransfeld, A.; Jiao, H.; Hommes, N. J. R. v. E. *J.*

Am. Chem. Soc. **1996**, *118*, 6317-6318.

(13) (a) Černušák, I.; Fowler, P. W.; Steiner, E. *Mol. Phys.* **2000**, *98*, 945-953. (b) Corminboeuf, C.; Heine, T.; Seifert, G.; Schleyer, P. v. R.; Weber, J. *Phys. Chem. Chem. Phys.* **2004**, *6*, 273-276. (c) Heine, T.; Schleyer, P. v. R.; Corminboeuf, C.; Seifert, G.; Reviakine, R.; Weber, J. *J. Phys. Chem. A* **2003**, *107*, 6470-6475. (d) Fallah-Bagher-Shaidaei, H.; Wannere, C. S.; Corminboeuf, C.; Puchta, R.; Schleyer, P. v. R. *Org. Lett.* **2006**, *8*, 863-866.

(14) Glendening, E. D.; Badenhoop, J. K.; Reed, A. E.; Carpenter, J. E.; Bohmann, J. A.; Morales, C. M.; Weinhold, F.; *NBO 5.0*; Theoretical Chemistry Institute: University of Wisconsin, Madison, WI, 2001.

CHAPTER 5

CYCLIC BORON CLUSTERS ENCLOSING PLANAR HYPERCOORDINATE COBALT, IRON, AND NICKEL[†]

[†] Keigo Ito, Zhifeng Pu, Qian-Shu Li, Paul von Ragué Schleyer *Inorg. Chem.* **2008**, *47*, 10906–10910. Reprinted here with permission of publisher.

5.1 Abstract

Planar cyclic boron clusters with cobalt, iron, and nickel atoms at their centers — singlet D_{8h} CoB_8^-, D_{9h} FeB_9^-, CoB_9, and NiB_9^+ — are computed to be stable minima at the BP86/TZVPP DFT level. Stochastic searches of the singlet and triplet potential energy surfaces show the planar hypercoordinate D_{8h} CoB_8^- (**1**) and D_{9h} FeB_9^- (**2**) singlet isomers to be the global minima. Their double aromatic character with 6 π and 10 radial electrons is documented by detailed $NICS_{zz}$ grid and CMO-$NICS_{zz}$ analyses at PW91/TZVPP. These results encourage gas phase investigations of these two exotic anions. Although isoelectronic with D_{9h} FeB_9^- (**2**), CoB_9 and NiB_9^+ prefer nonplanar structures, triplet **3-aT** for the former and singlet **4-a** for the latter.

5.2 Introduction

Molecules exhibiting planar hypercoordination captivatechemists because of their extreme violations of classical bonding principles.[1-7] Although the tetrahedral tetracoordination of carbon was proposed by van't Hoff[8] and Le Bel[9] in 1874, Monkhorst (1968) was the first to compute methane in its very high energy D_{4h} planar geometry.[10] Hoffmann, Alder, and Wilcox suggested strategies to stabilize planar tetracoordinate carbon (ptC) transition states in 1970,[11] but the first planar ptC *minimum* was computed by Schleyer, Pople, and co-workers in 1976.[12] Since then, numerous ptCs have been described, both experimentally and computationally.[1–6] A notable example is the 1999 Wang-Boldyrev-Simons verification[13] of the 1991 Schleyer-Boldyrev prediction of ptCs having only five atoms.[14] Even higher planar hypercoordination of carbon, for example, D_{6h} CB_6^{2-} [15] and many other of its hexacoordinate relatives are local minima.[16,17] Numerous planar

pentacoordinate carbon molecules, as well as the planar heptacoordinate carbon D_{7h} CB_7^- and the octacoordinate silicon D_{8h} SiB_8, were computed by Wang and Schleyer in 2001.[18] The D_{5h} pentacoordinate carbon CAl_5^+ cation has just been identified as being the global minimum.[19] The Hückel aromaticity of these planar species contributes to their stability. Although such unusual arrangements of carbon are startling, planar hypercoordination of other elements are just as interesting. Bonačić-Koutecký et al. computed the first theoretical molecules containing a planar hexacoordinate boron in 1991.[20] In addition, there are examples of hypercoordinate nitrogen, oxygen,[14] phosphorus, germanium, tin, etc.[20–27] Notably, anions with planar hypercoordinate borons, B_8^- and B_9^-, were characterized by photoelectron spectroscopy in the gas phase by Boldyrev, Wang, and co-workers.[28] Their computational study indicated that these species are doubly aromatic,[29] due to the presence of six π and six radial electrons. The concept of planar hypercoordination is not restricted to main group elements. Pseudoplanar hypercoordinate transition metal derivatives include Ni(TBC),30[Ni(P*t*-Bu)$_6$][31] and [In(Mn(CO)$_4$)$_5$].[32] Steric repulsion of the substituent groups in those molecules helps to achieve planarity. Frenking et al.[33] computed planar hypercoordinate transition metal (phTM) minima, singlet D_{5h} $FeBi_5^-$ and $FeSb_5^-$, in 2003. However, they found that the triplet C_s isomers were more stable than the D_{5h} singlets. Other phTMs, such as MAu_6^- (M = Ti, V, Cr),[34] Au_5Zn^+,[35] and Cu_7Sc,[36] also have been investigated, as have transition metal (TM) doped planar and nonplanar boron clusters.[37-42]

We now report theoretical predictions of planar B_8 and B_9 boron ring encapsulation of octa- and nonacoordinate cobalt, iron, and nickel, which parallel Qiong's recent and somewhat similar independent study.[42] Boron participates especially well in multicenter bonding due to its electrondeficient character.[43] Our phTM designs were based on the

Schleyer-Boldyrev geometrical and electronic match principles.[14] The size of the boron ligand ring must match the optimum lengths of the B-TM multicenter bonds between the central TM and the peripheral ligand atoms. The charge of the species is chosen on the basis of electron occupancy considerations to maximize the favorable TM-B bonding interactions.

5.3 Computational Methods

Geometry optimization and harmonic vibrational frequency computations at the BP86[44-46] DFT level with the TZVPP[47] basis set employed the Gaussian 03 program.[48] No wave function instabilities were found. Natural population analysis (NPA)[49] charge computations and Wiberg bond indices (WBI)[50] were computed at the same level using NBO 5.G.[51] Grids of nucleus-independent chemical shifts (NICS)[52,53] and their *zz* NICS shielding tensor components ($NICS_{zz}$)[54] were performed with the PW91 functional[55] and the TZVPP[47] basis set using the gauge including atomic orbital (GIAO)[56] method. Although NICS values are insensitive to the density functionals, it has been found that chemical shift computations are more accurate at PW91, so that this level was employed here.[57] The $NICS_{zz}$ shielding tensors also were dissected into the contributions of individual canonical molecular orbitals (CMO- $NICS_{zz}$).[58,59] Potential energy surface scans of phTM species were performed using Saunders' "Kick" stochastic search method.[60-62] A total of 3000 structures (singlet, triplet, or quintet) were randomly generated for each phTM species in a constrained box, which was varied from 2.5 to 4.0 Å. The initial Kick geometries were optimized first at the HF/STO-3G level of theory. All unique structures obtained from this initial Kick search were then reoptimized at theBP86/TZVPP level, followed by the harmonic vibrational frequency computations.

5.4 Geometry and Bonding Analysis

The singlet cyclic boron cluster minima encapsulating the planar hypercoordinate cobalt, iron, or nickel atoms, **1-4**, are shown in Figure 1. The Co-B bond distance in **1** (2.049Å, Figure 5-1) documents the significant bonding, as it is notably shorter than the typical Co-B value (2.16 Å).[63] The TM to boron separations (2.234, 2.240, and 2.264 Å, respectively) in **2**, **3**, and **4** are somewhat longer than the sum of the atomic radii of the TM and boron (2.14, 2.16, and 2.15 Å, respectively),[63] due to the larger cavity size of the nine-membered boron ring. The boron-boron bond distances of **1-4** (1.568, 1.528, 1.533, and 1.549 Å, respectively) are significantly shorter than the single boron-boron bond length, 1.622 Å, computed for D_{2d} B_2H_4 at the BP86/TZVPP level. However, the **1-4** bond lengths are comparable to the 1.560 Å B=B double bond distance reported by Robinson, et al.[64] The delocalized, multicenter bonding in the phTM species results in short B-B bond distances.

5.5 Molecular Orbital (MO) Analysis

As shown by the MO plot (Figure 5-2), **1** has six π electrons (MOs 26, 27, and 29). The boron ring contribution dominates the a_{2u} π MO (MO 29); there is little cobalt involvement. The energy of the cobalt $3p_z$ atomic orbital (AO) (MO17) is too low to efficiently interact with the boron ring π MO. The a_{2u} MO binds the peripheral boron atoms and helps to retain the planar geometry of **1**. The cobalt involvement is so effective in the degenerate π e_{1g} MO set (MO 26 and 27), formed by the overlap of the $3d_{(xz,yz)}$ cobalt AOs with the boron ring π MOs, that this MO set is lower in energy than the a_{2u} π MO (29). Similar d-π interactions are present in D_{5h} $FeSb_5^+$ and in $FeBi_5^+$.[24] Note that five MOs (25,

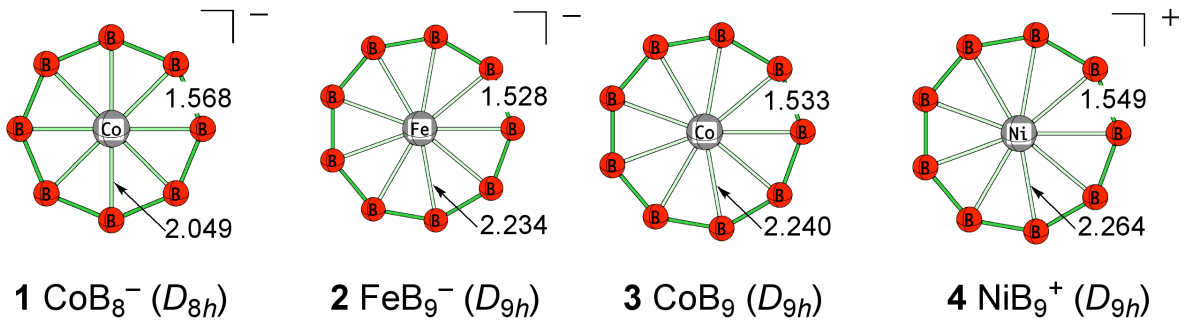

1 CoB_8^- (D_{8h}) **2** FeB_9^- (D_{9h}) **3** CoB_9 (D_{9h}) **4** NiB_9^+ (D_{9h})

Figure 5-1. Optimized geometries of the phTM minima at BP86/TZVPP. Bond distances are in angstroms.

Table 5-1. Summary of the total energies ($E_{Tot.}$ in a.u.), the zero point energy corrections (ZPE in kcal/mol) and the TM-B and B-B bond distances (r_{TM-B} and r_{B-B} in Å) computed at BP86/TZVPP.

	$E_{Tot.}$	ZPE	r_{TM-B}	r_{B-B}
1	-1581.80024	19.6	2.049	1.568
2	-1487.53869	21.4	2.234	1.528
3	-1606.50693	21.1	2.240	1.533
4	-1731.76914	20.6	2.264	1.549

30, 31, 33, and 34) have radial bonding character, as they are comprised of in-plane boron $p_{(x,y)}$ AOs pointing toward the center of the ring. The cobalt $3d_{xy}$ and $_{dx^2-y^2}$ AOs effectively overlap with the in-plane radial MOs, producing the bonding MOs (MO 30 and 31). The MOs 33 and 34 are primarily composed by theboron in-plane $p_{(x,y)}$ AOs. Like the a_{2u} π MO, the $3p_{(x,y)}$ involvement is negligible because the $3p_{(x,y)}$ AOs (MO 15 and 16) energies are too low compared to the boron ring radial MO. There is very little bonding between the central cobalt atom and the peripheral borons. In addition, the 4s and $3d_z^2$ cobalt AOs mix and interact with the lowest energy radial MO of the B_8 in a bonding and a nonbonding manner.

The resulting bonding radial MO 25 joins the central cobalt atom to the peripheral atoms of the boron ring and helps planarize the geometry. MO 32, the formally antibonding Co-B counterpart of MO25, is effectively nonbonding, dominated by the cobalt $3d_z^2$ AO. Hence, **1** has radial aromaticity with 10 (rather than 12) radial electrons. The formal electron count of the central cobalt atom in **1** satisfies the 18-electron rule, if MOs 15-17, 25-27, and 30-32 are included. Likewise, the transition metal atoms in **2-4** also have a formal 18-electron count, and their MOs are similar to **1**. However, the $d_{(xz,yz)}$-π interactions in **4** are diminished such that MOs 29 and 30 are mostly lone pair $d_{(xz,yz)}$. A smaller Ni-B interaction is also evident in the individual Ni-B WBI (WBI_{TM-B}, see the bond index analysis section and Table 5-1).

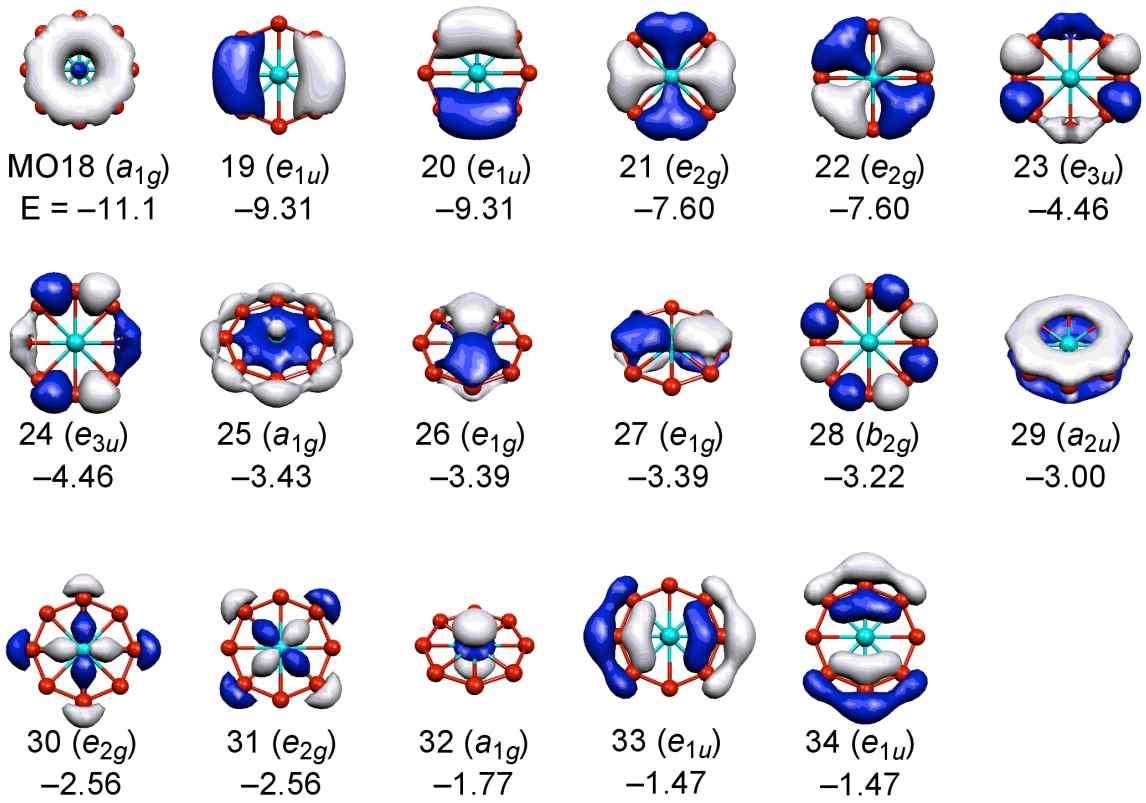

Figure 5-2. MOs of D_{8h} CoB_8^- (**1**) at the BP86/TZVPP level. MO energies are in eV.

5.6 Bond Index Analysis

The individual TM-B WBIs (WBI_{TM-B}) of **1-4** (0.39, 0.41, 0.37, and 0.28, respectively; see Table 5-2) reveal appreciable interactions between the TM and peripheral boron atoms. The total WBIs of the central TM atoms ($WBI_{TMTot.}$) range from 2.55 to 3.71 (see Table 5-2). This implies that each TM-B interaction is weak, but the unusually large number of partial TM-B bonds compensate. The individual boron-boron WBIs (WBI_{B-B}), in the 1.37 to 1.44 range (see Table 2), reflect the enhanced B-B bonding arising from the delocalized π and radial interactions. Moreover, the evenly distributed NPA charges on the peripheral boron atoms (NPA_B, see Table 5-2) in **1-4** further document the delocalized bonding nature of the phTMs.

Table 5-2. Wiberg Bond Indices of the Individual TM-B Bond, TM Total Bond Order, the Individual B-B Bond, the Boron Total Bond Order (WBI^{TM-B}, $WBI^{TMTot.}$, WBI^{B-B} and $WBI_{BTot.}$, Respectively), Natural Population Analysis Charges of the TM and Boron Atoms (NPA_{TM} and NPA_B, respectively), and $NICS(1)_{zz}$ (in ppm)[a]

	WBI_{TM-B}	$WBI_{TMTot.}$	WBI_{B-B}	$WBI_{BTot.}$	NPA_{TM}	NPA_B	$NICS(1)_{zz}$
1	0.39	3.15	1.44	3.61	0.45	-0.18	-84.5
2	0.41	3.71	1.44	3.63	0.54	-0.17	-85.8
3	0.37	3.29	1.40	3.54	0.71	-0.08	-85.4
4	0.28	2.55	1.37	3.44	0.88	0.01	-84.0

[a] WBIs and NPA charges were computed at the BP86/TZVPP level, and $NICS(1)_{zz}$ computations were performed at the PW91/TZVPP level.

5.7 Magnetic Aromaticity Analysis

The MO plot (Figure 5-2) suggests that **1** is doubly aromatic[29] due to the presence of 6 π and 10 radial electrons. The $NICS_{zz}$ at a point 1.0 Å above the ring centers $(NICS(1)_{zz})$[53,54,65] of **1-4** range from –84.0 to –85.8 ppm (see Table 5-2). Such diamagnetic $NICS(1)_{zz}$ values are much larger than those of benzene (–29.0), due to their very strong aromatic character.

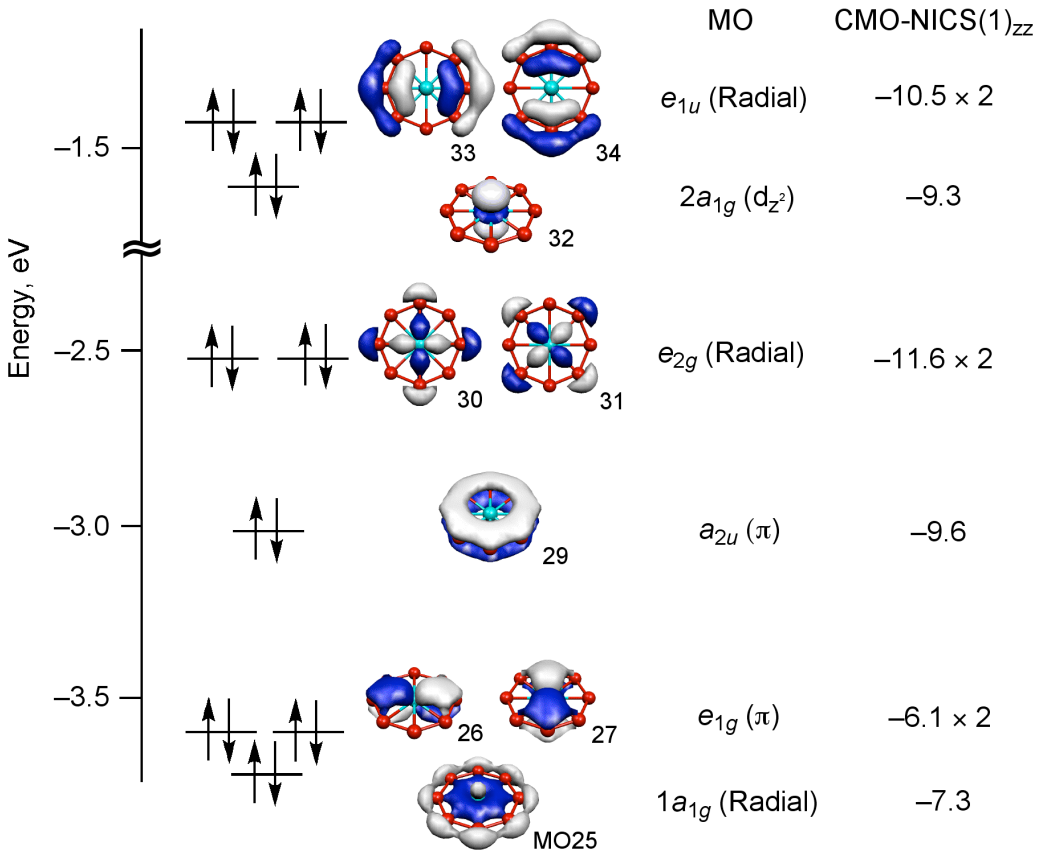

Figure 5-3. CMO-$NICS(1)_{zz}$ of D_{8h} CoB_8^- **(1)** at PW91/TZVPP level. NICS values are in ppm. *Total $NICS(1)_{zz}$ value includes include contributions from core, σ and d_{z^2} MOs.

More insights into the magnetic aromaticity are given by canonical molecular orbital

dissection of $NICS(1)_{zz}$ (CMO- $NICS(1)_{zz}$)[58] of **1**[66] using NBO5.G[51] (see Figure 5-3). The CMO- $NICS(1)_{zz}$ reveals that the contributions from both the π MOs (–21.7 ppm) and the radial MOs (–51.6) are both strongly diatropic, which depicts a double aromatic character.[29] Note that the total radial MO contribution is more than twice as large as that of the π MO total. Evidently, the radial MOs are even more important than the π MOs in determining the planar geometry preference of **1**.

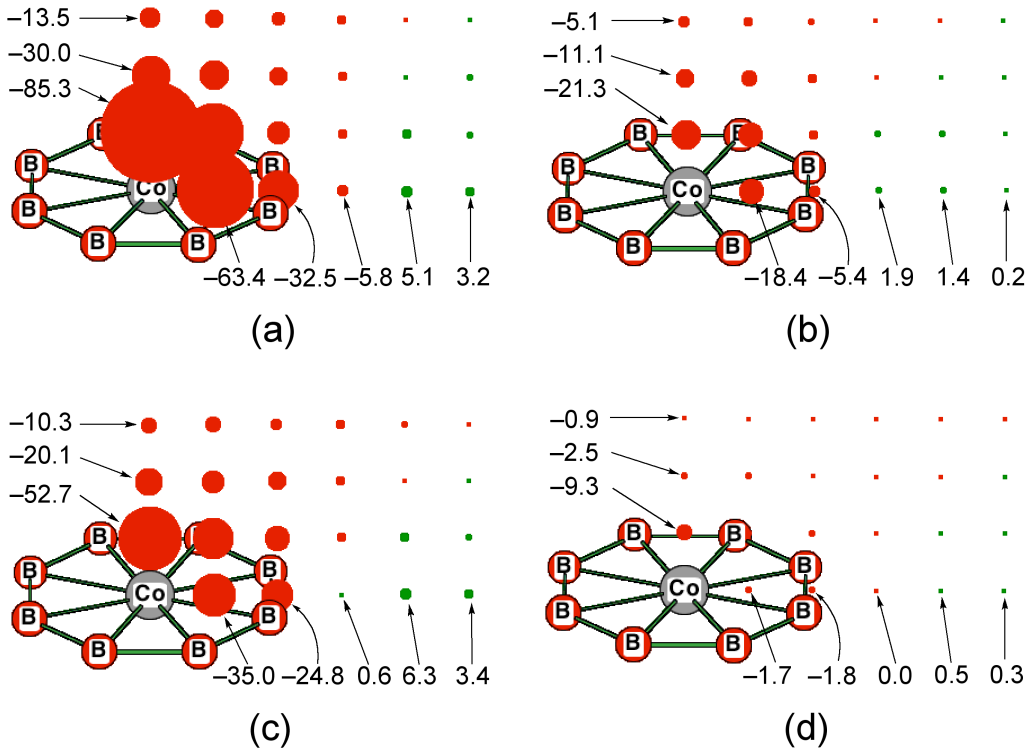

Figure 5-4. $NICS_{zz}$ grids of (a) $NICS_{zz}$, (b) $NICS_{\pi zz}$, (c) $NICS_{Radzz}$ and (d) $NICS_{d_{z^2}zz}$ of D_{8h} CoB_8^- (**1**) at PW91/TZVPP. Red points indicate diatropic and green points paratropic tensor contributions. NICS values are in ppm.

The magnetic properties of **1** were further elucidated by $NICS_{zz}$ grids (at points spaced 1.0 Å apart) partitioned into contributions from π, radial and d_{z^2} MOs ($NICS_{\pi zz}$,

$NICS_{Radzz}$, and $NICS_{dz^2zz}$)[59,65] (Figure 5-4). Both $NICS_{\pi zz}$ and the $NICS_{Radzz}$ grids reveal cone-shaped regions: diatropic shielding tensors(red points) inside and paratropic tensors (green points) outside the ring. These confirm the double aromatic character[29] of D_{8h} CoB_8^-. Such magnetic behavior is consistent with the ring current model[67] and is similar to that of C_5^{2-},[7] CCu_4^{2+},[68] and SiB[8,27]. Despite the nonbonding character of MO 32, its $NICS(1)_{zz}$ tensor contribution from MO 32 is moderately large (–9.3 ppm, see Figures 3 and 4). However, this contribution is only a local effect of the large cobalt $3d_{z^2}$ AO, as its magnitude attenuates quickly further away from the central cobalt atom (Figure 5-4d).

5.8 Chemical Viability

Of the four phTMs discussed here, **1** and **2** are most likely to be observable singlets in the gas phase. Although both are global minima, their HOMO-LUMO gaps (1.27 and 0.97 eV, respectively) and lowest harmonic vibration frequencies ($\nu_{min.}$) 26.7 and 15.2 cm^{-1}) are rather small (this also is true for **3** and **4**, see Table 5-3). The $\nu_{min.}$ vectors correspond to

Table 5-3. The lowest harmonic vibrational frequencies ($\nu_{Min.}$ in cm^{-1}) and the HOMO-LUMO gaps (Gap in eV) of the phTMs **1**-**4**, computed at the BP86/TZVPP level.

	$\nu_{Min.}$	Gap
1	46.7	1.27
2	15.2	0.97
3	38.3	1.03
4	77.8	0.68

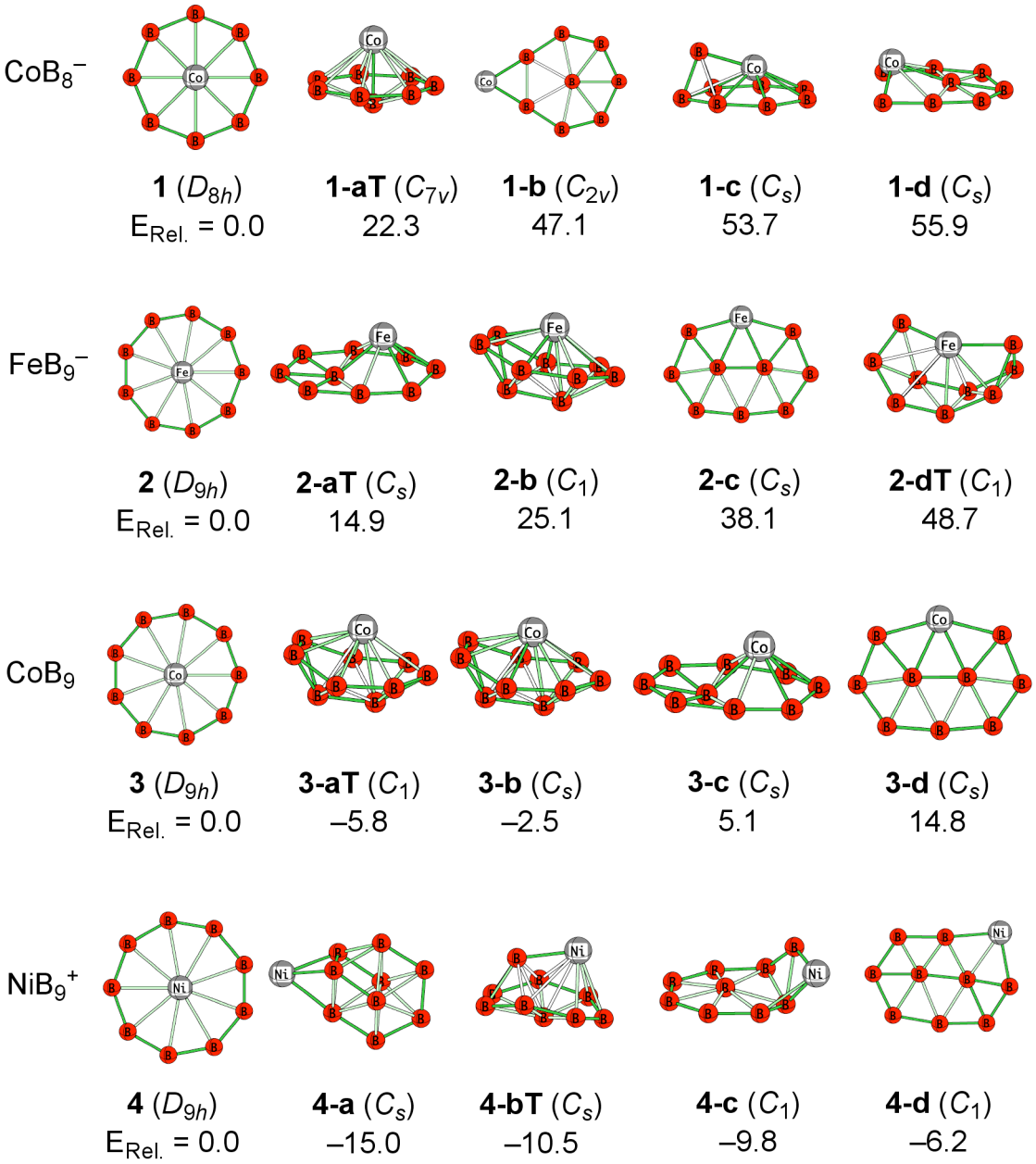

Figure 5-5. The optimized geometries of the five lowest energy minima of CoB_8^-, FeB_9^-, CoB_9 and NiB_9^+ at BP86/TZVPP. The relative energies (E_{Rel}) are based on the planar forms. Triplet states are indentified by **T'**s in the isomer designations.

out-of-plane pyramidal deformations (a_{2u} mode) for **1** and to out-of-plane ring flopping (degenerate e_{2u} modes) for **2-4**. The average atomization energy per atom of **3** (4.84 eV) are

comparable to those of D_{8h} SiB_8[27] (4.62 eV at BP86/TZVPP). The vertical detachment energy of **1** and **2** (4.09 and 3.48 eV, respectively) is similar to the experimentally characterized planar hypercoordinate boron ion with photoelectron spectroscopy (PES), the D_{8h} B_9^- (3.46 (PES), and 3.47 eV (BP86. TZVPP)).[28] The HOMO-LUMO gaps of **1-4** (see Table 5-3) are appreciable and resemble that of the D_{5h} $FeSb_5^{+3}$[33] gap (0.85 eV at BP86/TZVPP).[27] Additionally, the chemical viability of the phTMs **1-4** as isolated singlet, triplet, and quintet species were evaluated by the stochastic search "Kick" method,[60,61] as described above. The potential energy surface scans of **1-4** revealed that the singlet planar D_{nh} geometries of **1** and **2** were their global minima. Both anions are excellent candidates for gas phase detection (e.g., by laser ablation/photoelectron spectroscopy). The second-lowest energy isomers of **1** and **2** favor triplet spin states and are 22.3 and 14.9 kcal/mol higher than singlet **1** and **2**, respectively (see Figure 5, **1-aT** and **2-aT**). However, **3** and **4** were not the global minima. The lowest energy isomers of **3** and **4** (Figure 5-5) were 5.8 and 15.0 kcal/ mol more stable than the singlet planar geometries, respectively.

5.9 Conclusions

Our theoretical findings suggest that unconventional planar hypercoordinate transition metal compounds, D_{8h} CoB_8^- (**1**) and D_{9h} FeB^{9-} (**2**), are global minima and are excellent candidates for gas phase observation. Their unusual planar geometrical preferences and stabilization are due to the strong "double aromatic" interactions between the central TM *d* AOs and the π/radial MOs of the cyclic boron ligands. The 6 π and 10 radial electrons give rise to strong magnetic diatropicity. The formal electron count shows that the central TMs in **1-4** have 18 electrons. However, both **3** and **4** are less stable than nonplanar isomers,

triplet **3-aT** and singlet **4-a**, respectively. Nevertheless, even planar transition metal local minima with very high coordination are inherentlyinteresting. We have characterized many other phTM minima; details will subsequently be published.

Acknowledgment

This work was supported by the NSF (CHE-0716718) in the USA and by the 111 Project (B07012) in China. Some computations were performed at the Research Computing Center at the University of Georgia.

5.10 References

(1) Sorger, K.; Schleyer, P. v. R. *J. Mol. Struct. (THEOCHEM)* **1995**, *338*, 317–346.

(2) Röttger, D.; Erker, G. *Angew. Chem., Int. Ed. Engl.* **1997**, *36*, 812– 827.

(3) Radom, L.; Rasmussen, D. R. *Pure Appl. Chem.* **1998**, *70*, 1977– 1984.

(4) Siebert, W.; Gunale, A. *Chem. Soc. Re*V. **1999**, *28*, 367–371.

(5) Keese, R. *Chem. Re*V. **2006**, *106*, 4787–4808.

(6) Merino, G.; Méndes-Rojas, M. A.; Vela, A.; Heine, T. *J. Comput. Chem.* **2007**, *28*, 362–372.

(7) Merino, G.; Méndes-Rojas, M. A.; Beltrán, H. I.; Corminboeuf, C.; Heine, T.; Vela, A. *J. Am. Chem. Soc.* **2004**, *126*, 16160–16169.

(8) van't Hoff, J. H. *Arch. Neerl. Sci. Exactes Nat.* **1874**, *9*, 445–454.

(9) Le Bel, J. A. *Bull. Soc. Chim. Fr.* **1874**, *22*, 337–347.

(10) Monkhorst, H. *Chem. Commun.* **1968**, *18*, 1111–1112.

(11) Hoffmann, R.; Alder, R. W.; Wilcox, C. F. *J. Am. Chem. Soc.* **1970**, *92*, 4992–4993.

(12) Collins, J. B.; Dill, J. D.; Jemmis, E. D.; Apeloig, Y.; Schleyer, P. v. R.; Seeger, R.; Pople, J. A. *J. Am. Chem. Soc.* **1976**, *98*, 5419–5427.

(13) Li, X.; Wang, L.-S.; Boldyrev, A. I.; Simons, J. *J. Am. Chem. Soc.***1999**, *121*, 6033–6038.

(14) Schleyer, P. v. R.; Boldyrev, A. I. *J. Chem. Soc., Chem. Commun.***1991**, 1536–1538.

(15) Exner, K.; Schleyer, P. v. R. *Science* **2000**, *290*, 1937–1940.

(16) Minyaev, R. M.; Gribanova, T. N. *Russ. Chem. Bull.* **2000**, *49*, 783–793.

(17) Ito, K.; Chen, Z.; Corminboeuf, C.; Wannere, C.; Zhang, X.-H.; Li, Q.-S.; Schleyer, P. v. R. *J. Am. Chem. Soc.* **2007**, *129*, 1510–1512.

(18) Wang, Z.-X.; Schleyer, P. v. R. *Science* **2001**, *292*, 2465–2469.

(19) Pei, Y.; An, W.; Ito, K.; Schleyer, P. v. R.; Zeng, X. C. *J. Am. Chem. Soc.* **2008**, *130*, 10394–10400.

(20) Bonačić-Koutecký, V.; Fantucci, P.; Koutecký, J. *Chem. Rev.* **1991**, *91*, 1035–1108.

(21) Driess, M.; Aust, J.; Merz, K.; van Wüllen, C. *Angew. Chem., Int. Ed.* **1999**, *38*, 3677–3680.

(22) Gribanova, T. N.; Minyaev, R. M.; Minkin, V. I. *Mendeleev Commun.* **2001**, 169–170.

(23) Li, S.-D.; Miao, C.-Q.; Ren, G.-M. *Eur. J. Inorg. Chem.* **2004**, 2232– 2234.

(24) Li, S.-D.; Ren, G.-M.; Miao, C.-Q.; Jin, Z.-H. *Angew. Chem., Int. Ed.* **2004**, *43*, 1371–1373.

(25) Li, S.-D.; Ren, G.-M.; Miao, C.-Q. *Inorg. Chem.* **2004**, *43*, 6331– 6333.

(26) Li, S.-D.; Miao, C.-Q. *J. Phys. Chem. A* **2005**, *109*, 7594–7597.

(27) Islas, R.; Heine, T.; Ito, K.; Schleyer, P. v. R.; Merino, G. *J. Am. Chem. Soc.* **2007**, *129*, 14767–14774.

(28) Zhai, H.-J.; Alexandrova, A. N.; Birch, K. A.; Boldyrev, A. I.; Wang, L.-S. *Angew. Chem., Int. Ed. Engl.* **2003**, *42*, 6004–6008.

(29) Chandrasekhar, J.; Jemmis, E. D.; Schleyer, P. v. R. *Tetrahedron Lett.* **1979**, *39*, 3707–3710.

(30) Ferrara, J. D.; Tanaka, A. A.; Fierro, C.; Tessier-Youngs, C. A.; Youngs, W. J. *Organometallics* **1989**, *8*, 2089–2098.

(31) Ahlrichs, R.; Fenske, D.; Oesen, H.; Schneider, U. *Angew. Chem., Int. Ed. Engl.* **1992**, *31*, 323–326.

(32) Schollenberger, M.; Nuber, B.; Ziegler, M. *Angew. Chem., Int. Ed. Engl.* **1992**, *31*, 350–351.

(33) Lein, M.; Frunzke, J.; Frenking, G. *Angew. Chem., Int. Ed.* **2003**, *42*, 1303–1306.

(34) Li, X.; Kiran, B.; Cui, L.-F.; Wang, L.-S. *Phys. Re*V. *Lett.* **2005**, *95,* 253401-1-253401-4.

(35) Tanaka, H.; Neukermans, S.; Janssens, E.; Silverans, R.; Lievens, P. *J. Am. Chem. Soc.* **2003**, *125*, 2862–2863.

(36) Höltzl, T.; Janssens, E.; Veldeman, N.; Veszprémi, T.; Lievens, P.; Nguyen, M. T. *Chem. Phys. Chem.* **2008**, *9*, 833–838.

(37) Garnovsky, A. D.; Bren, V. A. *ARKIVOC* **2005**, *2005*, 1–10.

(38) Li, S.-D.; Miao, C.-Q.; Ren, G.-M.; Guo, J.-C. *Eur. J. Inorg. Chem.* **2006**, 2567–2571.

(39) Liu, X. L.; Zhao, G.-F.; Guo, L.-J.; Jing, Q.; Luo, Y.-H. *Phys. Re*V. *A* **2007**, *75*, 063201-1-063201-6.

(40) Yang, Z.; Xiong, S.-J. *J. Chem. Phys.* **2008**, *128*-1-8.

(41) Yao, J.-G.; Wang, X.-W.; Wang, Y.-X. *Chem. Phys.* **2008**, *351*, 1–6.

(42) Qiong, L. *Sci. China, Ser. B: Chem.* **2008**, *51*, 1–7.

(43) Averkiev, B. B.; Zubarev, D. Y.; Wang, L.-M.; Huang, W.; Wang, L.-S.; Boldyrev, A. I. *J. Am. Chem. Soc.* **2008**, *130*, 9248–9250.

(44) Becke, A. D. *Phys. Re*V. *A* **1988**, *38*, 3098–3100.

(45) Perdrew, J. P. *Phys. Re*V. *B* **1986**, *33*, 8822–8824.

(46) For molecules containing first row transition metal atoms, the BP86 functional performed slightly better than hybrid functionals, such as B3LYP. For more details,

see: Jensen, K. P.; Roos, B. O.; Ryde, U. *J. Chem. Phys.* **2007**, *126*, 014103-1-014103-14.

(47) Weigend, F.; Haeser, M.; Patzelt, H.; Ahlrichs, R. *Chem. Phys. Lett.* **1998**, *294*, 143–152.

(48) Frisch, M. J.; Trucks, G. W.; Schlegel, H. B.; Scuseria, G. E.; Robb, M. A.; Cheeseman, J. R.; Montgomery, J., J. A.; Vreven, T.; Kudin, K. N.; Burant, J. C.; Millam, J. M.; Iyengar, S. S.; Tomasi, J.; Barone, V.; Mennucci, B.; Cossi, M.; Scalmani, G.; Rega, N.; Petersson, G. A.; Nakatsuji, H.; Hada, M.; Ehara, M.; Toyota, K.; Fukuda, R.; Hasegawa, J.; Ishida, M.; Nakajima, T.; Honda, Y.; Kitao, O.; Nakai, H.; Klene, M.; Li, X.; Knox, J. E.; Hratchian, H. P.; Cross, J. B.; Adamo, C.; Jaramillo, J.; Gomperts, R.; Stratmann, R. E.; Yazyev, O.; Austin, A. J.; Cammi, R.; Pomelli, C.; Ochterski, J. W.; Ayala, P. Y.; Morokuma, K.; Voth, G. A.; Salvador, P.; Dannenberg, J. J.; Zakrzewski, V. G.; Dapprich, S.; Daniels, A. D.; Strain, M. C.; Farkas, O.; Malick, D. K.; Rabuck, A. D.; Raghavachari, K.; Foresman, J. B.; Ortiz, J. V.; Cui, Q.; Baboul, A. G.; Clifford, S.; Cioslowski, J.; Stefanov, B. B.; Liu, G.; Liashenko, A.; Piskorz, P.; Komaromi, I.; Martin, R. L.; Fox, D. J.; Keith, T.; Al-Laham, M. A.; Peng, C. Y.; Nanayakkara, A.; Challacombe, M.; Gill, P. M. W.; Johnson, B.; Chen, W.; Wong, M. W.; Gonzalez, C.; Pople, J. A.; Gaussian, Inc.: Wallingford, CT., 2004.

(49) Reed, A. E.; Weinstock, R. B.; Weinhold, F. *J. Chem. Phys.* **1985**, *83*, 735–746.

(50) Wiberg, K. B. *Tetrahedron* **1968**, *24*, 1083–1096.

(51) Glendening, E. D.; Badenhoop, J. K.; Reed, A. E.; Carpenter, J. E.; Bohmann, J. A.; Morales, C. M.; Weinhold, F. *NBO, 5.G*; University of Wisconsin: Madison, WI,

2001.

(52) Schleyer, P. v. R.; Maerker, C.; Dransfeld, A.; Jiao, H.; Hommes, N. J. R. v. E. *J. Am. Chem. Soc.* **1996**, *118*, 6317–6318.

(53) Schleyer, P. v. R.; Jiao, H.; Hommes, N. J. R. v. E.; Malkin, V. G.; Malkina, O. L. *J. Am. Chem. Soc.* **1997**, *119*, 12669–12670.

(54) Steiner, E.; Fowler, P. W.; Jenneskens, L. W. *Angew. Chem., Int. Ed.* **2001**, *40*, 362–366.

(55) Perdew, J. P.; Chevary, J. A.; Vosko, S. H.; Kackson, K. A.; Pederson, M. R.; Singh, D. J.; Foiolhais, C. *Phys. Re*V. *B* **1992**, *46*, 6671–6687.

(56) Ditchfield, R. *Mol. Phys.* **1974**, *27*, 789–807.

(57) Corminboeuf, C.; Heine, T.; Weber, J. *Chem. Phys. Lett.* **2002**, *357*, 1–7.

(58) Corminboeuf, C.; Heine, T.; Weber, J. *Phys. Chem. Chem. Phys.* **2003**, *5*, 246–251.

(59) Fallah-Bagher-Shaidaei, H.; Wannere, C. S.; Corminboeuf, C.; Puchta, R.; Schleyer, P. v. R. *Org. Lett.* **2006**, *8*, 863–866.

(60) Saunders, M. *J. Am. Chem. Soc.* **1987**, *109*, 3150–3152.

(61) Bera, P. P.; Sattelmeyer, K. W.; Saunders, M.; Schaefer, H. F., III.; Schleyer, P. v. R. *J. Phys. Chem. A* **2006**, *110*, 4287–4290.

(62) Loyd, L. D.; Johnston, R. L. *Chem. Phys.* **1998**, *236*, 107–121.

(63) Sutton, L. R. E., *Tables of Interatomic Distances and Configuration in Molecules and Ions*; Supplement 1956-1959; Chemical Society: London, 1965; Vol. *18*.

(64) Wang, Y.; Quillian, B.; Wei, P.; Wannere, C. S.; Xie, Y.; King, R. B.; Schaefer, H. F., III.; Schleyer, P. v. R.; Robinson, G. H. *J. Am. Chem. Soc.* **2007**, *129*, 12412–12413.

(65) Chen, Z.; Wannere, C. S.; Corminboeuf, C.; Puchta, R.; Schleyer, P. v. R. *Chem. Rev*. **2005**, *105*, 3842–3888.

(66) CMO-NICS(1)$_{zz}$ of **2**-**4** could not be computed due to a linear dependency of the basis set.

(67) Pople, J. A. *J. Chem. Phys.* **1956**, *24*, 1111–1112.

(68) Roy, D.; Corminboeuf, C.; Wannere, C.; King, R. B.; Schleyer, P. v. R. *Inorg. Chem.* **2006**, *45*, 8902–8906.

(69) Hoffmann, R.; Schleyer, P. v. R.; Schaefer, H. F., III. *Angew. Chem., Int. Ed.* **2008**, *47*, 7164-7167.

CHAPTER 6

CONCLUSIONS

This dissertation presents several simple and effective electron-counting rules for predicting molecules containing hypercoordinate hydrogens, carbons, and transition metals, based on a theoretical understanding of their bonding behavior. Based on such design principles, scandium hydride clusters, D_{3h} $Sc_2H_5^+$, D_{2d} Sc_2H_6, D_{3h} $Sc_3H_8^+$, and D_{4h} $Sc_4H_{13}^-$, as well as planar hypercoordinate transition metal (phTM) clusters, D_{8h} CoB_8^- and D_{9h} FeB_9^-, were identified as global minima. Hypercoordination in hydrogen in scandium hydride clusters can be achieved by the formation of highly ionic H-Sc bonds; due to their electronegativity differences, the hydride and scandium(III) atoms benefit from high coordination, which maximize electrostatic attraction. Hydrocarbon clusters containing three-dimensional hypercoordinate carbons (3dhC) utilize a synergistic bonding mechanism between the central 3dhC carbon and surrounding σ-donor/π-acceptor (acetylene and trannulene) ligands. Planar cyclic boron clusters enclosing transition metals also benefit from similar cooperative bonding (between the transition metal d-orbitals and boron ring), and exhibit π and radial double aromaticity.

Hypercoordinate bonding in molecules are not "rare exceptions" but have potential experimental viabilities. The computational findings presented in this dissertation also encourage experimental realization of myriads of non-classical bonding in molecules. In particular, we demonstrate the usefulness of grafting strategies and charge compensation methods in improving the kinetic stabilities of hypercoordinate element containing clusters. The chemical viability of the CB_6^{2-} planar hexacoordinate carbon (phC) cluster is enhanced through eliminating the unrealistic –2 charge by grafting appropriate hydrocarbon moieties,

while retaining its Hückel 4n+2 π aromaticity. The kinetic stabilities of the prototype 3dhC's, D_{3h} and D_{3d} $C_7H_6^{2+}$, a quasi-transition state and a true transition state, were greatly improved by adding two C_4H_7 moieties at the two ends of the $C_7H_6^{2+}$ units to form cage clusters. Replacement of apical carbons with boron in the cage clusters lead to two neutral minima, D_{3h} and D_{3d} $C_{13}H_{14}B_2$, which are attractive candidates for condensed phase synthesis.

Potential applications of hypercoordination in chemistry and material science, such as catalyses, hydrogen storage media, and semiconductors, are rudimentary but certainly should benefit from understanding the bonding mechanisms of hypercoordinate molecules from a theoretical perspective. Understanding the nature of hypercoordinate bonding not only helps predict new materials and molecules, but also enables us to exploit their full potential. Exciting development of hypercoordinate chemistry in the future can be foreseen.

CHAPTER 7

LIST OF PUBLICATIONS

1. "Copper(II) Fluoride is an Efficient Catalyst for Alkyne-Azide Huisgen [3+2] Cycloadditions" F. Friscourt, P. A. Ledin, **K. Ito**, P. v. R. Schleyer, G.-J. Boons. *In Preparation.*
2. "Synergistic Bonding in Three-Dimensional Hypercoordinate Carbons" **K. Ito**, P. v. R. Schleyer. To be submitted to *Org. Lett.*
3. "Scandium Hydride Clusters Containing Hypercoordinate Hydrogens" **K. Ito**, P. v. R. Schleyer. To be submitted to *Theo. Chem. Acc.*
4. "Planar Hepta-, Octa-, Ennea-, and Decacoordinate First Row d-Block Metals Enclosed by Boron Rings" Z. F. Pu, **K. Ito**, P. v. R. Schleyer, Q. S. Li *Inorg. Chem.* **2009***, 48,* 10679–10686.
5. "Cyclic Boron Clusters Enclosing Planar Hypercoordinate Cobalt, Iron and Nickel" **K. Ito**, Z. F. Pu, Q. S. Li, P. v. R. Schleyer *Inorganic Chemistry* **2008***, 47*, 10906–10910.
6. "Planar Pentacoordinate Carbon in CAl_5^+: A Global Minimum" Y. Pei, W. An, **K. Ito**, P. v. R. Schleyer, X.C. Zeng *J. Am. Chem. Soc.* **2008**, *130*, 10394-10400.
7. "Boron Rings Enclosing Planar Hypercoordinate Group 14 Elements" R. Islas, T. Heine, **K. Ito**, P. v. R. Schleyer, G. Merino *J. Am. Chem. Soc.* **2007**, *129*, 14767-14774.
8. "Myriad Planar Hexacoordinate Carbon Molecules Inviting Synthesis" **K. Ito**, Z. Chen, C. Corminboeuf, C. S. Wannere, X. H. Zhang, Q. S. Li, P. v. R. Schleyer *J. Am. Chem. Soc.* **2007**, *129*, 1510-1511.